
# The sedimentary petrology of carbonate nodules in the Elliot Formation, Karoo Supergroup, main Karoo Basin (South Africa)

by

Adam Moodley

Thesis presented for the degree of Master of Science in Geology

in the Department of Geological Sciences

University of Cape Town

July 2015

**Supervisor**: Dr. Emese M. Bordy

# Plagiarism Declaration

I know that plagiarism is wrong. Plagiarism is to use another's work and pretend that it is one's own. Each significant contribution to, and quotation in this thesis from the work of other people has been attributed and has been cited and referenced. I have not allowed, and will not allow anyone to copy my work with the intention of passing it off as his or her own work.

**Signature:** _____
Adam Moodley

**Date:** 6 July 2015

# Acknowledgements

The completion of this project was only possible because of the support offered by the following people:

Dr Emese M. Bordy my supervisor for giving me the opportunity to do this project. Thank you for your enormous academic support and guidance throughout this journey.

Prof John Compton for sharing his knowledge, advice and helpful nature throughout this project.

Prof Chris Harris for being an organised and helpful Head of Department.

Ms Lara Sciscio for assisting me in the field with the identification of features and advice about how to go about writing in a professional manner.

Mr William Krummeck for helping with the photography and field work.

Mr Nicholas Laidler for helping me operate the X-ray Diffraction machine and use the software in the Department of Geological Sciences.

Mr David Wilson and his assistant Mrs Rene van der Merwe for doing an extremely professional job at making the thin sections out of rocks that are difficult to cut and mount.

Mr Francisco Paiva for assistance with operating of the camera for the photomicrographs.

Ms Mhairi Reid for assistance with the drawing software used in generating some of the figures.

Mr John Harrison and Mr Ivan Wilson for taking care of the vehicle we used in the field.

The eastern Free State farmers and farm owners of Damplaats, Oldenburg, Paradys, Orange Spring, Twee Zusters, Rhodes, Nova Barletta, Saaihoek, St Fort, Sunnyside, Boshoek, and Bramleyshoek for their hospitality and for giving us access to the study sites.

The South African National Parks at Golden Gate Highlands National Park for allowing field work in the Park.

I would also like to acknowledge the following sources of financial support:

- National Research Foundation of South Africa for African Origins Platform Grant (# 82606: The Triassic-Jurassic boundary in southern Africa: a multidisciplinary investigation research) to my supervisor, Dr Bordy to cover operational costs and grantholder-linked student support in 2013 and 2014.
- Palaeontological Scientific Trust's (PAST) conference grant to my supervisor, Dr Bordy to attend the 18th Biennial Conference of the Palaeontological Society of Southern Africa, July 11 -14, Johannesburg, South Africa.
- National Research Foundation for Extension Bursary Support for Masters Students in 2015. (give details)
- My mother Mrs Perpetua Moodley **– whom I dedicate this project.**

# Abstract

In South Africa, fossils found in the upper part of the Elliot Formation (Stormberg Group, Karoo Supergroup) are often associated with genetically poorly-constrained carbonate nodules. The origin of carbonate nodules i.e., pedogenic versus diagenetic, is important as pedogenic carbonate nodules can be used as palaeoclimate indicators, while diagenetic nodules carry limited palaeoclimatic information on the depositional setting. This research aims to characterize the carbonate nodules of the Elliot Formation macroscopically, petrographically and geochemically and to establish a diagnostic set of criteria to enable the differentiation between pedogenic and diagenetic nodules and/or diagenetic overprint. The research techniques employed in this study range from a) macroscopic field observations of the stratigraphic relationships of the nodules to the sedimentary features of the host rocks; b) sedimentary petrography of the textural features in the nodules; and c) X-ray diffraction for the assessment of the clay composition trapped within the nodules as compared to host rocks. Macroscopic field observations have shown that carbonate nodules found in the UEF are strongly associated with host rocks that contain pedogenic features such as root traces, burrows, colour mottling, and desiccation cracks, and thus are suggestive of ancient soils. However, the microscopic analysis of the nodules reveal no evidence for biological activities but rather a range of abiotic features such as septarian cracks, circumgranular cracks, and micronodules which are more likely have resulted from physicochemical processes that may have occurred during diagenesis. Clay minerals identified by X-ray diffraction include illite, muscovite, and montmorillonite confirm the generation of the sediments under arid to semi-arid climatic conditions.

# Table of contents

# Chapter 1: Introduction

The carbonate nodules found in the Upper Triassic-Lower Jurassic Elliot Formation (Karoo Supergroup, Karoo Basin) in South Africa and Lesotho are potential palaeoclimate indicators, and their petrological and geochemical characterisation may assist in the reconstruction of ancient ecosystem ~200 Ma ago.

Globally, the boundary between the Triassic and Jurassic marks one of the Earth's largest mass extinction events, hence establishing the ecological changes that occurred some 200 million years ago in southern Africa has a potential to generate new knowledge on the Earth's history not only on regional, but also on global scale. The Elliot Formation in southern Africa contains a variety of terrestrial calcium carbonates which can act as repositories for environmental information detailing climatic changes during their formation (cf. Zhou and Chafetz, 2009 and 2010). The fundamental assumption for undertaking this project is that by characterising the carbonate nodules, protocol for identifying the difference between pedogenic carbonates and those that have been diagenetically altered can be established. The level of diagenesis can be ascertained and the influence of this alteration on the palaeoenvironmental information contained can be formalised.

This research project aims to:

(1) characterize the carbonate nodules macroscopically, petrographically, and geochemically;

(2) devise a descriptive petrographic (and geochemical) set of criteria to differentiate between pedogenic and diagenetic carbonate nodules.

It is important to note that in this study 'nodule' is used to refer to all glaebule types for simplicity and consistency. However, strictly speaking nodules are a type of glaebule with a massive interior.

## 1.1 Geological Background

The main Karoo Basin is a Late Palaeozoic to Early Mesozoic sedimentary basin covering about three quarters of South Africa. This basin formed on the pre-exiting Precambrian basement comprising the Archean Kaapvaal Craton, the Kheis Province, the Mesoproterozoic Namaqua-Natal Belt, and the Pan-African Saldania-Gariep Provinces (Andersson et. al, 2003).

## 1.2 Tectonic setting of the main Karoo Basin

Although other basin models have been proposed (e.g. Turner, 1999; Lindeque et al., 2007 and 2011; Tankard et al., 2009 and 2012), the main Karoo Basin is generally interpreted as a retroarc foreland basin which formed ahead of the developing Cape Fold Belt (CFB) found in the southwest of South Africa (Johnson et al., 1996; Theron, 1969; Visser, 1992). It is generally accepted that the CFB itself, formed in response to northward subduction of the paleo-Pacific plate underneath Gondwana during the Palaeozoic to Early Mesozoic Era (Lock, 1980 Winter, 1984; Johnson, 1991). In the regional context, the CFB formed part of the Pan Gondwanian Mobile Belt developed as a result of compression, collision and terrain accretion along the southern margin of Gondwana (Catuneanu et al., 1998). The associated foreland basin, later fragmented in process of the Gondwana break-up and parts of it are presently preserved in Australia (Bowen Basin), Antarctica (Beacon Basin), South Africa (Karoo Basin), and South America (Parana Basin) (Catuneanu et al., 1998). Late Proterozoic structural trends allowed for the development of the Cape Orogeny along the weakest and most deformed zones of the continental lithosphere (Tankard et al., 1982; Thomas et al., 1992). It was within this setting that the Karoo Foreland Basin developed in response to supralithospheric loading resulting from the crustal shortening and thickening of the CFB (Figure 1.1) (Catuneanu et al., 1998). According to this explanation the main Karoo Basin therefore qualifies as a retroarc (Dickinson, 1974) or retro-foreland setting and subduction happened beneath the basin (Johnson and Beaumont, 1995).

Turner (1999) proposes that evidence noted in the Upper Karoo (Upper Triassic – Jurassic) supports and extensional tectonic depositional environment. Extension is argued to have been the result of a thermal anomaly off the present day coast of southeast South Africa, while the lower Karoo is characteristic of a foreland basin (Turner, 1999). Based on geological and geophysical studies, Tankard et al. (2009) suggests that both the Cape and Karoo basin could

have formed as a result of crustal uplift, and later subsidence along crustal faults, finally culminating in extended periods of regional subsidence resulting from subduction-driven mantle flow (Pyklywec and Mitrovica, 1999).

Recently acquired seismic data has led to an alternative explanation for the formation of the main Karoo Basin. According to Lindeque et al. (2011), lithostratigraphic attributes usually associated with a foreland basin are absent from the Karoo sediments based on a reflection seismic profile in the southwestern Karoo (e.g. the lack of a notable foredeep basin). Furthermore, no basement deformation was observed on the seismic data. This suggests that the CFB and main Karoo basin formed in response to wide thin-skinned folding as a result of distant southward subduction leading to suturing south of the CFB (Lindeque et. al., 2011).

### 1.3 The main Karoo Basin

The main Karoo Basin contains the thickest and most complete Permo-Carboniferous to Jurassic megasequence in southwestern Gondwana (Figure 1.1) (Catuneanu et al., 1998). The sedimentary succession reflects changing environments from glacial to deep marine, deltaic, fluvial and aeolian (Smith, 1990; Smith et al., 1993). Generally, deposition of the Karoo Supergroup was associated with the single-phase, multiple event orogenesis of the CFB (Hälbich, 1983; Cole, 1992).

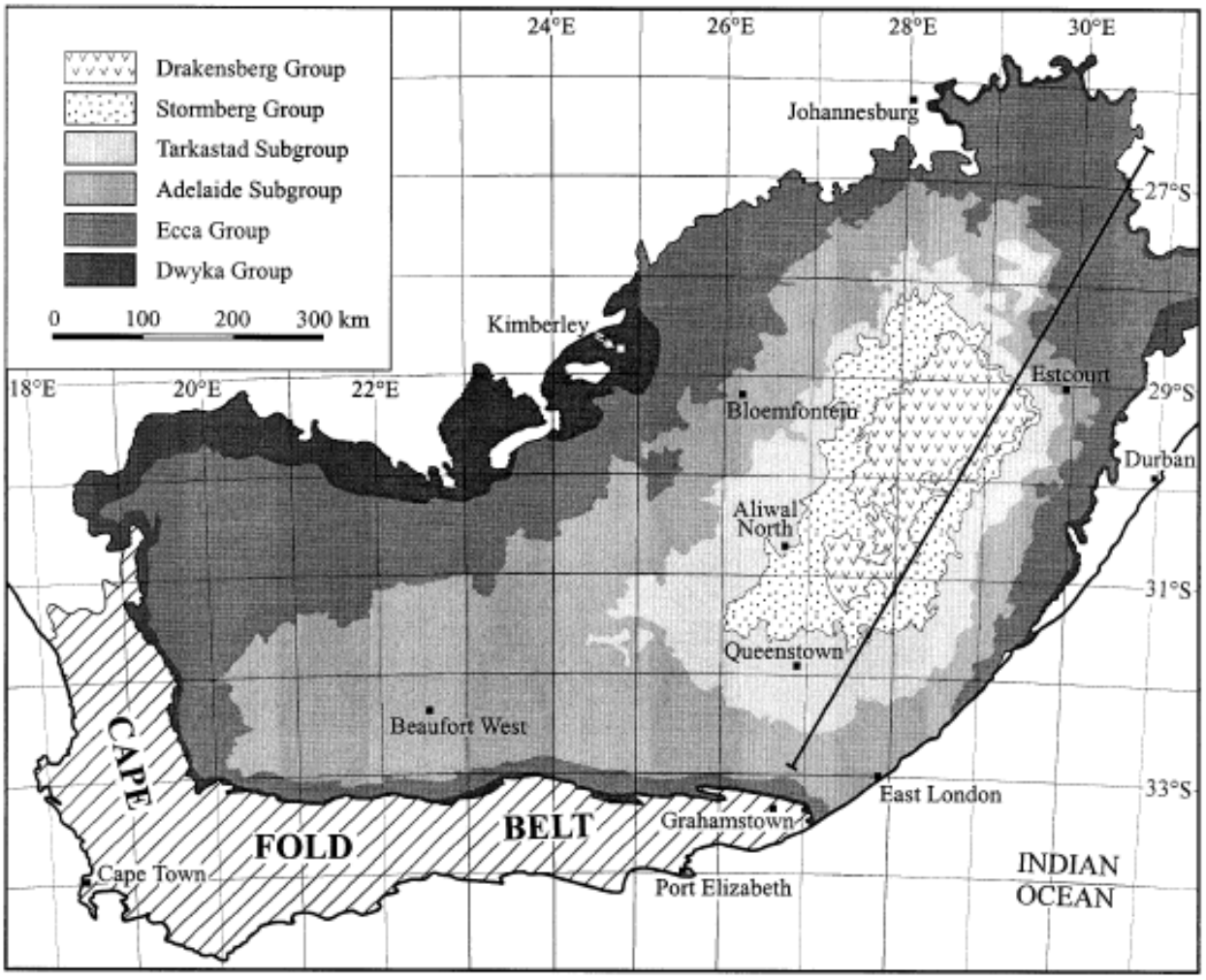


**Figure 1.1:** Schematic geological map of the main Karoo Basin in South Africa (Modified after Catuneanu et al., 1998).

The five main groups making up the Karoo Supergroup are the Dwyka, Ecca, Beaufort (Adelaide and Tarkastad subgroups), Stormberg and Drakensberg (Catuneanu et al., 1998). With the exception of the Drakensberg Group (igneous intrusive and extrusive rocks), the

entire Karoo Supergroup is a sedimentary rock succession (Catuneanu et al., 1998). The Dwyka, Ecca and Beaufort groups are separated from the overlying Stormberg Group by a major stratigraphic gap corresponding to the Middle Triassic Epoch (Catuneanu et al., 1998).

### 1.4 The Elliot Formation

The Late Triassic to Early Jurassic Elliot Formation is the middle unit of the Stormberg Group and is underlain by the Molteno, and overlain by the Clarens Formations (Figure 1.2) (Catuneanu et al, 1998). On a regional scale, the Elliot Formation has a sharp basal contact with the underlying Molteno Formation and is overlain by the gradational contact with the Clarens Formation (Bordy et al., 2004a).

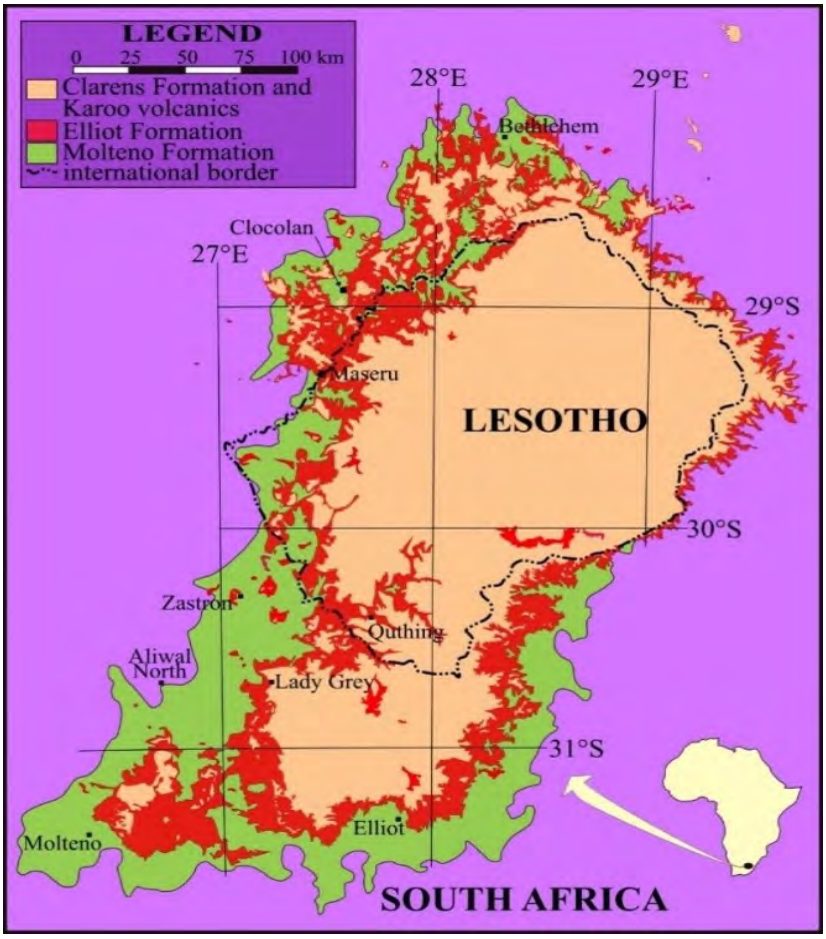


**Figure 1.2:** Simplified geological map of the upper Karoo Supergroup which comprises the fluvio-lacustrine Molteno, Elliot, mainly aeolian Clarens Formations, and igneous rocks of the Drakensburg Group. The latter, ~1400m of basaltic succession also known as the Karoo volcanics, conformably overlies the Clarens Formation (Duncan et al., 1997; Hawkesworth et al., 1999) (Modified after Bordy et al., 2004a).

The Elliot Formation is composed of reddish flood plain mudstone bodies and channel and crevasse splay sandstone bodies representing deposition within mixed-load-dominated meandering fluvial systems (Visser and Botha, 1980). Currently, the outcrops of the Elliot Formation enclave the Drakensberg Plateau (Smith and Kitching, 1997) reaching a maximum thickness of 480m in the south and thinning to less than 30m in the north (Du Toit, 1954). The change in thickness from south to north is gradual with the exception of an abrupt change between Lady Grey (Figure 1.2) and Zastron (Figure 1.2), where variable thicknesses have been observed (Bordy et. al., 2004a). Bordy et al., (2004a) were able to subdivide the Elliot Formation into the lower Elliot Formation (LEF) and upper Elliot Formation (UEF) based on vertical and horizontal facies relationships, sedimentary structures, palaeocurrents and provenance (Bordy et al., 2004a).

The boundary between the LEF and UEF is considered to represent a regionally significant surface developed as a result of the final orogenic loading event in the CFB (Bordy et al., 2004b). This orogenic loading would have caused the distal sector of the system to become elevated resulting in erosion due to uplift and southward migration of the forebulge, thereby creating a second order sequence boundary between the LEF and UEF (Bordy et al., 2004b). Subsequent to orogenic loading, the system was once again dominated by first-order unloading of the CFB, causing a depression in the distal sector, which was then filled by the upward coarsening UEF and Clarens Formations (Bordy et al., 2004b). The final tectonic event to affect the “Stormberg basin” was rifting during the Early Jurassic and has been linked to the break-up of Gondwana (Bordy et al., 2004b).

The features of sandstone bodies in the LEF and the UEF give insight into the fluvial styles operating at the time of deposition (Bordy et al., 2004a). The contrast in overall shape, thickness, lateral extent, geometry and sedimentary structures of the sandstone bodies of the LEF indicate that this lower part of the formation was deposited in a meandering fluvial system (Bordy et al., 2004a). The UEF sandstone bodies show no incision at their base and a suite of sedimentary features (e.g., abundant pedogenic features, closely spaced spaced, tabular sandstone bodies with higher feldspar content), which according to Bordy et al. (2004b) may be as a result of slower tectonic subsidence and the progressive aridification of the environment which resulted in less stable river banks and thus floodwaters that flowed in unconfined, shallow sheets rather than channels.

The main source of the Elliot sediments was material eroded from the CFB to the south during its tectonic unloading phases (Catuneanu et al., 1998). In the upper part of the Formation, an aeolian dust component is also present, which is thought to be derived from nearby deserts as wind-blown sediment (Eriksson, 1985). Furthermore, this upwards increase in aeolian features is considered as evidence for a gradual transition into more desert-like environments under which the bulk of the Clarens Formation was deposited (Catuneanu et al., 1998). The key evidence supporting the increasingly arid climatic conditions during the deposition of the Elliot Formation includes:

1. Palaeogeographic data indicating that southern Africa (within Gondwana) was situated in humid temperate to dry subtropical climatic latitudes from the Late Triassic to Early Jurassic (Figure 1.3) (Parrish, 1990; Scotese et al., 1999).
2. The gradual increase of reddening observed in mudrocks from the LEF to UEF due to diagenetic oxidation of iron held in ferruginous silicates and clays (Eriksson, 1986).
3. The very general changes in fauna from larger sized dinosaurs observed in the LEF ('*Euskelosaurus'* Range Zone comprising large prosauropods as well as cynodonts, amphibians) to smaller sized ones in the UEF (*Massospondylus* Range Zone comprising small sauropodomorphs and crocodilians - Haughton, 1924; Du Toit, 1954, Kitching and Raath, 1984; Gaffney and Kitching, 1994; Smith and Kitching, 1997; Warren and Damiani, 1999).
4. The relative abundance of petrified fossil wood in the southern LEF outcrops compared to the absence of petrified plant fossils in the UEF deposits (Bordy et al., 2004b).
5. The gradual increase in abundance of sediments with aeolian and affinity in the UEF (Kitching and Raath, 1984; Eriksson, 1985).
6. The conformably overlying aeolian sandstone bodies of the Clarens Formation (Beukes, 1970 and Eriksson, 1986).

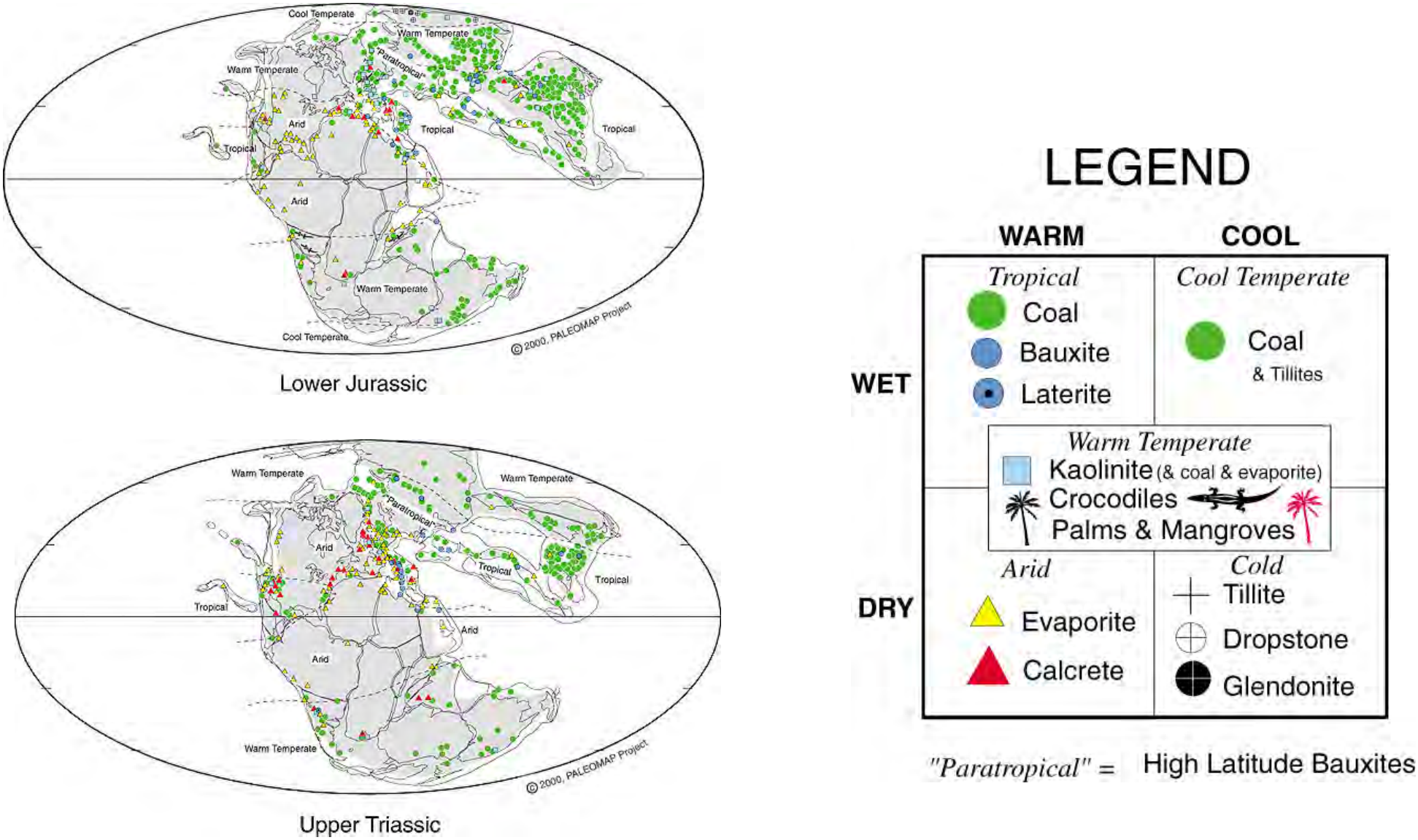


**Figure 1.3:** Upper Triassic – Lower Jurassic palaeographic map showing the climate boundaries and localisation of calcrete occurrences during the deposition of the Elliot Formation. (Scotese, 2015)

## 1.5 Pedogenic features in the Elliot Formation

In the southern Elliot Formation outcrops, especially in the LEF, pedogenic alteration is uncommon, compared to the northern part where the following features have been reported extensively: carbonate nodules, large-scale calcretized shrinkage cracks, clay-lined shrinkage cracks, small-scale desiccation cracks, irregular mottles, carbonized and calcretized root traces, terrestrial animal trace fossils (Smith and Kitching, 1997; Bordy et al., 2004a). Table 1.1 is a detailed summary of the pedogenic features reported from the northern outcrops of the UEF by Smith and Kitching (1997).

According to Bordy et al. (2004b), this contrast in pedogenic alteration features between the LEF and UEF can be explained as a consequence of tectonic and/or climatic changes. During LEF times, the higher tectonic subsidence rate in the foresag would have caused faster floodplain aggradation and slower soil profile development (Bordy et al., 2004b). However, during UEF times, reduction in orogenic unloading and cessation of thrusting, would result in lower rates of tectonic subsidence in the foresag, lower sedimentation rates and more pronounced pedogenesis on abandoned flood plain surfaces (Bordy et al., 2004b). These tectonic effects would have been enhanced by climatic conditions becoming more arid, thereby resulting in a reduced number of flooding events and therefore very low or no sedimentation (Bordy et al., 2004b) as supported by the abundance of preserved calcretized root moulds, sand-filled shrinkage cracks and invertebrate burrows and last, but not least, pedogenic carbonate nodules.

**Table 1.1:** Characteristics of palaeosols as identified by Smith and Kitching (1997) in the northern outcrops of the UEF.

| Palaeosol | Associated Features |
|---|---|
| Upper | Small calcareous nodules (diameter: <10mm)<br>Cylindrical calcareous rhizocretions<br>Fibrous root moulds<br>Desiccation cracks<br>Arenite filled vertical fissures<br>Mudrock clasts<br>Vertical laminae of dark reddish-brown claystone<br>Bioturbations<br>Fossils of *Massospondylus*, *Tritylodon* and 'fabrosaurid' ornithischians |
| *Tritylodon Acme Zone* conglomerate | Pebble sized (diameter: 10-60 mm) calcareous nodules<br>Rhizoliths (calcretized root moulds)<br>Sand-filled shrinkage cracks<br>Basal contact marked by erosional scour surface<br>Haematite-encrusted bones<br>Disarticulated, broken, reworked fossils of *Tritylodon, Massospondylus*, and 'fabrosaurid' ornithischians |
| Lower | Calcareous nodules (diameter: 10-25mm)<br>Oblate nodules (diameter: up to 60mm)<br>Calcretized shrinkage cracks<br>Sandstone filled vertical and horizontal fissures<br>Slickensided curved slip planes<br>Pseudo-anticlines lined with reddish-brown claystone<br>Discontinuous claystone laminae<br>Irregularly-shaped light grey mottles<br>Massive lenses of fine-grained sandstone with mudrock-lined burrows<br>Haematite-encrusted bones<br>Fossils of *Massospondylus, Tritylodon* and 'fabrosaurid' ornithischians |

## 1.6 Distinguishing criteria of pedogenic and diagenetic carbonate nodules

### 1.6.1 Definitions

The term ‘carbonate nodule’ is in use to refer to semi-spherical forms of calcium carbonate accumulations (Wright and Tucker, 1991). Carbonate nodules are discrete bodies which vary in shape from irregular, spherical to ellipsoidal or flattened to cylindrical (tubular) and are composed almost entirely of carbonate minerals. Those terrestrial, near surface carbonates that range in form from powdery to nodular to highly indurated are referred to as ‘calcrete’ since Lamplugh coined the term in 1902. Calcretes are in essence chemical sediments (duricrusts) comprising of carbonate crystals (mostly calcite) that form as a result of evaporation and/or evapotranspiration and degassing of carbon dioxide of mobile water saturated in calcium carbonate (Figure 1.3) (Wright and Tucker, 1991).

Calcretes can be classified according to the various textures and morphologies observed in them at a macroscopic scale (Netterberg, 1980; Wright and Tucker, 1991) or based on genesis. The former classification will be summarized in the next section, the latter, due to its importance and geological application, will be reviewed in more detail in the following paragraphs.

### 1.6.2 Genesis of pedogenic vs diagenetic calcretes

#### Pedogenic calcretes

Pedogenic or vadose calcretes are those that form closer to the surface in the soil moisture zone, usually in seasonally wet, semi-arid climatic conditions (Spötl and Wright, 1992). This has led many workers to use them as climatic indicators of such conditions (Spötl and Wright, 1992).

According to Miall (1996), pedogenic calcrete or nodule horizons could represent well-drained alkaline soils. Stable isotope analysis values of calcite $\delta^{13}C$ from carbonate nodules or concretions can help determine drainage conditions of the soil from which they precipitated (Gastaldo et al., 2014). Extremely negative calcite $\delta^{13}C$ values (-12 to -18‰) indicate poorly drained conditions, while calcite $\delta^{13}C$ values that are closer to zero (-8 to -4) reflect well drained soil conditions (Gastaldo et al., 2014). However, stable carbon isotope

values should be not be considered in isolation but in combination with other stable isotope values, palaeontological and sedimentological evidence before coming to any conclusions (Gastaldo et al., 2004; Herbert and Compton, 2007).

Today calcic soils are observed mostly in dry subtropical climates which receive around 500mm of rainfall per year and where evapotranspiration is greater than precipitation. The mean annual rainfall determines the depth of calcrete horizon development, generally forming closer to surface in dry areas and becoming deeper in wetter areas (Miall, 1996). In arid to semi-arid climates, rates of soil development are dependent on local rainfall patterns, sub-aerial exposure time, and $Ca^{2+}$ content (Wright, 1990). The sources of $Ca^{2+}$ can be assessed in calcretes using the $^{87}Sr/^{86}Sr$ ratios as proxies for the sources of $Ca^{2+}$ (Alonso-Zarza and Wright, 2010).

According to the widely accepted per *descensum* genetic model, during wet seasons meteoric (rain) water percolates downwards through the upper soil horizon, leaching carbonate in the process. Subsequently, during dry seasons, the higher temperatures cause carbonate precipitation as $CaCO_3$ or Mg-rich $CaCO_3$ in deeper parts of the soil profile (Leeder, 1975; Netterberg, 1980; Turner, 1980).

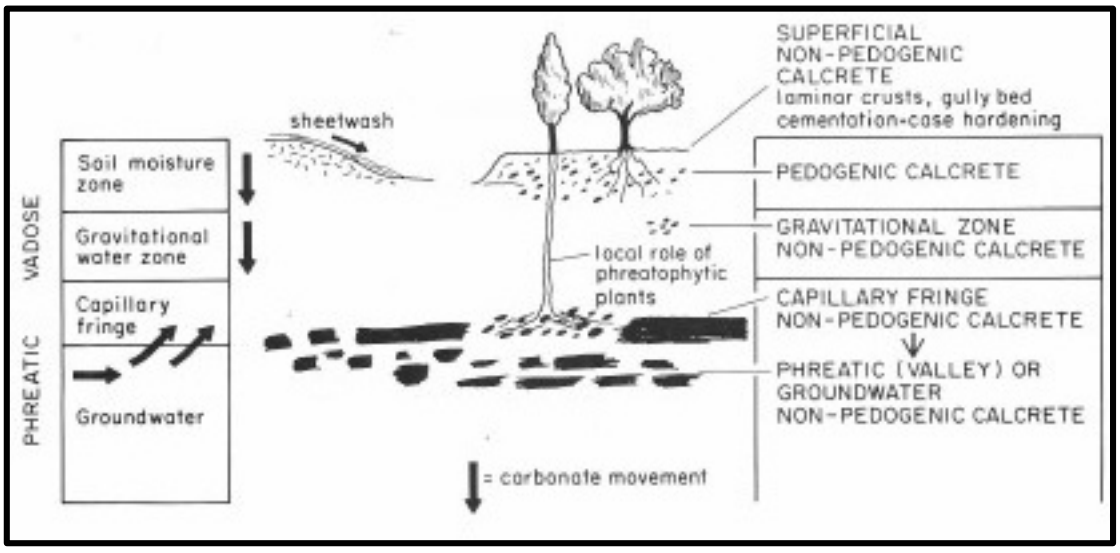


**Figure 1.4:** The main precipitation zones are defined relative to the water table position as the vadose zone (above the water table) and the phreatic zone (below the water table) (Arakel and McConchie, 1982).

It is thought that one of the major sources of $Ca^{2+}$ required for calcrete formation in semi-arid areas is from calcareous aeolian dust blown from nearby desert areas (Leeder, 1975; Turner, 1980). Other sources include: carbonate-saturated river water or sheet-floods flowing across

low relief geomorphic surfaces, from weathering upper catchment areas (Khadkikar et al., 1998). Klappa (1983) lists an entire range of calcium carbonate sources, including breakdown of Ca-rich primary minerals of the host sediments (e.g., anorthite or plagioclase containing more Ca); accumulation of carbonate within plant tissues, microbial synthesis of Ca-bearing minerals by biological (floral and fungal) processes, etc.

In summary, pedogenic calcretes form as a result of the displacive and replacive action of vadose carbonate percolating downwards through the upper soil horizon to deeper parts of the soil profile (Figure 1.3) (Netterberg, 1980; Wright and Tucker, 1991; Alonso-Zarza and Wright, 2010). The formation of pedogenic calcretes is dependent on repeated cycles of wetting and drying which results in the concentration and subsequent precipitation of carbonates (Leeder, 1975; Ekart et al., 1999).

**Diagenetic calcretes**

Diagenesis in continental settings has been described as the sum of physical and chemical changes that occur in sediments during burial and after lithification at temperatures and pressures lower than those required for metamorphosis (Armenteros, 2010). Eogenesis refers to early diagenetic changes taking place at or close to the sediment surface, mesogenesis includes changes occurring during burial where pore spaces are filled with solutions completely isolated from meteoric-derived water close to the surface (Morrow and McIlreath, 1990). Finally, telogenesis is characterized by the changes carbonate rocks undergo when exposed to meteoric water after uplift and erosion (Armenteros, 2010). Generally, diagenetic (also called groundwater) calcretes form at greater depths than pedogenic calcretes, i.e. below the main level of biological activity (Wright and Tucker, 1991). These are also referred to as phreatic calcretes as they form around the water table by the precipitation of carbonate minerals from laterally or vertically migrating groundwater through permeable substrates (Figure 1.3) (Netterberg, 1980). The carbonate is incorporated into the groundwater as it moves through subsurface carbonate-bearing formations. Precipitation later occurs due to water loss either by carbon dioxide degassing, evaporation or evapotranspiration, usually in groundwater discharge zones within topographic depressions (Wright and Tucker, 1991).

The processes of supersaturation and subsequent carbonate precipitation from groundwater are dependent on the following factors and their combinations: a) low annual rainfall; b) high evaporation rates c) the frequency and duration of rainfall. In alluvial settings, diagenetic calcretes are often found in association with sediments of high permeability (i.e., channel sand bodies rather than the fine grained overbank deposits) as these sediments allow the movement of the calcium carbonate charged groundwater more readily (Wright and Tucker, 1991; Spötl and Wright, 1992; Mozley and Davis, 1996). All in all, diagenetic (or groundwater) carbonate nodules form as a result of the precipitation of carbonate minerals from the vertical or lateral movement of groundwater in the vicinity of the water table in the phreatic zone (Figure 1.3) (Netterberg, 1980).

### 1.6.3 Macroscopic classification

This classification of calcretes is based on textural and morphological features observed on a large, hand specimen-scale. Various types include: calcareous soil, calcified soil, powder calcrete, nodular calcrete, calcrete pedotubules, honeycomb calcrete, hardpan calcrete, laminar calcrete and boulder/cobble calcrete (Netterberg, 1980; Netterberg and Caiger, 1983; Wright and Tucker, 1991). The observed morphological features of the various types suggest that they form in the order listed, e.g. nodular calcretes progressively developing into honeycomb calcrete and eventually into hardpan calcrete (Netterberg, 1980). Therefore on generic grounds this classification should include all possible types (Netterberg, 1980).

#### Calcareous soil

Calcareous soils are usually soft or loose and weakly cemented by a low carbonate content or not cemented at all (Netterberg, 1980). The carbonate occurs as grain coatings, patches of powdery carbonate, filaments (Ruellan, 1968 in Netterberg, 1980) and scattered nodules or concretions may also be present (Netterberg, 1980). The total carbonate content is expressed as $CaCO_3$ and ranges from one to ten per cent of the total sample weight (Netterberg, 1980).

**Calcified soil**

These are soils which have been cemented to a firm or stiff consistency by precipitated carbonate (Netterberg, 1980). Within the particular horizon, carbonate present can be evenly distributed throughout the profile as calcified sands and gravels or it can be confined to fissures (Netterberg, 1980). The term 'calcified' is used rather than 'calcareous' to indicate complete cementation of the entire horizon (Netterberg, 1980). The total carbonate content usually lies between ten and fifty weight percent (Netterberg, 1980). The sediment grain size appears to affect the horizon thicknesses as calcified sands are rarely more than a few metres thick, while calcified gravels more than ten metres thick have been observed (e.g. Sesriem Canyon, Namibia) (Netterberg, 1980).

**Powder calcrete**

Powder calcrete is a fine powder which may be loose or stiff and it is found *in situ* (Netterberg, 1980). It is high in silt-sized calcium carbonate with very little host sediment particles and little or no nodular development (Netterberg, 1980). These calcretes begin to form as irregular patches and lenses, in many cases along bedding planes and joints, and in clays and weathered mudrocks (Netterberg, 1980). They can potentially reach thicknesses of several metres of almost pure silt sized $CaCO_3$ crystals grading downwards into the host material (Netterberg, 1980). Powder calcretes may also contain nodules which are often weak and friable (Netterberg, 1980).

**Glaebular calcrete**

Glaebular calcretes are discrete, mostly intact, and soft to hard, concentrations of carbonate-cemented and/or replaced soil in a usually loose or sometimes strong calcareous soil matrix (Netterberg, 1980). These carbonate concentrations vary in shape from spherical through botryoidal to highly irregular, while platy, elongated and cylindrical shapes are also sometimes observed (Netterberg, 1980). Individual glaebules, or discrete botryoidal glaebule aggregations range in diameter from a few microns to more than 60 mm (Netterberg, 1980; Netterberg and Caiger, 1983). Diameters greater than 60 mm are less common because as glaebules grow larger they tend to come into contact and become cemented honeycomb

calcretes. The following glaebule classification criteria have been established by Netterberg, (1980):

1. Internal fabric: undifferentiated, concentric, lamellar, etc.;
2. Mineralogy: sesquioxidic, manganiferrous, calcareous, etc.;
3. Distinctness: sharpness of boundary and ease of removal of the glaebule from the host material;
4. Shape: spherical, botryoidal, tuberose, etc.

Using similar criteria to these, other workers (Pettijohn, 1957; Brewer and Sleeman, 1964) have classified glaebules into six types which are listed in Table 1.2 below.

**Table 1.2:** Main carbonate glaebule types and their key characteristics (based mainly on Pettijohn, 1957; Brewer and Sleeman, 1964).

| | |
|---|---|
| 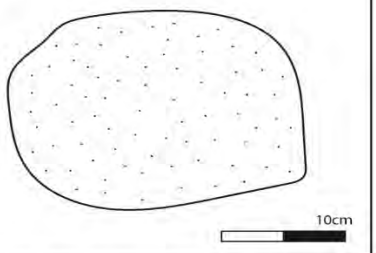 | 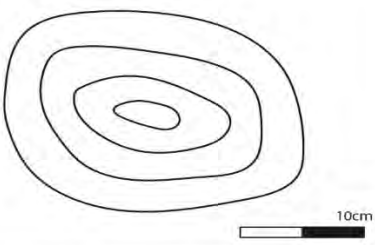 |
| Nodule: structureless internal fabric. | Concretion: concentric internal fabric |
| 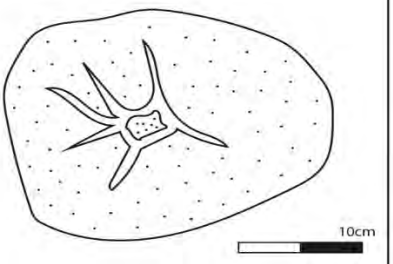 | 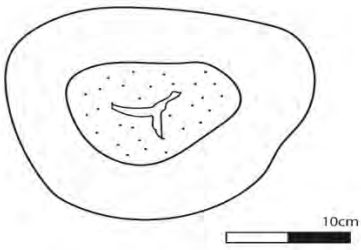 |
| Septarian: glaebule traversed by internal cracks filled with sparry calcite. | Glaebular halo: weakly cemented halo surrounding another glaebule |
| 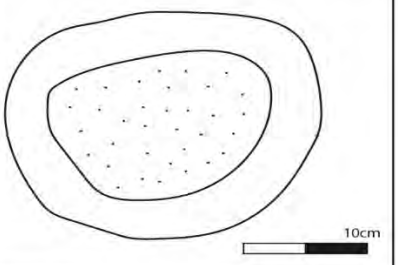 | 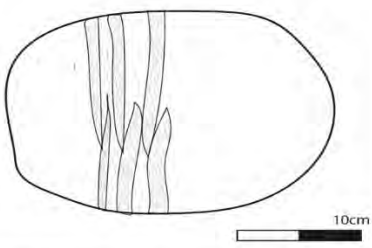 |
| Pedode: pedological equivalent of a geode. | Papule: composed of mostly clay with continuous and/or lamellar fabric. |

The most common forms of calcrete glaebules are nodules, concretions, and septaria; all other forms are rare (Netterberg, 1980). Nodular calcrete horizons are normally three to five metres thick, however some of up to thirteen metres thick have been observed on the Springbok Flats, north of Pretoria (Wagner, 1927 in Netterberg, 1980). The term nodular calcrete is more commonly used than glaebular calcrete as it encompasses other non-glaebular, secondary structures such as pedotubules and small crotovinas (Netterberg and Caiger, 1983). The term nodule in the strict sense refers to a glaebule that is massive internally. However, for the purpose of this study 'nodule' is used collectively to refer to all glaebule types for simplicity.

**Honeycomb calcrete**

This type of calcrete forms as a nodular calcite develops further and individual nodules become larger and more numerous until they become cemented together (Netterberg, 1980). Honeycomb calcretes are stiff to very hard with the interstitial voids often filled with the original host material (Netterberg, 1980). The voids are usually less than 30 mm in diameter and may be interconnected in less well developed honeycomb calcretes (Netterberg, 1980. Honeycomb calcrete profiles are rarely thicker than 500 mm (Netterberg, 1980).

**Hardpan calcrete**

Hardpan calcretes form progressively from honeycomb calcretes as the interstitial voids are filled with carbonate and the host material becomes suspended in carbonate cement (Netterberg, 1980). These calcretes are firm to very hard, relatively impervious sheet-like layers and often overlie softer or looser materials (Netterberg, 1980). Individual layers are rarely greater than 500 mm thick with a relatively sharp upper contact and a gradational or sharp lower contact (Netterberg, 1980). Hardpans may be unbroken and massive or may have some mechanical and chemical structures and textures.

**Calcrete boulders and cobbles**

Calcrete boulders and cobbles form as a result of weathering, disintegration and dissolution of calcrete hardpans to form discrete boulders (>200 mm in diameter) and cobbles (60-200 mm in diameter) (Netterberg, 1980). These calcretes are usually hard to very hard and often

occur in a red, sandy, non-calcareous soil matrix (Netterberg, 1980). Fragments with diameters smaller than cobbles and similar to that of cobbles are also common (Netterberg, 1980). Calcrete boulders and cobbles, along with those of smaller sizes are often mistaken for nodules (Netterberg, 1980). However, they can be distinguished from nodules by their usually greater size and hardness, lower grain/matrix ratio, sharper and smoother boundaries, and they are commonly partially or completely coated by a laminated rind (Netterberg, 1980).

### 1.6.4 Classification of pedogenic vs diagenetic carbonate nodules

Although these two calcretes form in different processes either virtually at the same time or after the deposition of the host sedimentary rocks, differentiation between them is difficult because they have many common macroscopic features (Wright, 1990; Wright and Tucker, 1991; Spötl and Wright, 1992). In spite of this difficulty, characterising and thus differentiating nodular calcrete types by formulating a protocol for identifying morphological and geochemical difference between them at various scales (micro to macro) is very important to gain a better understanding of the environmental and sedimentary conditions represented by pedogenic carbonate nodules at the time of their formation. The notion that pedogenic nodules can act as repositories for environmental, including climatic changes during sedimentation is based on the observation that atmospheric $CO_2$ concentration, present within soils, is stored in the precipitated pedogenic calcite in isotopic equilibrium with soil $CO_2$ (Zhou and Chafetz, 2009 and 2010).

### 1.6.5 Macroscopic classification

Many workers have concentrated their studies on pedogenic pisolitic, laminar, and massive calcretes (Reeves, 1970; James, 1972; Reeves, 1976; Esteban and Klappa, 1983; Goudie, 1983), while little attention has been given to the nodular forms (Blodgett, 1988). One of the key diagnostic features of elongated diagenetic carbonate nodules is that they tend to be parallel to one another and reflect the direction of groundwater flow at the time of formation as well as the primary permeability pattern in the host rock (Mozley and Davis, 1996).

Because of the close morphological similarities of pedogenic and diagenetic carbonate nodules, a more useful approach in differentiating them is to observe the characteristics of the host rock the nodules are found in. Characteristics of the host rock my give insight into the

depth of the groundwater table during the time of nodule formation. By considering the palaeosol constituents (clay and carbonate) and constituent properties (content, colour, form, distribution, and boundaries) an interpretation of the groundwater table influence can be made. For example, in palaeosols formed above the groundwater table clay content is highest above the carbonate enriched zone and it is brown or red in colour, while in palaeosols formed within the influence of the groundwater table clay content is variable and its colour also varies from brown or red to grey or greenish. Table 1.3 below summarizes these key features and the rest of the section gives a more in-depth explanation to the processes of formation and features associated with these two calcrete types.

**Table 1.3:** Summary of the characteristics that are commonly found in association with pedogenic and diagenetic carbonate nodules (based on Blodgett, 1988; Wright and Tucker, 1991; Spötl and Wright, 1992; Gustavson and Holiday, 1999).

| Host rock features of pedogenic carbonate nodules | Host rock features of diagenetic carbonate nodules |
|---|---|
| Destruction of primary sedimentary structures | Pristine primary sedimentary structures |
| Colour mottling | No colour mottling |
| Upper contact of nodule bearing unit: sharp | Upper contact of nodule bearing unit: sharp or diffuse |
| Lower contact of nodule bearing unit: diffuse | Lower contact of nodule bearing unit: typically sharp |
| Voids due to roots decay, often filled by meniscus pedant cement | No vadose cement |
| Poorly-sorted, floating-grain structures | Euhedral grains |
| Microbially coated grains | |
| Early diagenetic cementation: e.g. carbonate cement | |
| Sparry calcite veins due to calcite precipitation within desiccation cracks | |
| Development/preservation of soil horizons | No soil horizons |
| Abundant plant and animal bioturbation features: e.g., root traces, burrowing by soil biota (earth worms, termites) | No plant and animal bioturbation features (from well below the zone of main animal activity), however features associated with phreatotypes (deep-rooted plants) might be present |
| Various terrestrial features: e.g., desiccation cracks, slickensides | No terrestrial features |

While the above differentiation seems comprehensive, assessing these criteria in practice is more difficult, because in environments, where the position of the groundwater table is shallow (i.e., close to the surface), it can influence or even overprint the primary characteristics of the soils (Slate *et al*., 1996). Soils which form well-above the influence of groundwater have abundant clay and the highest fine-to-coarse clay or fine-to-total clay ratios in what is referred to as an argillic (Bt) horizon in soil terminology (Soil Survey Staff, 1975). These argillic soil horizons are depleted in $CaCO_3$ and are brown, red, or reddish in colour (Slate *et al*., 1996).

However, soils formed around the groundwater table show more variability in their colours which vary from brown/red to grey/greenish to a combination of the two (Slate *et al*., 1996). Grey/green-coloured or grey/green-mottled horizons have been interpreted as forming under gleying conditions or as a result of diagenesis where organic matter may have been present and preserved due to reducing conditions (Slate *et al*., 1996).

### 1.6.6 Microscopic classification

The key microscopic features of pedogenic and diagenetic calcretes are listed in Table 1.4 below. At microscopic level, a major difference between the diagenetic and pedogenic calcretes is that in diagenetic calcretes, the pore spaces between larger grains is filled with simple (sparry) cement, while pedogenic calcretes are composed of mostly micritic cements (Retallack, 1991). These micritic cements often replace the host rock matrix and enclave matrix supported grains with irregular edges showing dissolution embayment textures (Retallack, 1991). Furthermore, displacive and replacive growth features in diagenetic calcretes are more pronounced as compared to the smaller sized micritic/sparry mottled textures seen in pedogenic calcretes.

**Table 1.4:** Microscopic features of pedogenic and diagenetic calcretes (based on based on Retallack, 1991; Tandon and Narayan, 1981).

| Microscopic Feature | Pedogenic | Diagenetic |
|---|---|---|
| *Cement* | Micrite | Simple/sparite |
| *Displacive & replacive growth* | Less pronounced | More pronounced |
| *Detrital grains* | Dissolution embayments | Etched and fractured |
| *Septaria* | Present | Present |
| *Micritic laminae* | Smaller and indistinct | Larger and distinct |

Septarias of various forms (i.e., curvilinear circumgranular and radial wedge-shaped cracks filled with sparry cement) and concretions occur in both pedogenic and diagenetic calcretes. However, pedogenic concretions usually consist of less abundant micritic laminae, which are usually indistinct and smaller in size than those formed by groundwater (Tandon and Narayan, 1981).

According to Blodgett (1988), circumgranular crystallaria and septaria form due to "differential drying and cementation between the interior and exterior" of the nodules, and between nodules and the surrounding soil matrix. In well-drained soils, pedogenic septarias reflect fluctuation of oxygenation, while concretions indicate fluctuation of pedochemical conditions (Spötl and Wright, 1991).

One of the most useful and comprehensive summary of the microscopic features and pedogenic and diagenetic calcretes is by Wright (1990) who identified two end-member types of microstructures: the alpha- and beta-types. Alpha fabrics appear to be associated with abiotic (non-biogenic) processes; while beta-types are mainly biogenic in origin (Figure 1.4) (Wright, 1990; Alonso-Zarza and Wright, 2010). Biogenetic processes result in more variable microscopic features than abiogenic processes (Zhou and Chafetz, 2009). Because diagenetic calcretes form beneath the main level of biological activity they tend to be associated with alpha-type microstructures. Pedogenic calcretes form closer to the surface in the soil moisture zone allowing them to develop more beta-type microstructures. However, due to the previously mentioned groundwater overprinting of pedogenic features in settings with shallow groundwater tables, many calcretes show a combination of alpha and beta microstructures (Wright, 1990; Alonso-Zarza and Wright, 2010).

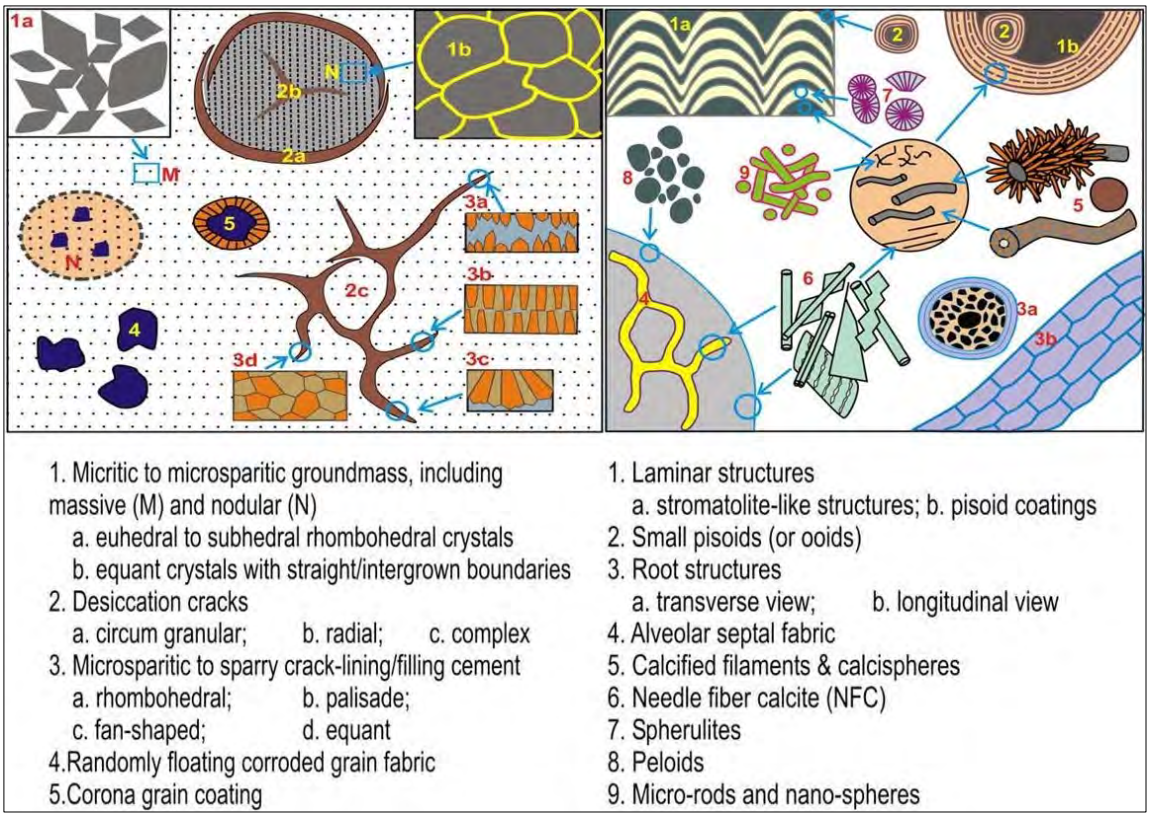


**Figure 1.5:** The microscopic difference between alpha-type microstructures (1 to 5 on the left) and beta-type microstructures (1 to 9 on the right) (Zhou and Chafetz, 2009).

# Chapter 2: Methodology

In order to answer the proposed research questions, an essentially qualitative approach was applied at both macroscopic and microscopic scales. This qualitative approach to carbonate nodules found in the Elliot Formation was coupled with a comparison of other carbonate nodules from similar dryland formations (not limited to the Triassic-Jurassic) by utilizing published literature. On a macroscopic scale, the study began in the field where first, sedimentary facies analysis was carried out to better understand the overall context in which the carbonate nodules have been preserved. The sedimentary facies analysis was then followed by sample collection from each of the selected sites within the study area for more detailed analysis in the laboratory. Laboratory analysis involved petrography to establish internal microscopic features of the nodules and X-ray diffraction to more precisely identify the minerals present in the samples. All analytical work was performed in the Department of Geological Science, University of Cape Town including preliminary sample preparation which involved cutting of samples before thin section preparation and drilling and crushing of samples before powder x-ray diffraction could be carried out.

## 2.1 Study area

The study area is located in the Eastern Free State of South Africa (Figure 2.1). A total of fourteen sites of the UEF (Table 2.1 and Figure 2.1) within the study area were selected for detailed sedimentary facies analysis and sample collection based on work done previously by Kitching and Raath (1984); Smith and Kitching (1997) and Bordy et al. (2004a, b). The reason for most study sites being in the UEF is that carbonate nodules are most commonly found in this portion of the Elliot Formation and especially in the northern part of the basin (Bordy et al., 2004b).

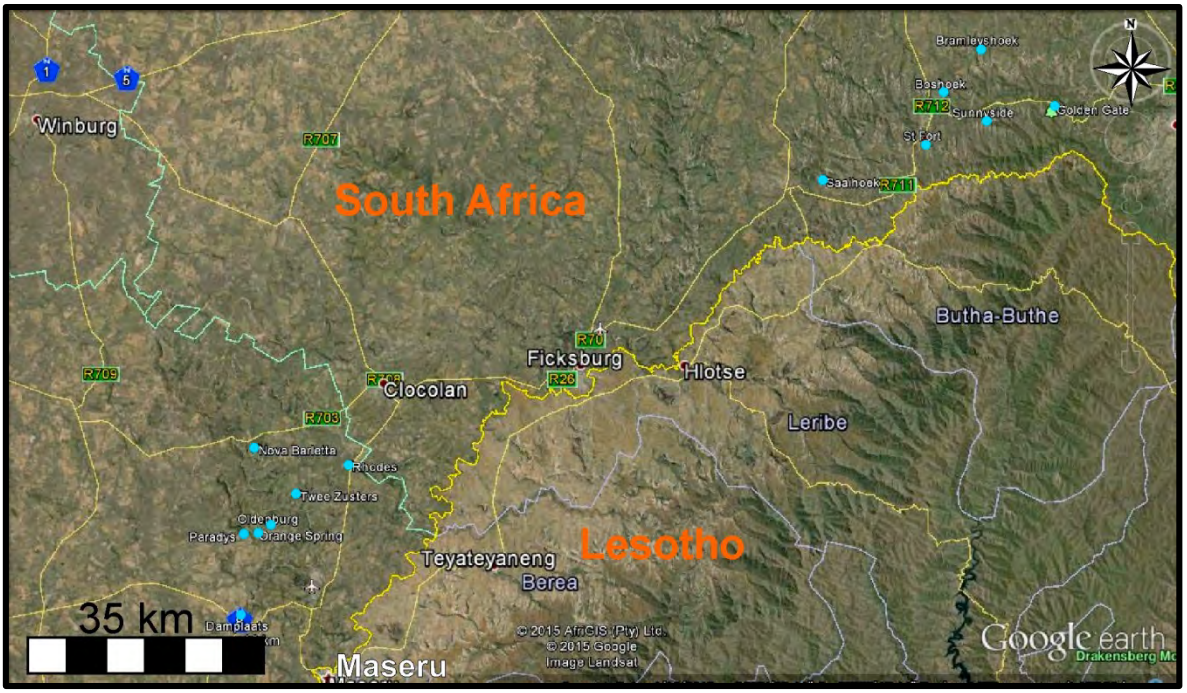


**Figure 2.1:** Study area (Eastern Free State, South Africa). Farms visited are labelled and marked with blue dots. For the GPS coordinates of the sample sites, see **Table 2.1**.

**Table 2.1 :** Sample site localities in the UEF of the eastern Free State, South Africa. NP – National Park

| District | Farm name | Coordinates |
|---|---|---|
| Bethlehem | Bramleyshoek | 28°26'S 28°30'E |
| | Boshoek | 28°29'S 28°27'E |
| | Golden Gate NP | 28°31'S 28°38'E |
| | Sunnyside | 28°32'S 28°31'E |
| Fouriesburg | St Fort | 28°34'S 28°25'E |
| | Saaihoek | 28°37'S 28°16'E |
| Clocolan | Nova Barletta | 28°59'S 27°22'E |
| Ladybrand | Rhodes | 29°01'S 27°31'E |
| | Twee Zusters | 29°03'S 27°26'E |
| | Oldenburg | 29°05'S 27°23'E |
| | Paradys | 29°06'S 27°21'E |
| | Damplaats | 29°13'S 27°20'E |
| | Orange Spring | 29°06'S 27°22'E |

## 2.2 Field work

At each site visited within the study area, the farm name, geographic location (i.e., relative to the nearest town or landmark), GPS coordinates, and height and length of the outcrop were recorded. This preliminary data capture was followed by the description of relevant outcrops,

sedimentary features and *in situ* carbonate nodules within them in the form of photo mosaics, sketches, field notes, summary diagrams, detailed stratigraphic profiles and sedimentary logs. Each site visit was then concluded by systematically photographing, collecting and preparing carbonate nodule samples in the field for further description and investigation.

### 2.2.1 Sedimentary facies analysis

Study of the vertical and regional changes in the host sedimentary facies architecture was achieved by applying the principles of facies analysis as described in Miall (1996). This method was primarily applied to establish the stratigraphic context of the carbonate nodules relative to the lower and upper boundary of the UEF. The five major characteristics used to describe a sedimentary facies are: geometry, lithology, fossil content, sedimentary structures, and palaeocurrent direction. In this study, it was also important to take note of the colour of the different sedimentary beds and nodules if present. The geometry of each unit refers to the thickness, lateral extent, and shape of the beds. Grain size variations within beds and within successions were determined for each lithology. The type of sedimentary structures in the beds (e.g., massive, horizontally laminated, cross laminated) along with bed-top and bed-bottom sedimentary features was also established. These sedimentary features provided insight into processes involved in the transportation of the sediment, i.e. energy levels and flow direction. In addition to the observation of syn-depositional features, observations of post-depositional features such as desiccation cracks and mottling of the sediment were also made. For the stratigraphic aspect of the study, it was also important to distinguish between the physical, chemical and biological aspects of the sedimentary beds and lateral changes within a succession of beds. This study does not give a detailed sedimentary facies analysis on the Elliot Formation as this work has been already covered to great lengths. Detailed explanations on the facies analysis of the Elliot Formation can be found in Bordy et al., 2004a,b,c, and d; Bordy et al., 2005a and b.

Once the sedimentary facies analysis of the entire outcrop was completed, special attention was given to the one or more carbonate nodule horizons present. It was necessary to take note of the areas of high and low nodule concentrations within the outcrop, trying to specify the upward or lateral increase or decrease in abundance of nodules. The quantification of the nodules involved specifying the percentage occupied within each outcrop, as well as within

each stratigraphic occurrence. The following descriptors were used for the percent occurrence of nodules: few (<2%); common (2 to 20%); and many (>20%). Specification of the categories of the nodules was made using the following descriptors: fine (<2 mm); medium (2 to <5 mm); coarse (5 to <20 mm); very coarse (20 to <76 mm); and extremely coarse (>76 mm). It is important to note that this size range used is strictly for the nodules in the sediment and not for the sediment itself. An effort was also made to put outcrops from different sites and multiple nodule horizons within an outcrop into a time order relative to the always present and clearly defined upper contact of the Elliot Formation with the overlying Clarens Formation.

### 2.2.2 Sample collection

Subsequent to the sedimentary facies analysis of the entire outcrop, systematic sample collection of the carbonate nodule samples was undertaken, but they were not physically removed from the outcrop before the following procedures were carried out:

- Stratigraphic positions of carbonate nodule horizons identified and recorded.
- Individual nodules representative of the nodule horizon labelled *in situ* with a sample number and way up arrow to indicate the sample orientation.
- Labelled *in situ* samples along with the associated sedimentary features in the outcrop sketched and photographed.
- Carbonate nodule samples carefully removed from the outcrop by excavating around each individual nodule using the pick end of a geological hammer to avoid damage to the external morphology of the carbonate nodule.
- Individual collected samples were placed in labelled sample bags and the farm name and GPS coordinates recorded.

The number of samples collected at each site within the study area was dependent upon the following factors: number of nodule horizons present, relative percentage of nodules in the horizon and variation of external morphologies observed in a particular nodule horizon.

## 2.3 Laboratory analysis

All sample preparation and laboratory analysis was carried out in the Department of Geological Sciences at the University of Cape Town. Petrography and X-ray diffraction were the two methods of analysis used to further investigate the samples collected from the field.

### 2.3.1 Petrography

After the external morphology of the collected carbonate nodules was observed and photographed the samples were split using a Diamant Boart electric diamond tipped saw. The macromorphological features where then observed using a Carl Zeiss binocular microscope fitted with Vickers lenses and samples with similar features were grouped. Of the grouped samples, the most representative samples in each group were selected for thin sectioning.

The prepared transmitted light thin sections (75mm in length, 25mm in width and 1mm thick) were examined under a Leica transmitted light microscope. The transmitted light thin sections were then examined again using a computer linked Nikon Optiphoto microscope fitted with an Olympus SC20 digital camera used to photograph the microscopic features. This examination allowed the visual assessment of the minerals present and description of the microscopic textures invisible to the naked eye.

### 2.3.2 X-Ray diffraction analysis

**Bulk rock samples**

The X-ray Diffraction (XRD) analysis with a Phillips X-ray Diffractometer assisted in the more precise mineral identification. Internally, the carbonate nodule samples are very heterogeneous (see section 3.9 Micromorphology of the carbonate nodules in the Elliot Formation). This means that specific areas had to be sampled separately for a more accurate analysis and the entire nodule could not be crushed as a whole. To extract sample material from the different parts of the nodule, a Proxxon hand held drill was used to drill into these different parts. The powdered fraction generated from the cores was then evenly smeared onto a perspex slide placed into the X-ray diffractometer. The instrument used was a Philips

PW 1390 XRD (Department of Geological Sciences, UCT), which uses a Copper K-α X-Ray tube with x-ray wavelength of 1.542 Å (Angstrom), accelerating voltage= 40kv and current=25mA. Bragg 2Θ angles between 20° and 52° were used for analysis. A continuous scan step size of 0.02° was applied with a scan step time of 0.75s. The resultant XRD pattern of 2theta vs. Intensity was used to calculate the d-spacing of the most intense peaks by solving for the Bragg equation.

The high calcite content of the samples meant that the minor clay minerals could not be picked up on the generated profile and therefore the clay fraction had to be separated from the bulk rock samples and run separately.

**Clay samples**

The rock samples were first crushed using a jaw crusher. After crushing they were not milled to avoid breaking down minerals such as quartz and feldspar to the same size as the clay minerals and thus defeated the object of isolating the clay minerals.

Instead the crushed samples were then placed into labelled beakers and one percent hydrochloric acid was added to them in order to dissolve out the calcite. When the effervescence stopped, the dissolution of the carbonates was considered complete. The samples were then left to settle for twelve hours to ensure that all the clay was given time to settle and minimize the amount lost during decanting of the acidic water twelve hours later.

After the acidic solution was carefully poured off, washing of the samples was done by adding 300 to 400 ml of water to each sample and stirring them, before allowing them to settle for at least twelve hours and then pouring the clear water faction off. The washing procedure was repeated 4 times to ensure all the acid was removed and no salts could form.

To separate the clay minerals, 300 to 400 ml of water was added to each of the thoroughly washed samples and stirred in order to put all the clay minerals into suspension. The samples were then left to settle for 30 minutes to allow for all the silt and sand sized particles to settle before pouring the suspended clay fraction off into a separate beaker. The clay fraction was then left to settle out for a 14 hour period before finally pouring the water fraction off and

concentrating the clays in a slurry. The clay slurry was then mounted onto glass slides and left to dry at room temperature for more than 24 hours. Finally, the glass slides with the mounted, dried clay where then placed into the X-ray diffractometer. The instrument used was a Philips PW 1390 XRD (Department of Geological Sciences, UCT), which uses a Copper K-α X-Ray tube with x-ray wavelength of 1.542 A, accelerating voltage= 40kv and current=25mA. Bragg 2Θ angles between 5° and 75°, then 2° and 62° were used for analysis. A continuous scan step size of 0.02° was applied with a scan step time of 0.5s for the angles between 5° and 75°, then later refined to a continuous scan step size of 0.03° with a scan step time of 1.50s for the angle between 2° and 62°. The resultant XRD pattern of 2theta vs. Intensity was used to calculate the d-spacing of the most intense peaks by solving for the Bragg equation.

# Chapter 3: Results

All the study sites visited during this work expose the UEF with the exception of farm Damplaats 55 where most of the UEF and a few meters of the uppermost LEF are also outcropping.

### 3.1 Lithology

The lithologies present within the study area are fine to very fine grained silty sandstone and interbedded mudstone bodies with those in the LEF being red, purple, light red or pink with green and grey mottling, whereas those of the UEF being dark red or maroon, with occasional light grey mottling, particularly in sections where carbonate nodules are present. The UEF generally display a slight coarsening upwards in grain size with fine to very fine sandstone bodies in the lower parts of the succession into fine to medium grained sandstone bodies towards the upper most parts (Figure 3.1A).

#### 3.1.1 Sandstone bodies

Sandstone bodies observed in the study area are pale red, moderate red and dark reddish brown in colour. The geometry of most sandstone bodies is sheet like, with a few lenticular shaped bodies in the upper most parts below the overlying Clarens Formation (Figure 3.1). The sheet like sandstone bodies are laterally extensive, extending for several tens of meters (Figure 3.1 A). These sheet like sandstone bodies are 5 to 6 m thick and composed of individual beds (Figure 3.1B), which range in thickness from 0.2 to 1 m. The lower and upper bedding plane surfaces are parallel, sharp and laterally persistent with rare undulating irregularities of not more than a few decimetres. Interbedded mudstone bodies are around 0.5 m thick or less and are either massive or finely laminated.

The lenticular sandstone bodies have been interpreted as channel sandstones based on their composition and geometry. In general, rivers transport large volumes of sediment as either bedload (sand material or coarser saltating, rolling, or dragging along the river bed) or as suspended load (very fine-grained clay or silt material carried in suspension) (Reineck and

Singh, 1980). Channel deposits comprise of predominantly arenaceous coarse member sediments, resulting from the deposition of the bedload. Generally, meandering river channel-deposits are thought to form as a result of lateral accretion due to lateral channel migration, which is the means of deposition and crucial diagnostic feature of the aggrading alluvial surface (Reineck and Singh, 1980).

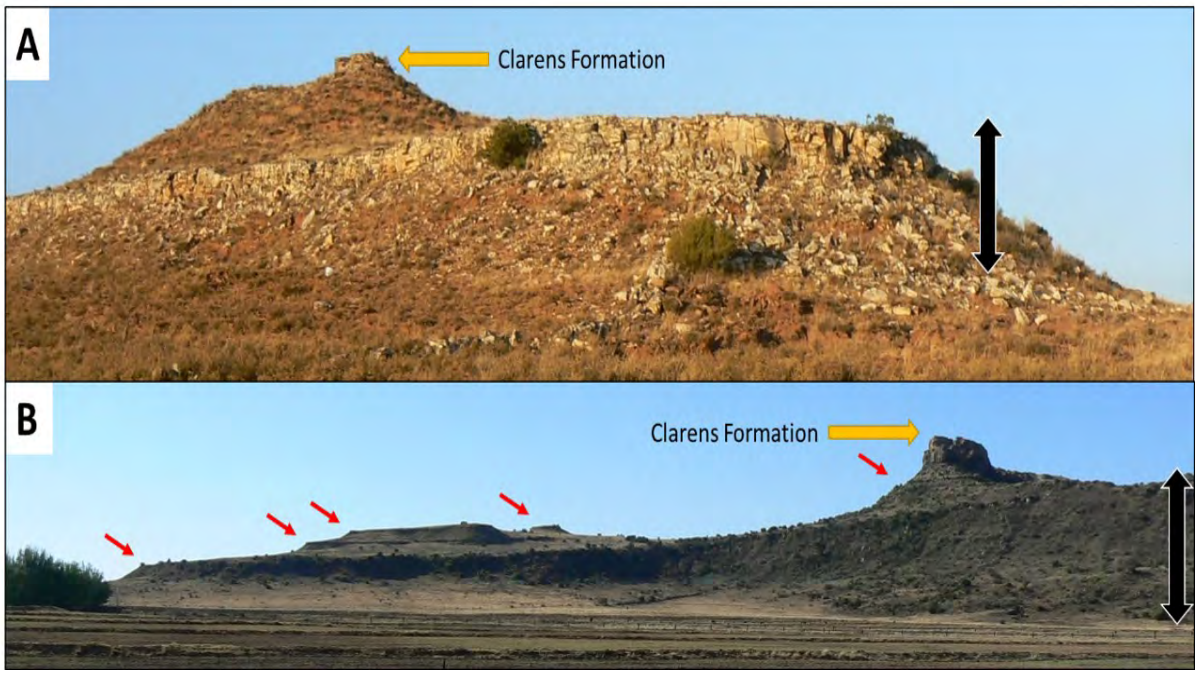


**Figure 3.1: A.** The last major sheet sandstone body in the UEF some 20 m below the contact with the conformably overlying Clarens Formation on the farm Damplaats 55 (GPS coordinate: S29° 13' 15.0" E27° 20' 29.2"). Scale: double black arrow 10 m long. **B**. Laterally extensive sheet sandstone bodies (marked with red arrows) separated by mudstone bodies in the UEF viewed from the R26 (GPS coordinate: S29° 13' 58.39" E27° 20' 31.83"). Note the uppermost sandstone is part of the Clarens Formation at elevation 1820 m. Scale: double black arrow 200 m long.

### 3.1.2 Mudstone bodies

Mudstone bodies found in the study area are red to very dark red in colour and sometimes reddish brown with bluish grey and light greenish grey mottles (Figure 3.2A). Mudstone bodies are 0.5 to 10 m thick and separate the sheet-like sandstone bodies. In terms of grain size, the mudstone bodies range from pure claystone to siltstones, with the latter being much more common. These mudstone bodies are laterally continuous (Figure 3.2B) extending for tens of meters. The majority of mudstone bodies are massive and less commonly finely laminated (Figure 3.3). The upper and lower contacts are sharp and straight, but rare undulating surfaces are also present.

The mudstone bodies have been interpreted as floodplain or overbank deposits as they are composed of mostly silt and clay (mudrocks) together with pedogenic features. Overbank deposits form away from the river channel and beyond the levees (Reid and Frostick, 1994) during floods when fine suspended load sediment can be transported to overbank interchannel areas (Galloway and Hobday, 1983). In the overbank areas sedimentation is inconsistent and the rates of sedimentation are low. During periods of no sedimentation pedogenic processes, plant growth, bioturbation (burrowing) rework the sediment, thereby destroying the primary sedimentary structures.

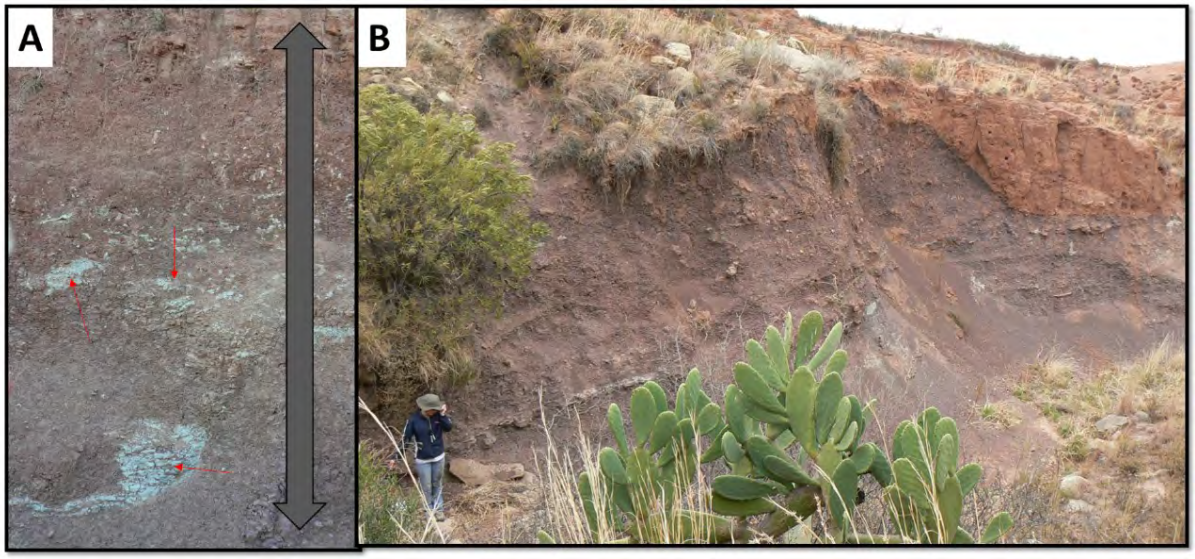


**Figure 3.2: A.** Reddish brown mudstone with bluish grey mottles pointed out with red arrows. Scale: double arrow 40 cm long. **B**. A 4 to 5 m thick massive mudstone unit with some bluish grey mottling. Note the incised unit on the right is recent colluvium. Scale: person 1.57 m tall in bottom left corner. Both photographs are taken on the farm Damplaats 55 (S29° 13' 25.63" E27° 20' 14.87").

**Figure 3.3:** Finely laminated reddish brown, 20 to 30 cm thick mudstone, overlain by reddish brown silty, very fine grained sandstone with light greenish grey discolouration on the top and followed by massive reddish brown mudstone body below a thick palaeosol horizon. Picture taken on the farm Damplaats 55 (S29° 13' 19.95" E27° 20' 16.26"). Scale: geological hammer 33 cm long.

### 3.2 Sedimentary structures

The syn- and post depositional sedimentary structures observed in the sandstone bodies and mudstone bodies of the UEF within the study area are shown in **Figures 3.4 and 3.5** below, repetitively.

**Figure 3.4:** Sedimentary structures observed in the UEF sandstone bodies within the study area.

<table>
<tr><td>  </td><td> 
</td></tr>
<tr><td>Massive sandstone</td><td>Horizontal lamination</td></tr>
<tr><td>  </td><td>  </td></tr>
<tr><td>Low-angle cross-bedding</td><td>Planar cross-bedding</td></tr>
<tr><td>  </td><td>  </td></tr>
<tr><td>Ripple marks</td><td>Climbing ripple cross-lamination (top)</td></tr>
</table>

**Figure 3.4 (cont.):** Sedimentary structures observed in the UEF sandstone bodies within the study area.

Mud-draped foresets in cross-beds

Convolute bedding

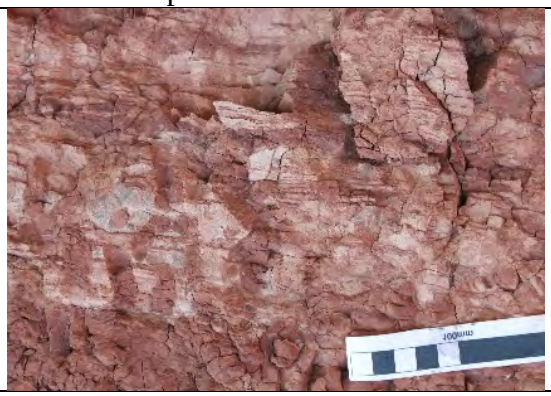

Burrows in very fine, silty sandstone

**Figure 3.5:** Sedimentary structures observed in the UEF mudstone bodies within the study area.

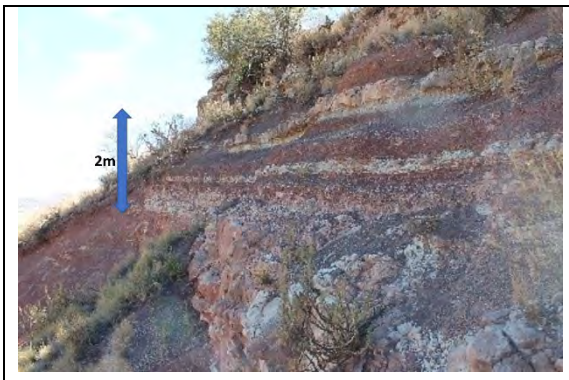


Bedded mudstone body with fine laminations


Massive bedding

Calcretized root traces

Irregular light greenish grey mottles

Sandstone-filled desiccation cracks

Large-scale desiccation cracks

Fine to extremely coarse carbonate nodules

Falling water-level marks

### 3.3 Fossils

In the floodplain deposits, fragmented fossil bones (Figure 3.6) were found occasionally. The associated sedimentary features and the close proximity to the Clarens Formation made it clear that these fossil bones are within the UEF and therefore part of the *Massospondylus* Range Zone of Kitching and Raath (1984). Channel sandstone bodies were devoid of fossil remains, but some of their basal channel-lags contained fossil bone fragments in association with mud chip (Figure 3.7A) and reworked carbonate nodule conglomerates (Figure 3.7B).

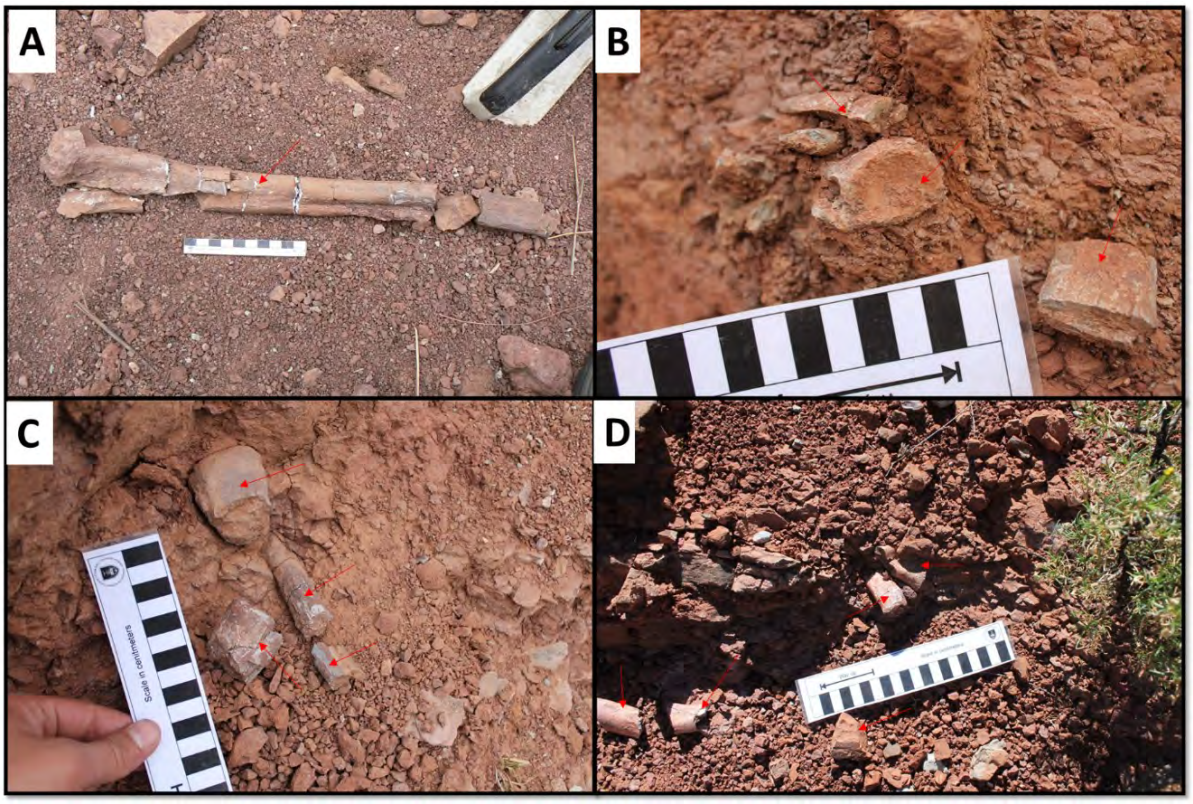


**Figure 3.6: A.** Reconstructed broken femur bone on the Farm Damplaats (GPS coordinate: S29° 13'18.03" E27° 20' 17.43"). Scale bar 10 cm long. **B**. and **C**. Fossil bone fragments at Golden Gate Highlands National Park (GPS coordinate: S28° 30' 38.40" E28°37' 31.20"). Scale bar intervals 1 cm wide. **D**. Fossil bone fragments on the Farm Nova Barletta (GPS coordinate: S28° 59'14.60" E27° 22' 16.02"). Scale bar 20 cm long.

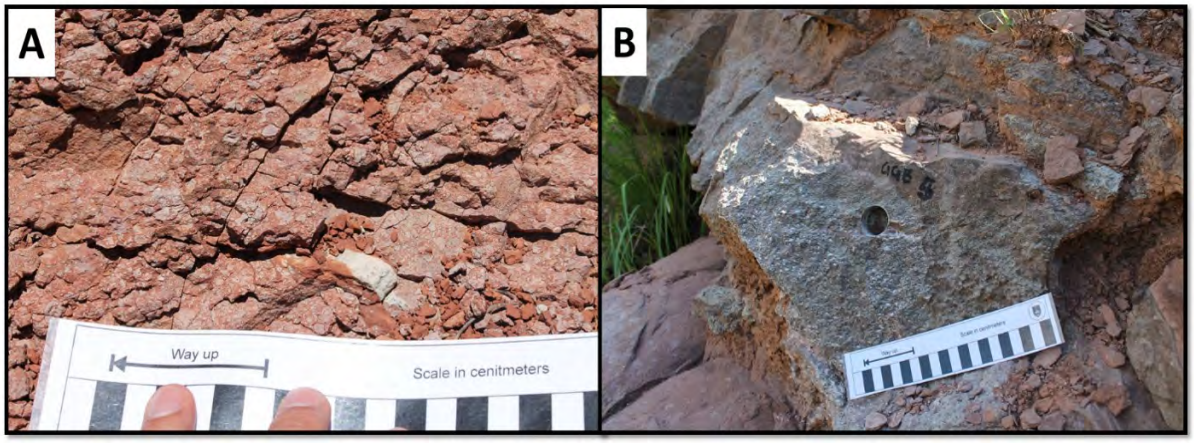


**Figure 3.7: A.** Mud chip conglomerate with mud clasts 2 to 5 mm in size in a mudrock matrix on the Farm Nova Barletta (GPS coordinates: S28 59 16.52 E27 22 10.74). Scale bar in 1 cm intervals. **B**. Reworked carbonate nodule conglomerate with many (>20%) medium (2 to <5 mm) to coarse sized (5 to <20 mm) nodules in a reddish brown muddy silty, very fine grained sandstone matrix at Golden Gate Highlands National Park (GPS coordinates: S28 30 40.08 E28 37 33.49). Scale bar 20 cm long.

Trace fossils are rare and associated with shallow bedding plane features. These are horizontal or sub-horizontal, straight, simple and unlined burrows that are massively filled with the same material as that of the host rock. Similar traces in the UEF have been interpreted as feeding traces (Fodichina) of arthropods and vermiform animals (Bordy et. al., 2004b). Traces less than 10 mm in diameter with crescent-shaped backfilling were also occasionally observed, and were previously interpreted as feeding burrows characteristic of a low-energy, shallow water environment where the burrows were actively back-filled by the organism(s) (Frey et al., 1984 and Buatois et al., 1998).

### 3.4 Palaeosol features

It is important to note that in this study is the *Tritylodon* Acme Zone described by Kitching and Smith (1997 as an almost continuous regional marker horizon was not observed in the study area. Because of this, the *Tritylodon* Acme Zone could not be used a reference surface (datum) for the assessment of the stratigraphic position of the studied palaeosol horizons. Instead, in this study the clearly identifiable regional contact between the UEF and Clarens Formations was used as a marker surface, and the stratigraphic positions of the palaeosols and the carbonate nodules collected from the UEF in this study were measured relative to this datum.

Pedogenic features such as rhizoliths, burrows, colour mottling and desiccation are useful in helping to identify fossil soils or soil horizons. In addition to pedogenic features helping to identify soil horizons, they may also give insight into the hydrological, chemical, climatic and depositional conditions prevalent during pedogenesis (Mack and James, 1994; Retallack and Alonso-Zarza, 1998; Retallack, 1999; Sheldon, 2006)

### 3.4.1 Root traces

The organo-sedimentary structures produced by roots in the sediments are termed "rhizoliths", and are defined as "the accumulation and/or cementation around, cementation within, or replacement of higher plant roots by mineral matter" (Klappa, 1980: 615). Ancient root traces provide evidence for sub-aerial exposure of the sediment surface and colonization by plant life (Retallack, 1988).

In many of the palaeosols rhizoliths such as root casts, root moulds and rhizocretions are common. Root casts and moulds are thin and fibrous measuring just a few millimetres in thickness and calcareous rhizocretions are cylindrical (Figure 3.8) (2.5-50 mm in diameter). The root casts, moulds, and rhizocretions are in a vertical to sub-vertical orientation, tapering downwards as they penetrate into the siltstone below. These rhizocretions appear to be in the same orientation they would have been during the lifetime of the plants. The top of the palaeosol is taken to represent the ancient surface from which the root traces emanate. At some the sample sites where more than one palaeosol has been observed, in the upper palaeosols there are reworked rhizoliths resembling those found in lower palaeosols.

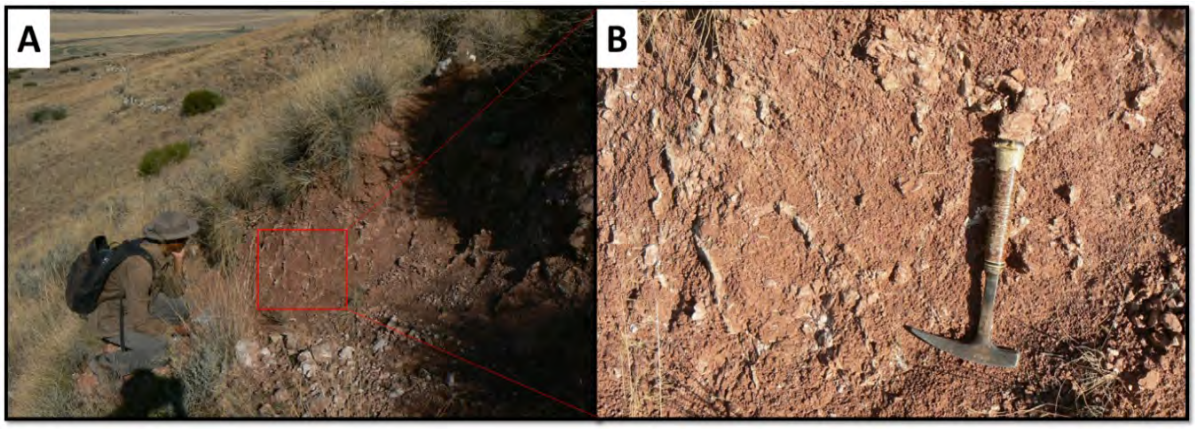


**Figure 3.8: A** and **B.** Rhizocretions on Damplaats Farm (GPS coordinates: S29° 13' 18.59" E27° 20' 28.62"). Scale: Person crouched ~1m high in A and geological hammer 33 cm long in B.

### 3.4.2 Burrows

Burrows, especially made by soil-dwelling invertebrates, are common biological sedimentary features in soils and are considered vital in ecosystem engineering (Jones et al., 1994). Invertebrates such as earthworms, termites, ants and crayfish affect the availability of resources to other plant and animal species, by changing the physical state of soils (Brussard, 1998). For example, these organisms can increase the porosity and permeability of the soil and as a result increase the drainage and the likelihood of carbonate precipitation under favourable physicochemical conditions (Jones et al., 1994; Brussard, 1998). Distinguishing between root traces and vertical to subvertical, shaft like burrows can be difficult, and because of this, the non-generic term ‘pedotubule’ was introduced by Brewer (1964). Generally, burrows are distinguished from root traces by the absence of downward bifurcation and/or tapering common to most root traces (Bown and Kraus, 1981; Retallack, 1983).

Burrows were observed in lenses of massive fine-grained sandstone that are light brown in colour (Figure 3.9: A and B) in the lower palaeosol horizons that are more than 60 m below the contact of the Elliot and Clarens Formations. These sandstone bodies contain shaft-like semi-vertical burrows with a uniform diameter of about 2 cm and lined with reddish brown mudrock (Figure 3.4). The burrows are range from 5 to10 cm in length and may be anastomosing.

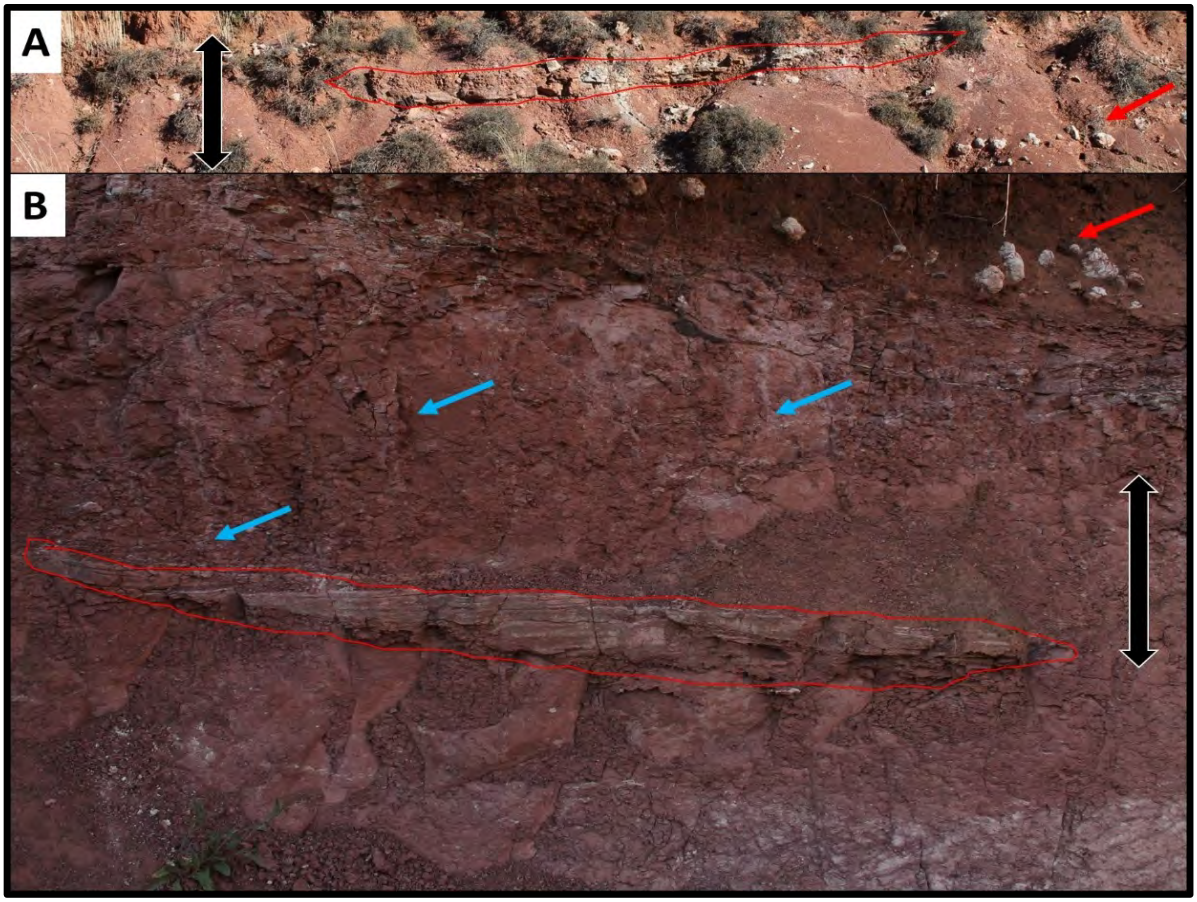


**Figure 3.9: A.** Fine-grained light brown sandstone lens (outlined in red) in a lower palaeosol exposed in a road cutting on the R26 next to Rhodes Farm (GPS coordinate: S29° 00' 39.01" E27° 31' 04.88"). The sandstone lens is interpreted as deposit of a crevasse splay (internally heterogeneous: highly variable grain-size and lamination, as a result of their formation by shallow flowing water conditions, extremely fast rates of sedimentation and multiple flood events (Galloway and Hobday, 1983)). Note the very coarse (20 to <76 mm) to extremely coarse (>76 mm) size *in situ* carbonate nodules marked with a red arrow on the right. Scale: double black arrow 2 m long. **B**. Fine-grained sandstone lens (<30 cm thick and outlined in red) with grey discolouration enclaved by a lower palaeosol on Sunnyside Farm (GPS coordinate: S28° 31' 35.78" E28° 30' 54.64"). Note the very coarse (20 to <76 mm) to extremely coarse (>76 mm) size in situ carbonate nodules (marked with a red arrow) on the right, light grey mottles 20-30 cm long resembling downward penetrating roots in reddish brown mudstone (marked with blue arrows). Scale: double black arrow 1 m long.

### 3.4.3 Colour mottling

Colour mottles are defined as irregularly shaped diffuse aggregations or patches of amorphous or very finely crystalline minerals, and generally occur as irregular patches of discolouration (Retallack, 1990). Mottles may represent the elementary stages of nodule

development and/or concretion differentiation (Retallack, 1990), or may form as a result of faunal and floral bioturbation and the associated organic decomposition (Blodgette, 1988).

Colour mottling in the UEF is mostly observed in the lower palaeosol horizons (>60m below the Elliot to Clarens Formation contact) and become less distinct in palaeosols closer to the overlying Clarens Formation. The lower palaeosols contain in abundance distinct, coarse (>15 mm in the greatest dimension) light greenish grey mottles which occupy 2-20 % of the exposed surfaces (Figure 3.2A). In some palaeosols, mottles appear to take the form of roots penetrating downwards and occasionally bifurcating (Figure 3.9). The abundance of mottles often increases from common to many (occupying >20 % of the exposed surface) in sections of the palaeosols where carbonate nodules are numerous.

### 3.4.4 Desiccation cracks

Desiccation or shrinkage cracks are classified as shrink-swell features which commonly form in sediments with >30% clay content (Gustavson, 1991). Well-developed desiccation cracks indicate multiple episodes of swelling under wet conditions (flooding or rainfall) followed by shrinkage under warm and drier conditions (Pettijohn, 1975). The cracks develop a polygonal surface pattern and vary in width. The cracks may be infilled with carbonate, clay, silt or sand from the overlying sand or silt layer that gets deposited in the first flood after a drying period (Pettijohn, 1975; Gustavson, 1991; Driese and Foreman, 1992).

The carbonate nodules of the UEF are associated with desiccation cracks infilled with micrite and/or fine-grained sandstone (Figure 3.10). The desiccation cracks (Figure 3.10) can be more than 2 cm wide on the upper surfaces of the palaeosols and taper downwards to occasionally penetrate the underlying palaeosol layers if present. The sandstone fill in the wider cracks (3-4 cm wide) is characterized by discontinuous lamination running semi-parallel to the walls of the cracks.

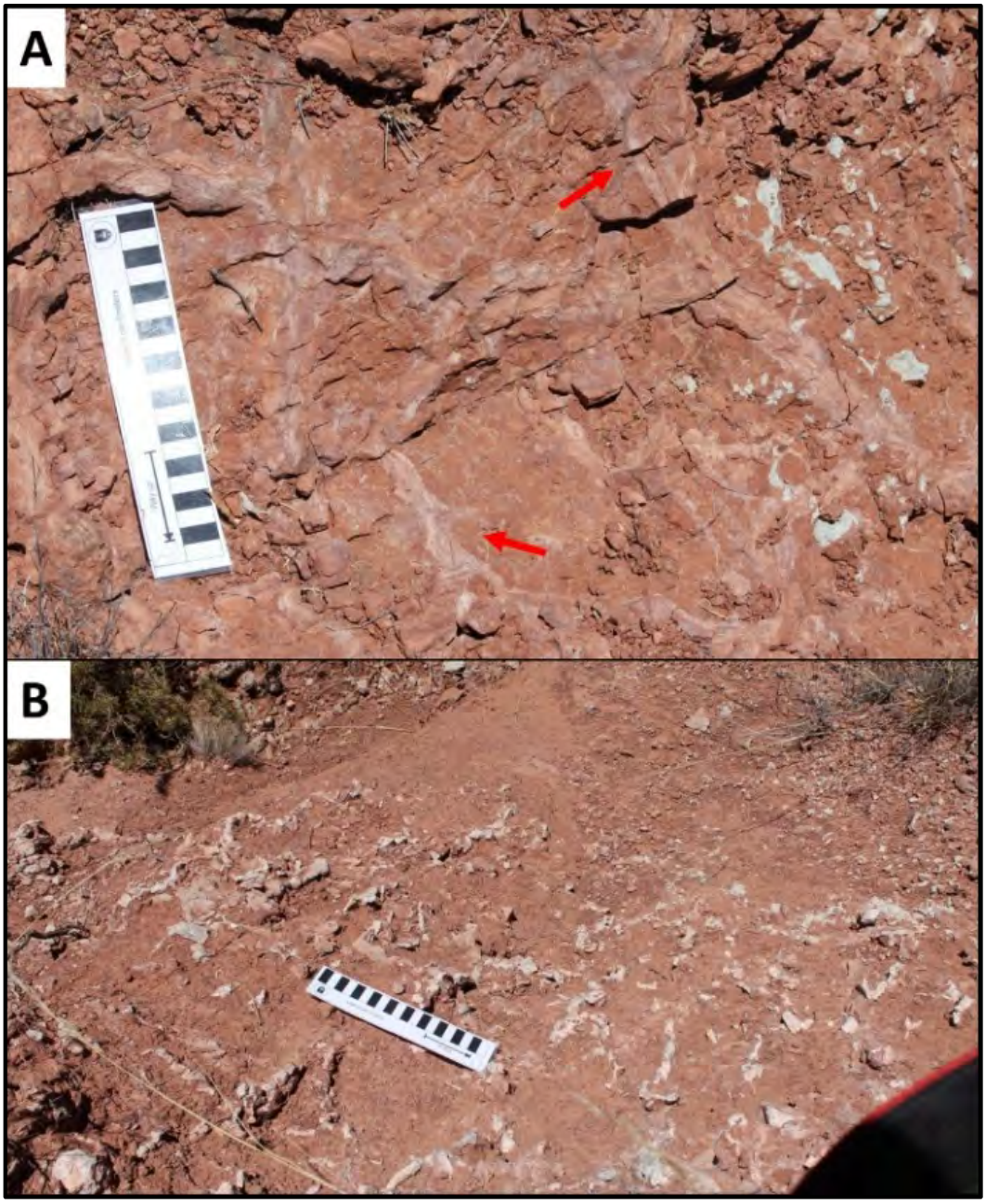


**Figure 3.10: A.** Sandstone filled desiccation cracks (marked with red arrows) in an upper palaeosol on Nova Barletta Farm (GPS coordinate: S28° 59' 16.99" E27° 22' 08.99"). Scale bar 20 cm long. **B**. Carbonate filled desiccation cracks in the upper palaeosols on Nova Barletta Farm (GPS coordinate: S28° 59' 16.29" E27° 22' 10.79"E). Scale bar 20 cm long.

### 3.5 Carbonate nodules in the field

Carbonate nodules were primarily hosted in mudstone bodies with various shades and hues of red in the UEF (Figures 3.11 and 3.12). In addition to carbonate nodules, these mudstone bodies also contained pedogenic features such as: calcretized root traces, falling water level marks, colour mottling, and desiccation cracks (Figure 3.4). According to Kitching and Raath

(1984), Smith and Kitching (1997), and Bordy et al. (2004b), the co-occurrence of these sedimentary features within the mudstone bodies suggests that they are components of palaeosols which are lithified, ancient soils and/or soil horizons (Smith, 1990). Non-generic terms used to identify palaeosols include red beds, variegated beds, cornstone or ganister (Walker, 1967; Turner, 1980; Tandon and Narayan, 1981; Retallack, 1990).

At each of the sample sites, several (up to three) successive palaeosol horizons, ranging in thickness from less than 50 cm to greater than 1.5 m, were identified. The sizes and abundances of carbonate nodules at each site were measured and the stratigraphic position of each palaeosol were recorded as the distance relative to the contact between the UEF and Clarens Formations (Table 3.1 and Figures 3.13 to 3.14). This surface is therefore used as a physical, but not a temporal marker surface (datum) as it is assumed that this contact is most likely diachronous. Although, it was attempted, correlation of the palaeosols even between neighbouring sample sites was impossible to establish.

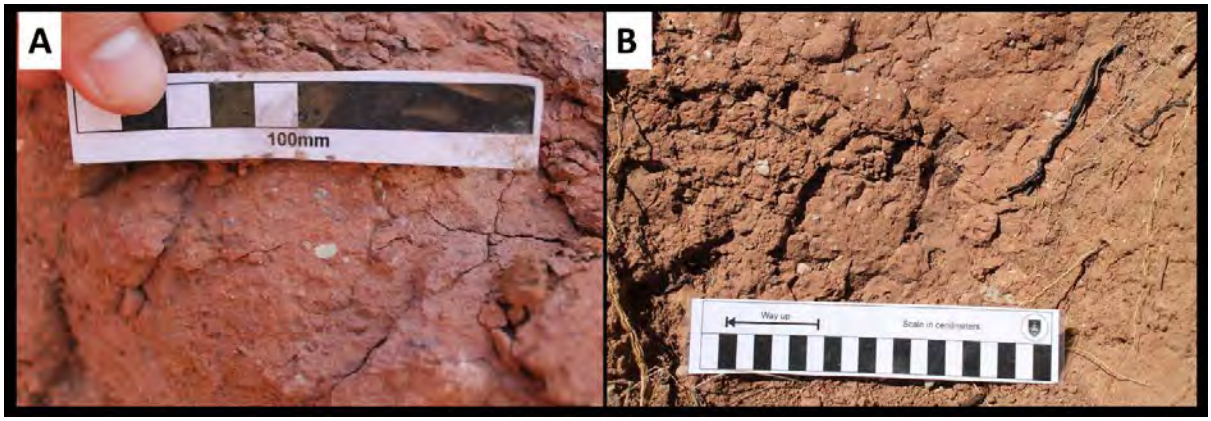


**Figure 3.11:** Massive muddy siltstone with small, scattered carbonate nodules in upper palaeosols. **A**. Deep red mudrock matrix on the farm Paradys Farm (GPS coordinate: S29° 06' 27.43" E27° 20' 46.99"). Scale bar 10 cm long **B**. Brownish red mudrock matrix on the farm Saaihook Farm (GPS coordinate: S28° 36' 50.71" E28° 15' 46.61"). Scale bar 20 cm long.

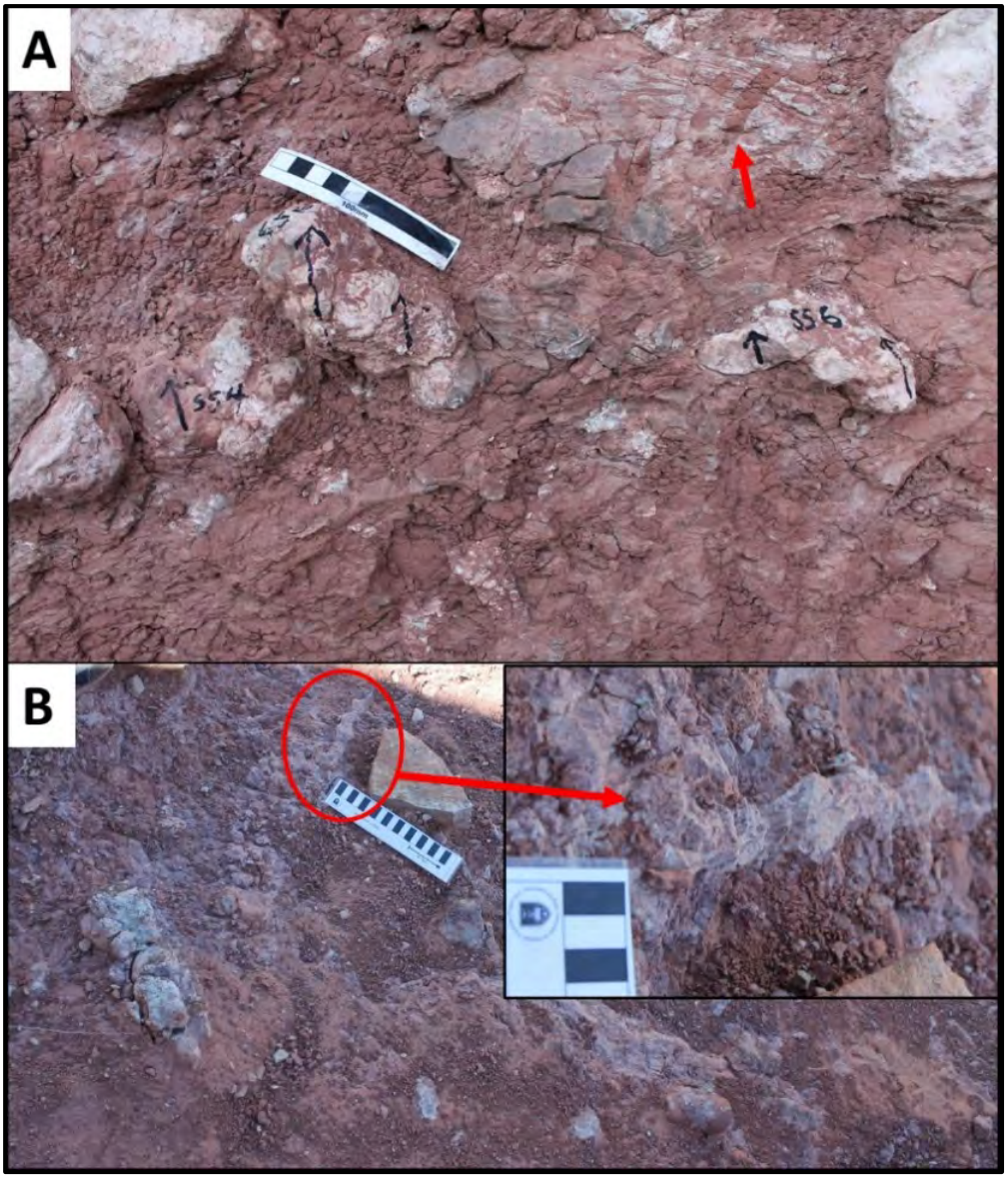


**Figure 3.12: A.** Extremely coarse (>76 mm) oblate and irregularly shaped carbonate nodules and well-developed burrows (marked with red arrow) in the lower palaeosol on the Farm Sunnyside (GPS coordinate: S28° 31' 35.88" E28° 30' 53.32"). Scale bar 10 cm long. **B**. Desiccation cracks filled with micrite and fine-grained sandstone in the lower palaeosols on Saaihoek (GPS coordinate: S28° 36' 51.32" E28° 15' 47.17"). Scale bar 20 cm long.

### 3.6 Macroscopic carbonate nodule description

Carbonate nodules are most commonly found in massive and compact mudstone bodies with red and/or green mottling, in an orientation mainly horizontal to bedding. Table 3.1 below gives characteristics of the nodule horizons observed at each site within the study area. The percent occurrence and size categories descriptors used for macroscopic carbonate nodule assessments are given in Chapter 2. Based on their relative distance from the contact of the

UEF and Clarens Formations, the carbonate nodules have been assigned to the following three distance ranges referred here as 'horizon categories': a) 'lower' when the nodules are >59 m, b) 'intermediate' when the nodules are 30m to 59 m, and 'upper' when the nodules are <30 m below the contact, respectively (Table 3.1). The distribution of the sizes and the abundance of the nodules within the horizon categories and across the study area are shown in Figures 3.13 and 3.14, respectively.

**Table 3.1:** Characteristics of nodule horizons present at sites within study area in the UEF. NP – National Park.

| Farm | Horizon category | Distance (in m) below the contact of the UEF and Clarens Fms. | Quantification | Size Categories |
|---|---|---|---|---|
| Bramleyshoek | Upper | 30 | common | very to extremely coarse |
| | Intermediate | 40 | common | very to extremely coarse |
| Boshoek | Lower | 70 | few | very coarse |
| Golden Gate NP | Intermediate (2) | 35 | many | very to extremely coarse |
| | Intermediate (1) | 50 | common | medium to coarse |
| Sunnyside | Lower | 75 | common | very to extremely coarse |
| St Fort | Upper | 25 | few | very coarse |
| Saaihoek | Upper (2) | 15 | common | medium to coarse |
| | Upper (1) | 20 | many | very to extremely coarse |
| Nova Barletta | Intermediate | 50 | common | coarse |
| | Lower | 65 | many | very to extremely coarse |
| Rhodes | Intermediate | 40 | many | very to extremely coarse |
| Twee Zusters | Upper | 25 | common | coarse |
| | Intermediate | 35 | common | very coarse |
| Oldenburg | Intermediate | 35 | many | very coarse |
| Paradys | Intermediate | 55 | common | very to extremely coarse |
| | Lower | 60 | many | coarse |
| Orange Spring | Lower | 60 | few | very coarse |
| Damplaats | Lower (2) | 70 | common | very coarse |
| | Lower (1) | 90 | common | very to extremely coarse |

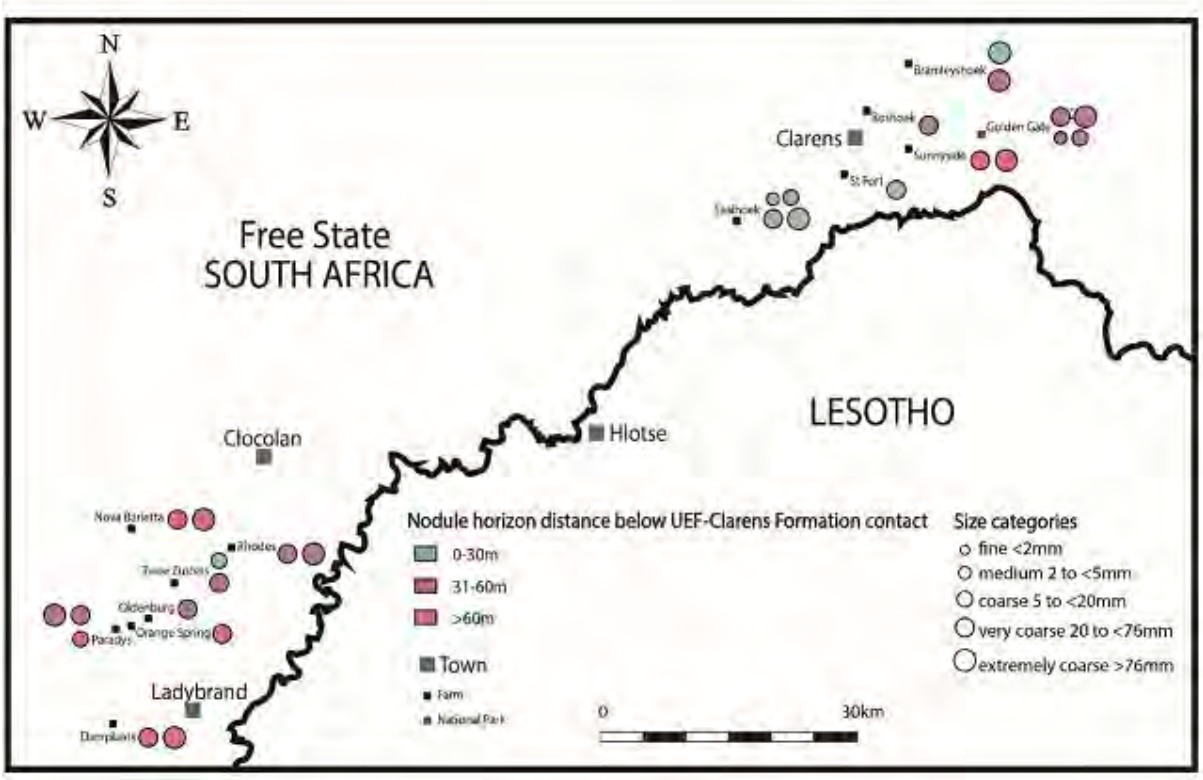


**Figure 3.13**: Distribution of carbonate nodule sizes within horizon categories and across the study area.

The nodules in the lower horizon (>60 m below the contact of the UEF and Clarens Formation) are predominantly very coarse to extremely coarse in size. The nodules in the middle horizon (i.e., 31 to 60 m below the contact of the UEF and Clarens Formation) are also mostly very coarse to extremely coarse, with the only exception observed at Golden Gate National Park where medium to coarse sized nodules were observed in this vertical distance range. The upper horizon (< 30 m below the contact of the UEF and Clarens Formation) generally host smaller sized nodules than the other two lower horizons as it is dominated by coarse sized rather than very coarse to extremely coarse sized nodules. Overall, nodules in the study area mostly fall into the coarse to extremely coarse size category, and smaller nodules are observed more frequently in the upper 60 m of the UEF.

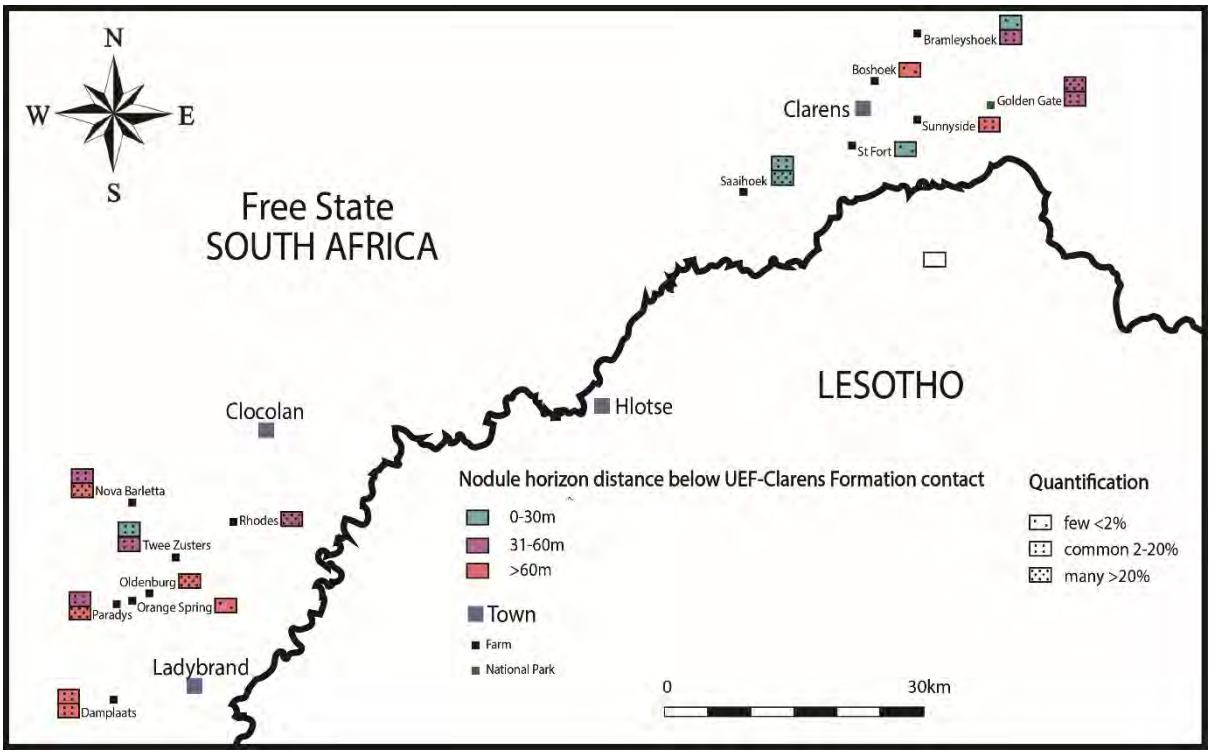


**Figure 3.14:** Distribution of carbonate nodule abundances within horizon categories and across the study area. Note that at Damplaats nodules were observed at 70 m and at 90 m below the contact between the Elliot and Clarens Formations (both fall into the 'lower' category); similarly, nodules were noted at 50 m and at 35 m at Golden Gate (within the intermediate horizon) as well as at 20 and at 15 m at Saaihoek (within the upper horizon).

Between Ladybrand and Clocolan, nodule abundances are high in the stratigraphic horizons that are more than 60 m below the contact of the UEF and Clarens Formation, with the exception of Orange Spring Farm where nodule abundances are low. In the Clarens region, where the lower horizons can be observed only at two sites of the five visited, the nodules are moderately abundant. The intermediate horizon, again only observed at two sites out of the five visited, shows moderate to high nodule abundances. In the upper horizon, where relatively speaking smaller nodules dominate (Figure 3.13), the nodule abundances are low, with the exception of Saaihoek Farm where nodules are common to abundant in the upper 20 m of the Elliot Formation. A more quantitative and systematic assessment of the nodule abundances across the region and within the preserved stratigraphy however is hard to undertake due to the widely spaced study sites.

### 3.7 External morphology of carbonate nodules

The most of the calcrete the Elliot Formation fall into the calcrete category of carbonate nodules or strictly speaking, glaebules. The carbonate nodules are discrete, very hard, spheroidal, irregularly shaped (Figure 3.15A) or semi cylindrical (Figure 3.15B) with a high concentration of carbonate minerals (calcite in the current case). They are usually much harder than the host rock in which they are found with sharply defined boundaries and mostly smooth surfaces (Figure 3.15C). In most outcrops, the more elongated nodules are parallel to sub-parallel to the overall bedding in the formations (Figure 3.15D). Locally the smaller nodules may be semi-perpendicular to the bedding (Figure 3.15E). Although most horizons contain sparsely scattered individual nodules, some twinned nodules can also be found. Where nodules become numerous or very large, reaching diameters of more than 20 cm, they merge and form coalesced horizons (Figure 3.15F) and/or a solid carbonate layer.

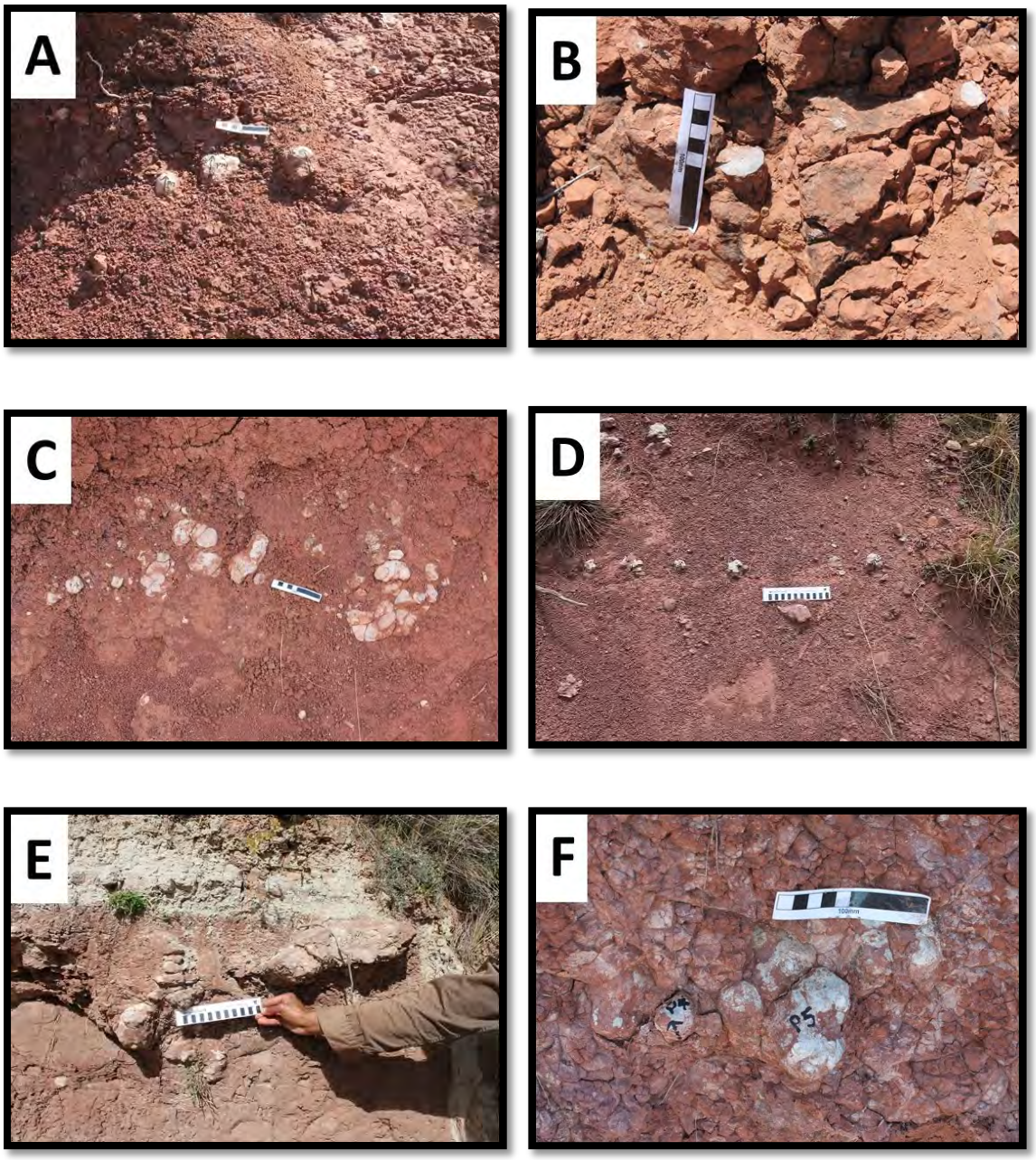


**Figure 3.15: A.** Discrete spheroidal and irregularly shaped carbonate nodules in massive reddish brown mudrock on Paradys Farm (GPS coordinates: S29° 06' 26.99" E27° 26' 06.43"). Scale bar 10 cm long. **B**. Semi-cylindrical or tubular carbonate nodule in light a light red massive mudrock on Twee Zusters Farm (GPS coordinates: S29° 03' 06.44" E27° 26' 06.43"). Scale car 10 cm long. **C**. Sharply defined boundaries and smooth surfaces of carbonate nodules in a massive red mudrock on the Farm Orange Spring (GPS coordinates: S29° 06' 20.83" E27° 22' 13.66"). **D**. Irregularly shaped carbonate nodules are in a horizontal orientation in a massive dark red mudrock on Bramleyshoek Farm (GPS coordinates: S28° 25' 33.63" E28° 30' 19.68"). Scale bar 20 cm long. **E**. Vertically stacked carbonate nodules in massive reddish brown mudrock on Boshoek Farm (GPS coordinates: S28° 29' 15.70" E28° 26' 52.03"). Scale bar 20 cm long. **F**. Coalesced carbonate nodules in a dark red massive mudrock on Paradys Farm (GPS coordinates: S29° 06' 27.12" E27° 20' 47.06"). Scale bar 10 cm long.

### 3.8 Internal fabric of carbonate nodules

Carbonate nodules are distinguished by observing their internal features, because from the exterior little differences, apart from size and shape, can be established. It is noteworthy to mention that in the strict sense the term ‘nodule’ should be used for those carbonate glaebule that are massive internally. However, to maintain consistency and simplicity across the thesis, all glaebules are referred to as nodules, except in this section. The glaebule types observed in the study area include: papules, septarian glaebule, mature and immature typic glaebules, pedodes, and nodules (the massive glaebules) (Figure 3.16).

Papules (Figure 3.16A) are glaebules composed of mostly clay with continuous and/or lamellar fabric. Separian type glaebules (Figure 3.16B) are relatively common throughout the study area and contain distinct cracks filled with well-developed calcite crystals in a radiating pattern or sometimes forming polygon shapes and lenses. Typic glaebules (Figure 3.16C and D) are generally softer than septarian glaebules and have an irregular array of internal cracks filled with a mixture of mud from the host rock and/or carbonate minerals. The cracking and filling of typic nodules appears to be cyclic where different compositions can be found in the different generations of cracks. Typic glaebules containing more carbonate, less cracks and appearing less differentiated are more mature (Figure 3.16D), while those composed of relatively less carbonate, more mud and more cracks with varying compositions are immature (Figure 3.16C). Pedodes (Figure 3.16E) are often referred to as the pedological equivalent of geodes because of the similar core and cortex regions they display internally. The core region, containing relatively more mud and sometimes well-developed sparry calcite, is less impregnated than the carbonate-rich cortex. As mentioned above, strictly speaking, glaebules referred to as nodules are those with no internal structure (Figure 3.16F).

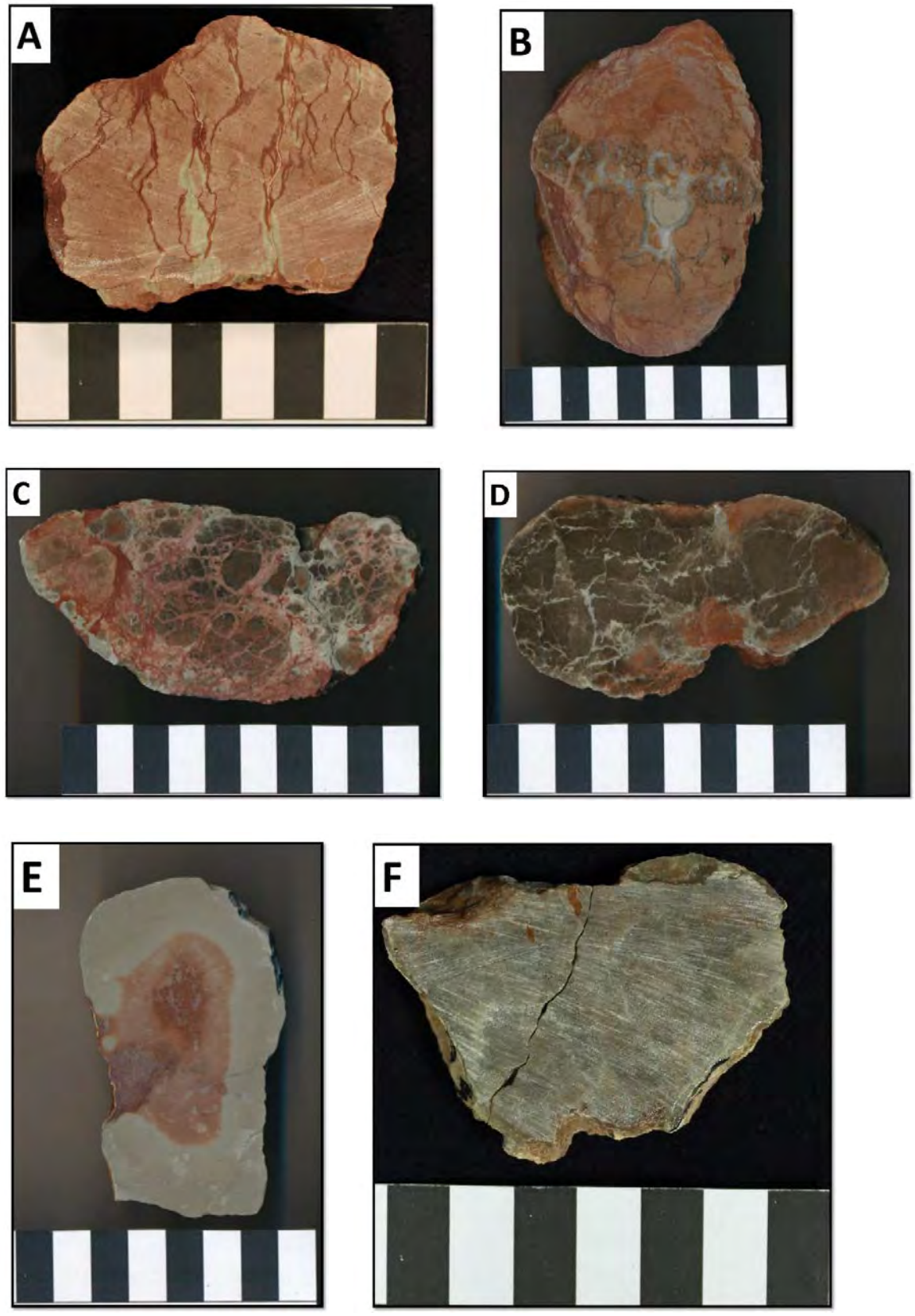


**Figure 3.16:** Glaebule types observed in the study area and their associated internal macroscopic features. **A**. Papule; **B**. Septarian glaebule; **C**. Immature typic glaebule; **D**. Mature typic glaebule; **E**. Pedode; **F**. Nodule which is a massive, structureless glaebule. Scale bar is in centimetres.

## 3.9 Micromorphology of the carbonate nodules in the Elliot Formation

In thin sections, the nodules found in the Elliot Formation show certain microscopic characteristics (see section 3.9.1 below) that are regularly found in all nodules as well as some unique features (e.g., septarian cracks, microcodium, micronodules, circumgranular cracks) that are only observed in some of the samples (see section 3.9.2 below).

### Common characteristics

#### Mineral composition

Minerals identified in the nodules of the Elliot Formation include calcite, quartz and feldspar, along with some iron staining and micritic carbonate cement. No rock fragments were observed. In terms of proportions, calcite is the most abundant (80-95%) followed by quartz (10-15%) (Figure 3.17: A and B) and then feldspar (>5%) (Figure 3.17: E and F). Calcite grains show good cleavage and lamellar twining, while the feldspar grains may exhibit some multiple twining (Figure 3.17: F).

#### Colour

In plane polarized light (ppl) sparite, quartz and feldspar are colourless (Figure 3.17: G). Micrite and microsparite are greyish brown in colour (Figure 3.17: C and E) and areas containing some iron staining are reddish brown (Figure 3.17: I) or opaque.

#### Grain size

Calcite grains show the widest range in terms of grain size varying from micrite (< 4 μm), through microsparite (4-15 μm), to sparry calcite (>15 μm). Quartz and feldspar grains are clay to coarse silt in size (< 3.9 μm to < 62.5 μm).

#### Grain morphology

Calcite grains are subhedral to euhedral, whereas the quartz and feldspar grains are xenomorphic (Figure 3.17: A and B). All mineral grains present are angular to subangular, with low sphericity.

**Grain fabric**

Calcite grains show an annealed texture with grain boundaries intersecting at 120° (Figure 3.17: A and G). Quartz and feldspar grains are generally not in contact (i.e. floating grains) and are normally surrounded by micritic cement with some iron staining (Figure 3.17: E and F).

**Variation in characteristics**

In thin section, the following variations in the composition and texture can be observed. Some of the features (e.g., septarian cracks, microcodium, micronodules, and circumgranular cracks) can be found in isolation or in different combinations together within one sample.

**Colour**

Generally, those thin sections that are reddish brown when examined with the naked eye contain higher proportions of quartz, feldspar and iron staining, while those that are more transparent and grey contain more calcite. The coarser the calcite grains present, the more transparent the thin section will appear with the naked eye.

**Mineral composition**

Most samples show a higher proportion of calcite (>95%) and a lower proportion of quartz and feldspar (>5%) (Figure 3.17: A and B). While other samples show a relatively lower proportion of calcite (80-85%) and a relatively higher proportion of quartz and feldspar (15-20%) (Figure 3.17: I and J). It is also important to note that the proportion of quartz is always more than that of the feldspar, and this relative distribution is similar in the nodule-free host rocks of the formation. An increase in calcite is also marked by a decrease in iron staining which is normally associated with the quartz and feldspar (Figure 3.17: G and H).

**Texture**

As calcite grains become coarser grained, the 120° grain boundary intersections become more apparent and the nodules become more homogeneous in terms of mineral composition and overall texture (Figure 3.17: A and G). Some features are observed in some samples and not in others. These include:

**Septarian cracks**

These are internal irregular cracks that are sometimes bifurcating and range in thickness from less than 1 mm to greater than 4 mm. Septarian cracks cut across all other fabrics present in the nodules indicating that these were the last features to develop within the nodules. These cracks are filled with fine to coarse (8-63μm) sparite grains (Figure 3.17: K and L).

**Microcodium Glück**

Microcodium Glück are 'flower-like' features characterised by elongated petal-like grains radiating from a central coarser grain in a circular structure (Figure 3.17: M and N). The central grain is usually coarser grained quartz with finer more elongated calcite grains radiating outwards. Microcodium Glück features vary in size from less than 100 μm to greater than 400 μm in the longest dimension.

**Micronodules**

Micronodules are irregular in shape and composed mostly of dense micrite and some angular quartz fragments floating within the micrite. They are often cracked internally and the cracks filled with coarser grained microsparite (Figure 3.17: O and P). The grain size contrast between the finer grained micrite, which the micronodule is composed of, and relatively coarser gained enclaving material makes these micronodules easy to identify.

**Circumgranular cracking**

Circumgranular cracks are partly circular cracks observed around the circumference of micronodules. They are usually more than 100 μm wide and infilled with microsparite, similar in grain size to the crack fillings within the micronodules (Figure 3.17: Q and R).

| | |
|---|---|
| 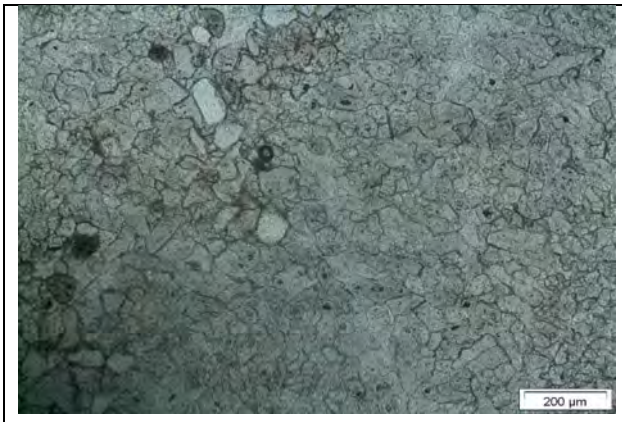 | 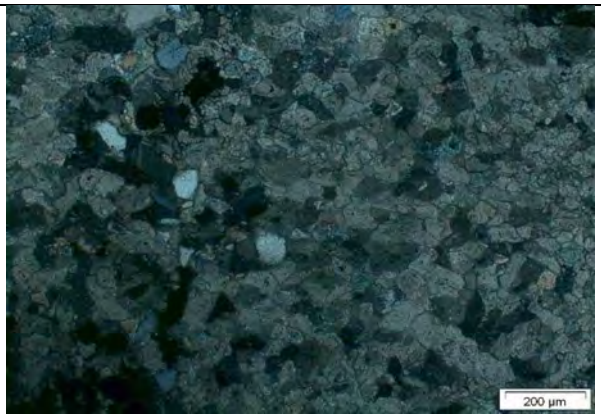 |
| A. Sample NB1 in plane polarized light (ppl) showing grains of calcite and quartz (Nova Barletta Farm). | B. Sample NB1 in cross polarized light (xpl). Notice the distinction between the calcite with higher interference colours and the quartz with low interference colours. |
| 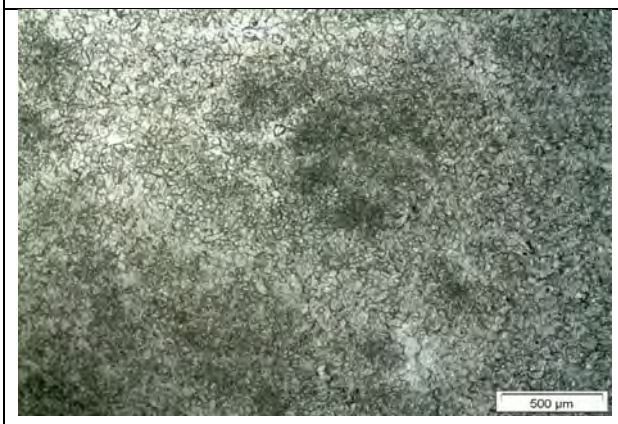 | 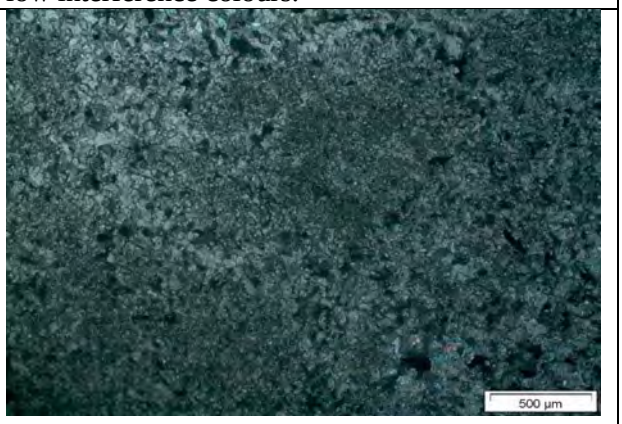 |
| C. Sample NB1 in ppl showing the difference between the finer grained grey micrite and relatively coarser grained microsparite. | D. Sample NB1 in xpl. |
| 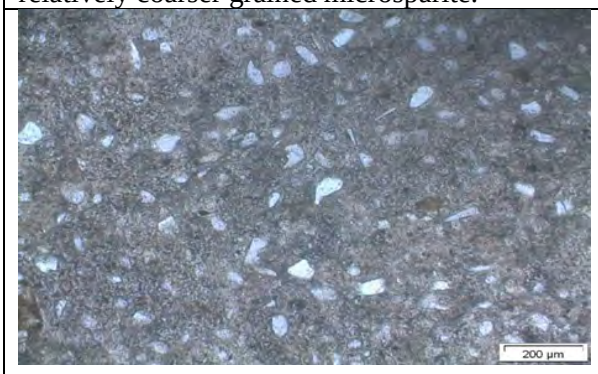 | 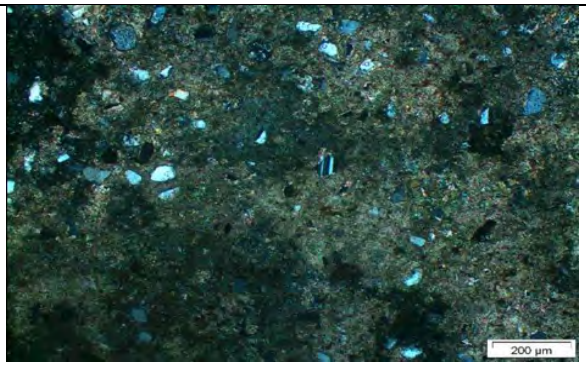 |
| E. Sample GG4 in ppl showing the brownish grey micrite and colourless quartz and feldspar grains (Golden Gate Highlands National Park). | F. Sample GG4 in xpl showing the distinction between the silicate (quartz and feldspar) and carbonate (micrite) minerals. Notice the multiple twinning of the feldspar grain in the central area of the field of view. |

**Figure 3.17**: Microscopic features of carbonate nodules in the Elliot Formation.

| | |
|---|---|
| 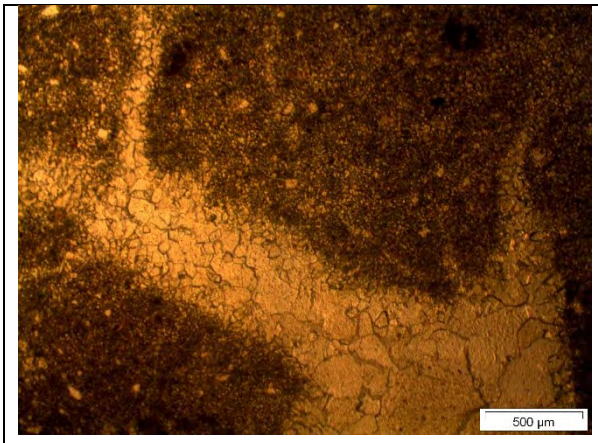 | 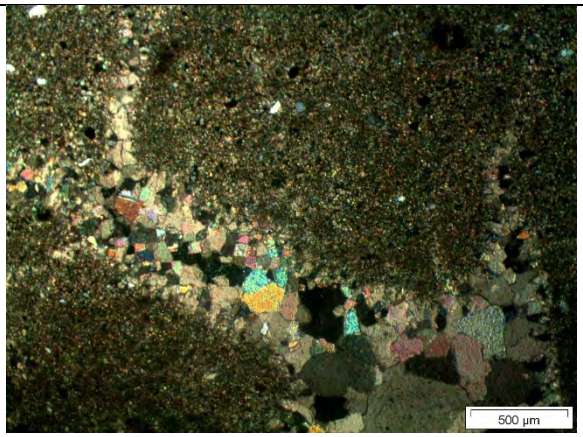 |
| G. Sample ZH2 in ppl illustrating the 120° grain intersections i.e. annealed grains in a bifurcating septarian crack (Saaihoek Farm). | H. Sample ZH2 in xpl. |
| 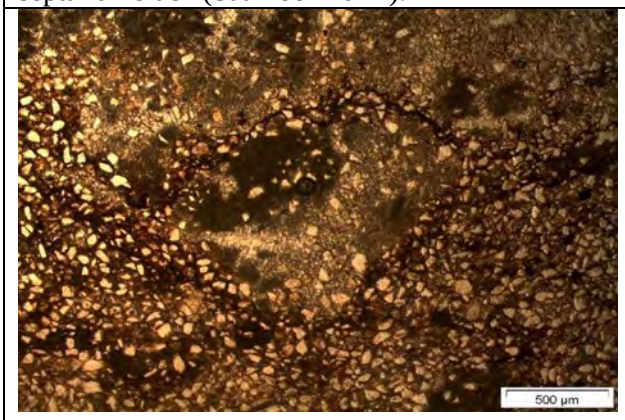 | 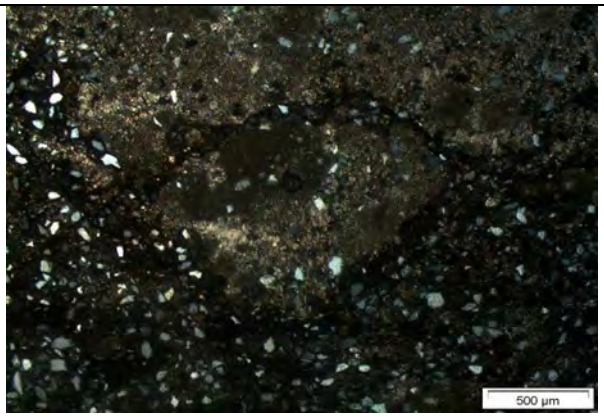 |
| I. Sample ZH2 in ppl showing abundant quartz and feldspar grains associated with red-brown iron staining and micrite (Saaihoek Farm). | J. Sample ZH2 in xpl. Notice the iron staining becomes opaque in xpl. |
|  | 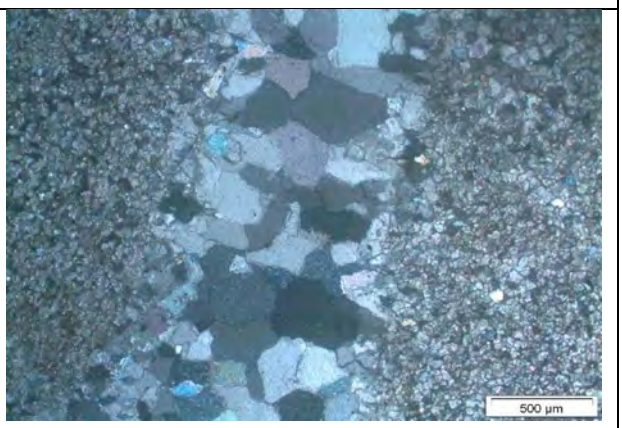 |
| K. Sample SS1 in ppl showing a septarian crack filled by coarser grained sparite cutting across a finer grained micrite and quartz matrix (Sunnyside Farm). | L. Sample SS1 in xpl. |

**Figure 3.17 (cont.)**: Microscopic features of carbonate nodules in the Elliot Formation.

| | |
|---|---|
|  | 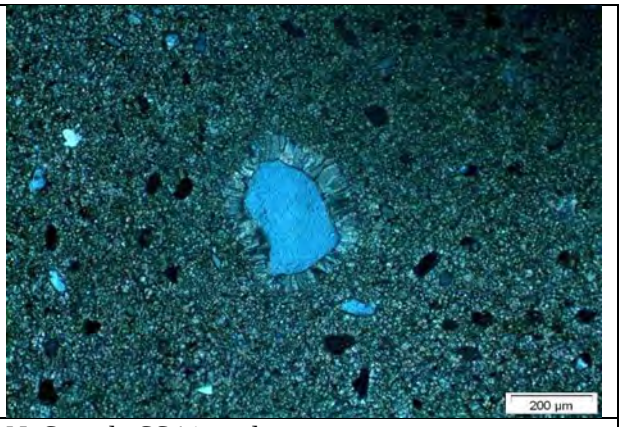 |
| M. Sample SS4 in ppl showing Microcodium Glück structure with a central quartz grain and finer elongated calcite grains radiating from it in a circular arrangement (Sunnyside Farm). | N. Sample SS4 in xpl. |
|  | 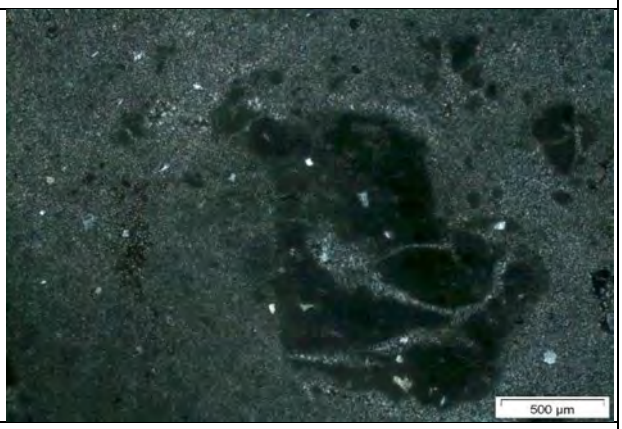 |
| O. Sample T3 in ppl showing a micronodule composed of dark brown finer grained micrite being cross cut by thin calcite veins containing relatively coarser grained calcite (Twee Zusters Farm). | P. Sample T3 in xpl. |
| 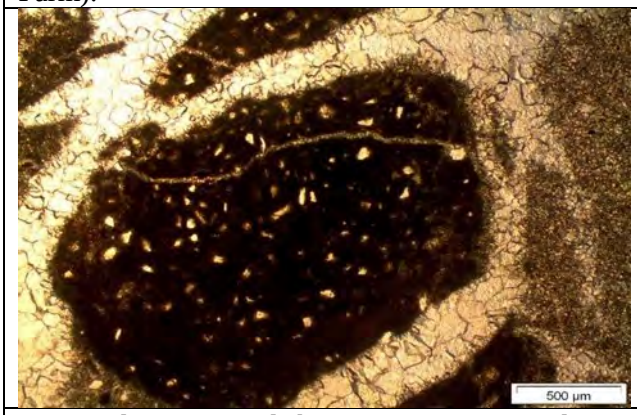 | 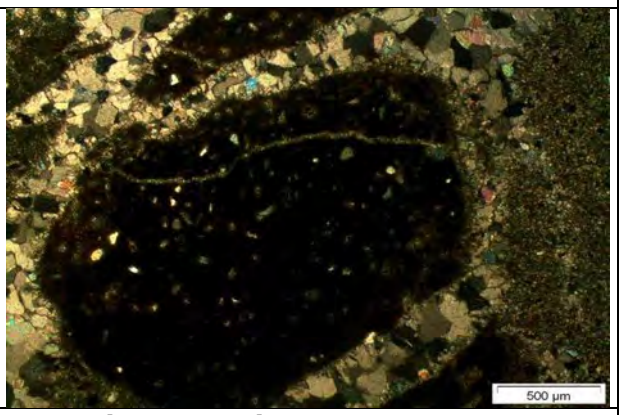 |
| Q. Sample ZH2 in ppl showing a circumgranular crack, filled by sparite, around a micrite micronodule containing some quartz grains (Zaaihoek Farm). | R. Sample ZH2 in xpl. |

**Figure 3.17 (cont.)**: Microscopic features of carbonate nodules in the Elliot Formation.

The microscopic features observed, including internal cracks such as septarian and circumgranular cracks, micro nodules and microcodium glück (corona grain coating), are similar to the so-called alpha-type microscopic features which are interpreted as products of predominantly physicochemical processes (see section 1.6.6 Microscopic Classification Wright, 1990; Zhou and Chafetz, 2009; Alonso-Zarza and Wright, 2010). Based on this, and in the absence of features that could be interpreted as beta-types microscopic features, it is not unreasonable to conclude that original pedogenic nodules in the UEF were diagenetically overprinted during burial diagenesis. However, neither the macro- nor the microscopic analyses could confirm this interpretation with confidence.

### 3.10 Powder X-ray diffraction

The powder samples were initially analysed as bulk rock samples. The bulk rock samples confirmed the presence calcite, quartz and feldspar as observed in the petrographic study (Appendices). However, the high calcite content present made it impossible to identify the clay mineral peaks on the diffractograms.

The clay minerals positively identified using the X-ray diffractometer on the separated clay rich samples are: illite, montmorillonite, muscovite, analcime and clay sized quartz (Figure 3.18). The majority of the samples analysed contained illite and muscovite, while montmorillonite and analcime were less common (Appendices).

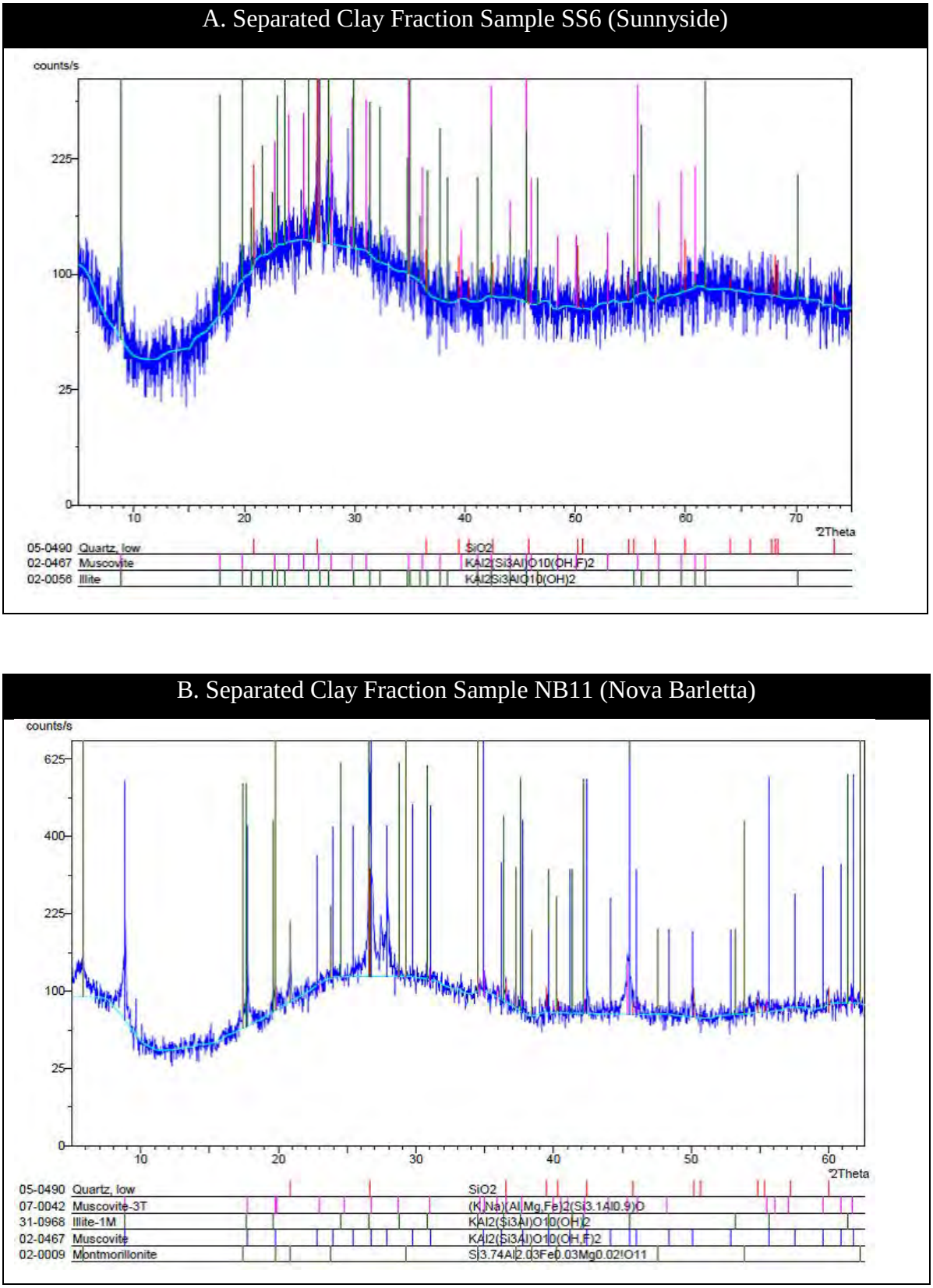


**Figure 3.18:** Representative diffractograms for the separated clay samples SS6 and NB11 collected from the farms Sunnyside (A) and Nova Barletta (B) respectively.

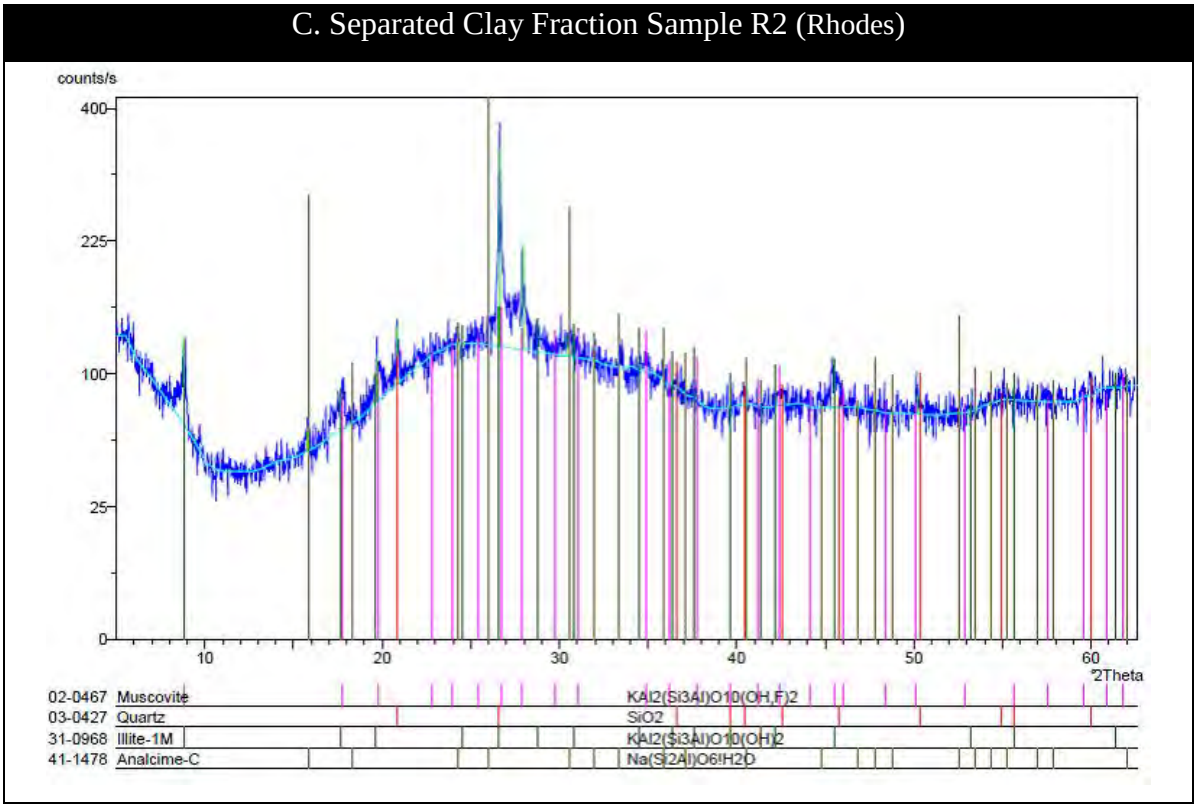


**Figure 3.18 (continued):** Representative diffractogram for the separated clay sample R2 collected from the farm Rhodes (C).

The clay mineral diffractograms were compared with X-ray results of Sciscio (2015) who analysed mudstone samples from the UEF at Likhole Mountain, Mafeteng, Lesotho. Sciscio (2015), who studied the mudstone samples with the same machine as in this current study, ran clay fraction samples and positively identified the following minerals: illite, quartz, kaolinite-montmorillonite, tosudite (chlorite-montmorillonite group), rectorite (illite-montmorillonite group), goethite and hematite (Figure 3.19). All in all, illite, montmorillonite and quartz were identified in abundance the UEF mudstone bodies in both this study and that of Sciscio (2015). The additional minerals identified by Sciscio (2015) may be as a result of the mudrocks analysed having been exposed to later diagenetic alteration as compared to the clay analysed in this study that was extracted from the interior of the carbonate nodules. The effort in this study to separate the clay minerals from the carbonate nodules themselves was made, because it was assumed that the clay within the nodules is a more truthful representation of the clay compositions present in the sediment prior to diagenetic alterations which likely affected the clays outside the entombing environment of the carbonate nodules.

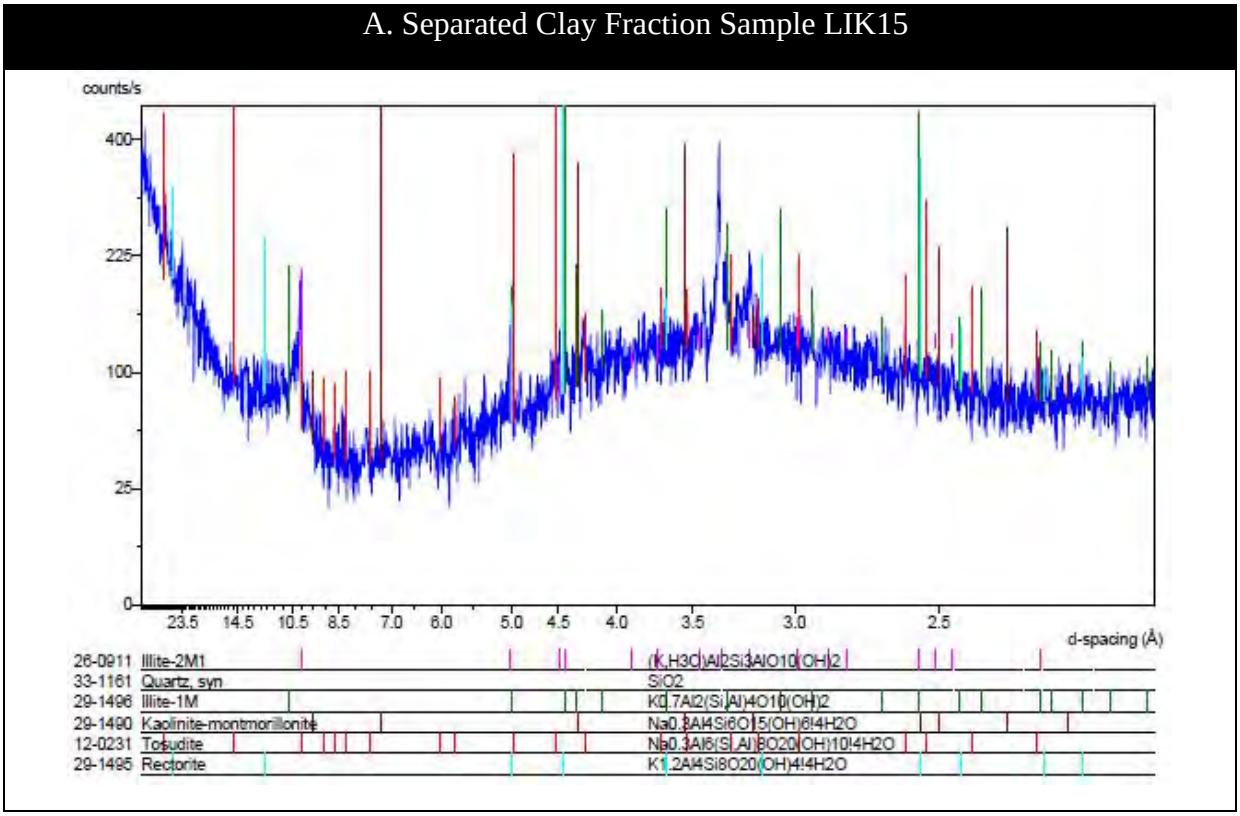


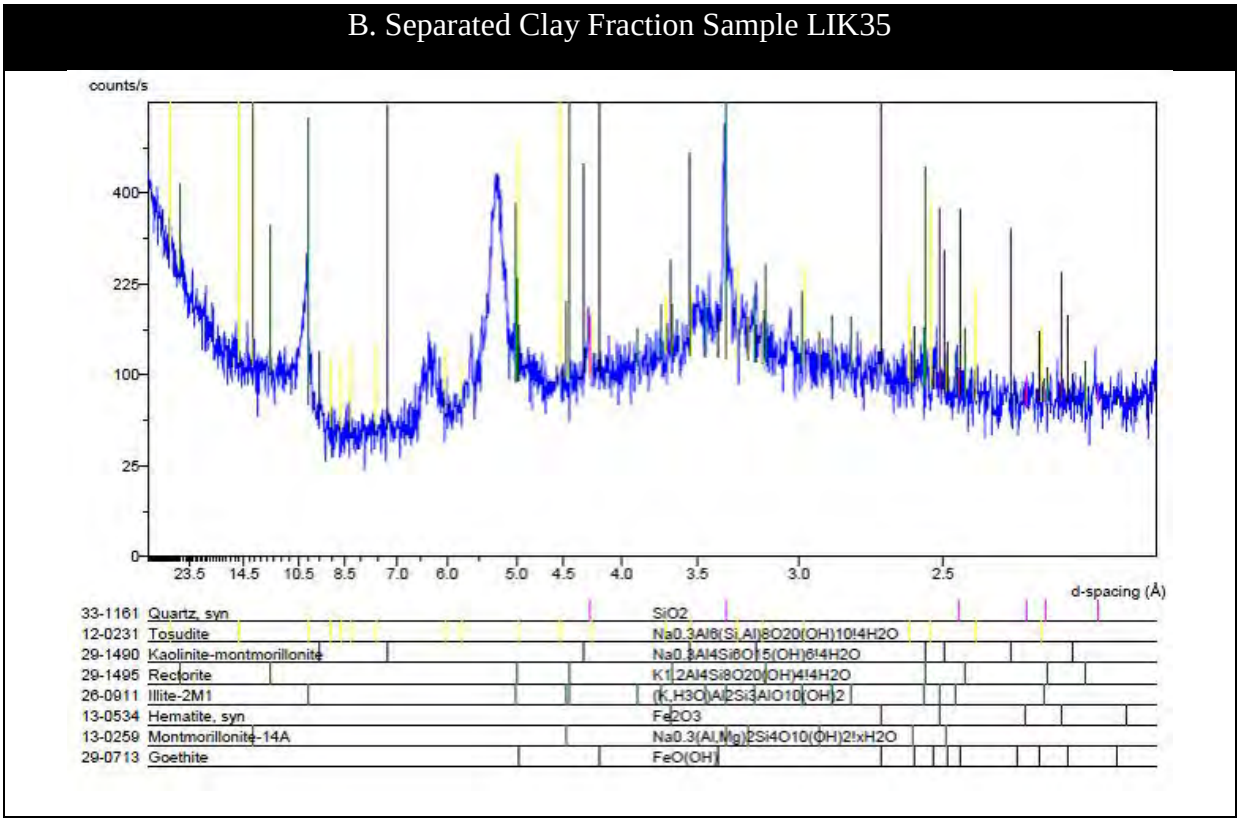


**Figure 3.19:** Diffractometers for clay samples LIK15 and LIK35 separated from mudstones in the UEF from Likhole Mountain, Mafeteng, Lesotho (taken from Sciscio, 2015).

**The origin of clay minerals**

Strictly speaking, clay minerals are those grains that measure <2 μm equivalent spherical diameter (Wilson, 1999; Sheldon and Tabor, 2009). However, the term 'clay' is also used to refer to finely crystalline sediments forming as a result of pedogenic alteration and is often applied to phyllosilicates, oxides and oxyhydroxides (Sheldon and Tabor, 2009). In several reviews, clay minerals from both continental and marine sediments have been correlated with climatic conditions during sedimentation, because factors such as temperature and availability of water strongly impact on the amount and intensity of weathering and thus clay formation (Singer, 1984; Sheldon and Tabor, 2009; Chaudhri and Singh, 2012). Sediments with high proportions of chlorite, illite, palygorskite and quartz have been interpreted as corresponding to relatively dry periods (Singer, 1984). Relatively more stable clays such as kaolinite have been interpreted as forming under humid conditions with more intensive weathering and leaching (Singer, 1984). Furthermore, the presence of smectite is considered to imply climatic conditions with contrasting wet-dry seasons, but with a more dominant dry season (Singer, 1984).

It has been however shown (e.g., Wilson, 1999) that clays only provide indirect information on the syndepositional palaeoclimatic conditions, because of the complexities of clay genesis that can result from any combination of the following processes: a) detrital inheritance, b) transformation and c) neoformation. Detrital inheritance refers to those clay minerals that are derived from pre-existing rocks and soils (Wilson, 1999). For example, illite could be derived from the weathering of feldspar- and mica-rich crystalline rocks, whereas chlorite may be the weathering product of intermediate and basic crystalline and low grade metamorphic rocks. Kaolinite can be derived from the weathering of granitic and basic rocks rich in potassium feldspars and micas, but the subsequent leaching of Si and Al is also required in this case (Chaudhri and Singh, 2012). Transformation refers to the development of a new clay mineral as a result changes in the interlayer region of the silicate structure. For example, illite transforms to vermiculite and then to smectite through the process of depletion and exchange of interlayer K and concomitant decrease of layer charges (Wilson, 1999). Neoformation is the formation of new clay minerals as a result of the crystallization of gels or solutions under appropriate physicochemical conditions during diagenesis (Wilson, 1999).

# Chapter 4: Discussion

In the UEF, rhizoliths, calcretized root moulds and fibrous roots as well as desiccation cracks, burrows, colour mottling, etc. are sedimentary features found in the immediate vicinity of the carbonate nodules. This collective evidence suggests that pedogenic processes were active during the history of the Elliot Formation. Furthermore, the presence of rhizoliths, calcretized roots and burrows suggests a period of low sediment supply and the development of soils inhabited by soil biota (plants, animals) which could modify the sediment surface via their complex biogeochemical activities (Bown and Kraus, 1981; Retallack, 1990). Desiccation cracks and slickensides indicate cyclic periods of wetting and drying along with short periods of sedimentation cessation under seasonal, semi-arid to dry sub-humid climatic conditions (Gustavson, 1991; Driese and Foreman, 1992). Desiccation cracks form in subaerially exposed sediments with more than 30% clay content (Gustavson, 1991). During wet periods clay minerals swell due to the absorption of water and during dry periods, moisture is lost through evaporation resulting in shrinkage and usually cracking of the sediment (Gustavson, 1991; Leeder, 1982). All in all,–the sedimentary facies analysis conducted in this study, especially the sedimentary features observed in the host rocks of the carbonate nodules in the UEF are consistent with those made by previous workers such as Kitching and Raath (1984); Groenewald (1986); Smith and Kitching (1997); Bordy et al. (2004a, b).

While the origin of carbonate nodules in the UEF is without much doubt pedogenic, not only due to the above listed evidence, but also because reworked carbonate nodule conglomerates are common in the UEF, assessing whether the nodules were diagenetically overprinted remains difficult. Calcretes found in the UEF are predominantly carbonate nodules (Figures 3.11, 3.15, and 3.16) which are commonly interpreted as components of soils in semi-arid to arid climates (Blodgett, 1988). Based on macroscopic morphological features, carbonate nodules can be nodules, concretions, septarian, pedotubules and nodular haloes (Brewer, 1964; Netterberg 1980; 1983; Blodgett, 1988). The most common nodule types are nodules and concretions, which are identified by observing their internal structures (Retallack, 1990). Nodules are internally massive which may reflect formation by continuous growth and compared to concretions displaying internal concentric layering, formed around a central point, plane or line, which may reflect discontinuous and probably seasonal growth (Brewer, 1964; Retallack, 1990). However, the macroscopic appearance of nodules alone, does not

provide conclusive evidence as to whether nodules are diagenetic or pedogenic in origin. Therefore their higher resolution examination was necessary in petrographic thin sections.

Microscopic features observed in carbonate nodules have been subdivided into two end-member types: alpha and beta-types (Wright, 1990; Zhou and Chafetz, 2009 Alonso-Zarza & Wright, 2010). Alpha-type appear to be products of predominantly physico-chemical processes, while beta-types are mainly biogenic in origin (ibid). The microscopic features observed in the carbonate nodules in the UEF include internal cracks such as septarian and circumgranular cracks, micro nodules, and microcodium glück. The most dominant features are internal cracks whose biogenic origin has been widely debated for over a century (Pratt, 2001). Raiswell (1971) suggested septarian cracks develop as a result of shrinkage of an early gel-phase which was subsequently modified to form the nodule. This proposal was rejected by Astin (1986) based on textural and chemical evidence and instead offered an alternative explanation based on the development of overpressure in the enclaving mudrock. Astin's hypothesis was expanded upon by Hounslow (1997: 1145) who showed that septarian cracks form "in a tensile regime as a result of locally increased pore pressure at the concretion site which is caused by permeability reduction initiated by cementation". In summary, despite the field sedimentological evidence of pedogenesis as a process being active in the UEF, the carbonate nodules themselves contain no biological features when viewed at the microscopic level (i.e., no univocal beta-type features were found). Therefore, the absence of beta-type microstructures in the nodules may be considered as a result of diagenetic overprinting of the previously formed pedogenic microstructures. It must be pointed out however, that this interpretation is based on negative evidence only, and therefore would require further testing.

The use of geochemical analysis of the clay mineral extracted from the nodules proved to be useful in gaining a more detailed understanding of the palaeo-environmental messages recorded by the carbonate nodules in the UEF. Clay minerals form primarily as products of weathering parent rocks and soil forming processes, therefore clay mineral assemblages are useful indicators of palaeoclimate (Singer, 1984; Chaudhri and Singh, 2012). In this study the identification of clay minerals extracted from carbonate nodules from the UEF using powder x-ray diffraction was applied to gain insight into the palaeoclimatic conditions that prevailed during the time of nodule formation. Because clay minerals have large surface areas, they are very reactive to the ions in the depositional setting. Therefore, it is necessary to consider which ions are in abundance and if there is a leaching mechanism that can remove them.

Leaching becomes more efficient under warm humid climatic conditions as compared arid climates characterised by incomplete leaching. The clay minerals identified in this study included: illite, montmorillonite, muscovite and analcime (Figure 3.18; Appendices).

Under arid climatic conditions acid rocks weather to illite due to their high abundance of K ions and basic rocks weather to form montmorillonite and to a lesser extent chlorite and vermiculite (Folk, 1980). The presence of muscovite in the spectra suggests deposition under arid climatic conditions and excludes the possibility of a warm humid climate (Folk, 1980). However, montmorillonite may form by neoformation in poorly drained soils under alkaline conditions, with high concentrations of $Mg^{2+}$ and $Ca^{2+}$ and where Al, Si and Fe tend to accumulate (Wilson, 1999). Moreover, illite may be formed by transformation from other clays during deep burial, slight metamorphism and marine diagenesis (Deer et al., 2004). Therefore, the palaeoclimatic interpretation of clay minerals may be limited by the fact that distinguishing authigenic and detrital clay minerals is problematic, particularly with regards to the smectite group (which includes montmorillonite) (Singer, 1984). The presence of illite, muscovite and clay-sized quartz in the UEF suggests formation probably as a result of detrital inheritance being derived from the weathering of feldspar and mica-rich crystalline rocks under relatively dry warm conditions. In the UEF the identification of montmorillonite suggests the possible transformation of illite to the smectite through the depletion and exchange of interlayer K and concomitant decrease of layer charge (Wilson, 1999). The use isotope geochemistry analytical techniques may help overcome these limitations although they go beyond the scope of this project.

Testing the validity of the explanation offered here with regards to the origin of the carbonate nodules is limited by the methods used in this study which are primarily based on physical observations made at the macroscopic and microscopic scale. In other carbonate nodule studies, stable isotopes of oxygen and carbon have been used to gain insight into palaeoclimatic and palaeohydrologic conditions at the time of formation (e.g., Ehleringer, 1989; Lohmann and Walker, 1989; Herbert and Compton, 2007; Gastaldo et al., 2014). More specifically, oxygen isotopes from carbonate and clay minerals have been used successfully to determine the composition of meteoric water which is in turn influenced by the mean annual temperature (Cerling, 1984; Cerling and Quade, 1993; Stern et al., 1997). With regard to carbon isotopes, very negative $\delta^{13}C$ values (i.e. >-10‰) could suggest some of the carbon was derived from the degradation of organic matter by microbial activity (Ehleringer, 1989)

or be indicative of water-logged conditions (Gastaldo et al., 2014). Whereas more positive values $\delta^{13}C$ (i.e. >+2‰) may suggest carbon derived from limestone bodies or abiotic marine calcites with typically higher values (Lohmann and Walker, 1989). The provenance of Ca in calcretes has been assessed using $^{87}Sr/^{86}Sr$ ratios as proxies for the sources of Ca because Sr and Ca share similar chemical properties, and therefore Sr shows strong affinity with Ca (Dart et al., 2007). The $^{87}Sr/^{86}Sr$ ratio expressed will reflect the source of carbonate, e.g. old continental rocks, volcanic rocks, marine carbonate, aeolian dust (Quade et. al., 1995). Carbonate provenance studies may give clues as to whether the calcretes in question formed under pedogenic or diagenetic conditions, for example, a source associated with surface or above transportation of sediment (e.g., aeolian dust) may be more likely to form calcretes under pedogenic conditions as soils are found on the surface.

Finally, an unexpected outcome of this study is the discrepancy between this work and that of Kitching and Smith (1997) is that their *Tritylodon* Acme Zone described as an almost continuous regional marker horizon, which was not observed in the study area. Because of this, the *Tritylodon* Acme Zone could not be used a reference surface (datum) for the assessment of the stratigraphic position of the studied palaeosol horizons. Instead, in this study the contact of the UEF and Clarens Formations was a regional marker surface, and the stratigraphic positions of the palaeosols and the carbonate nodules collected from the UEF in this study were measured relative to this datum. However, it is important to note that the use of this surface as a stratigraphic datum for the palaeosols and samples collected beneath is only possible if one assumes (a) that this is an even surface of similar age; and (b) a laterally and vertically uniform depositional rate and post-depositional compaction rate in the UEF. Both of these are rather unlikely in fluvial systems where the deposition and the compaction of heterolithic facies are heterogeneous, because depositional volume will be controlled by highly variable gradients, flow regimes and other factors across time and space (Figure 4.1 - Wright and Marriot, 1993; Gibling, 2006).

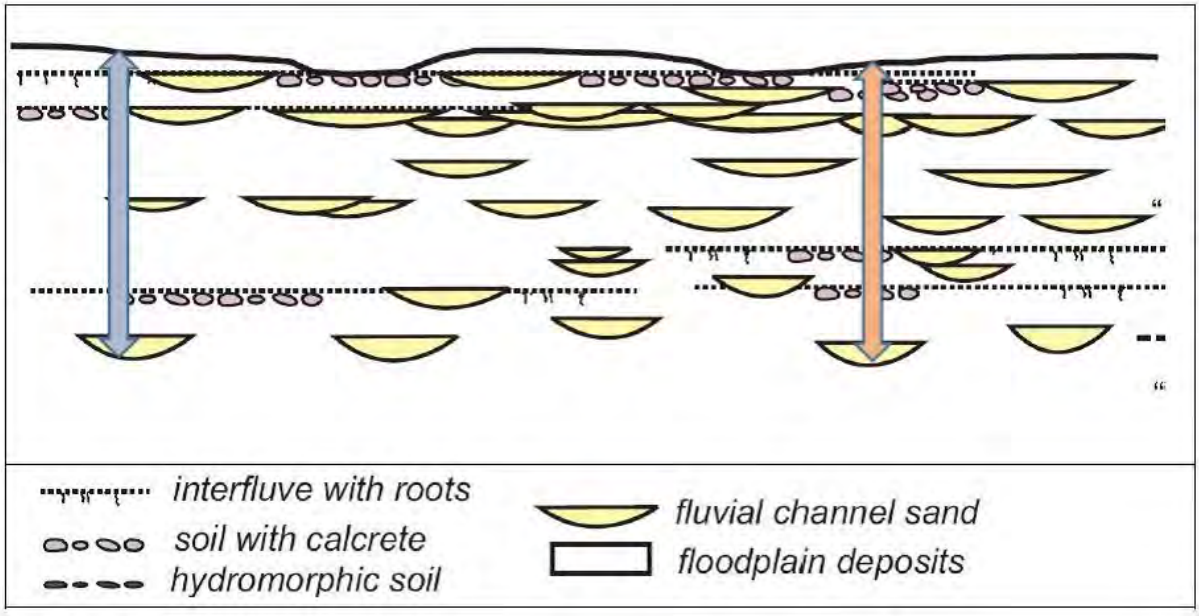


**Figure 4.1:** Fluvial deposits are both heterogeneous and laterally restricted, notice the two logs illustrated by blue and red arrows cannot be correlated (Wright and Marriott, 1993).

An alternative explanation to the pedogenic origin of the carbonate nodules and later diagenetic overprinting may be that the nodules formed independently at a later stage under diagenetic conditions. It may be possible that the carbonate nodules formed through the eogenesis pathway, which refers to diagenetic changes that occur at or near the sediment surface were dissolution and porosity are relatively high (Morrow and McIlreath, 1990). If this was indeed the case, then the host rock would have been a soil as the internal features (rhizoliths, burrows, colour mottling, etc.) suggest and shortly before sediment lithification the nodules have developed through the eogenetic pathway. The development of the carbonate nodules through the eogenetic pathway may explain the presence of abiotic microstructures observed and absence of microstructures of biological origin common in nodules formed by pedogenic processes. Although in most cases diagenesis commonly postdates pedogenesis, these processes can in part operate simultaneously and hence the term pedodiagenesis has been proposed by Klappa (1983). Finally, the exclusively diagenetic origin of the carbonate nodules is very unlikely, because of the well-documented bone-bearing, reworked carbonate nodule conglomerates that are a reliable stratigraphic marker of the UEF (Bordy et al., 2004a, b). The presence of such intraformational conglomerates clearly suggests high energy, fluvial erosion that could rework the nodules during floods. Considering all the evidence for the sheet flood dominated, semi-arid UEF conditions (Bordy et al., 2004a, b), among others the absence of deeply incised sandstone bodies, these

carbonate nodules had to be in shallow subsurface positions, and thus likely associated with ancient soils.

### 4.1 Further research

Further research on these carbonate nodules should be concerned primarily with geochemical analysis of stable isotopes such as oxygen, carbon and strontium which might help provide more conclusive evidence on origin and geological evolution of the carbonate nodules found in the UEF. A complete isotope geochemical analytical study would provide an interdisciplinary approach together with the data derived from the clay minerals in this study to better interpret the palaeoclimatic conditions at the time when the nodules were forming. For comparative purposes and for better defined geochemical signatures, it would be useful to conduct isotope analysis not only on samples collected from the Elliot Formation but also on other calcretes from other similar sedimentary sequences with a more constrained climatic regime (i.e., modern Sub-Saharan African calcretes).

# Chapter 5: Conclusion

Carbonate nodules found in the Lower Jurassic UEF are associated with a series of palaeosols that have been stratigraphically defined ('lower', 'intermediate', and 'upper' horizons) based on their distances below the contact of the Elliot and Clarens Formations. The palaeosols were identified by the presence of root traces, burrows, and colour mottling and desiccation cracks. The close association between carbonate nodules and palaeosol features observed in the field suggest that the carbonate nodules most likely formed under pedogenic conditions. Moreover, the observed internal macroscopic and microscopic features of the Elliot nodules, such as septarian cracks, circumgranular cracks, and fractured micronodules, suggest formation due to predominantly abiotic physicochemical processes. Therefore, it is possible that the nodules, after a primary genesis in soils, underwent a subsequent diagenetic overprinting.

The widely accepted mode of deposition the Elliot Formation under a seasonally wet, semi-arid climate and in a flash flood dominated, fluvio-lacustrine setting is supported by the findings of this study. Firstly, this is reinforced by the close association of carbonate nodules and calcretized desiccation cracks which are collectively taken as supportive evidence for a setting with seasonal rainfall where repeated drying and wetting periods occurred. Furthermore, the identified of clay minerals (illite, muscovite, and montmorillonite) that were extracted from the interior of the nodules also support an arid to semi-arid palaeoclimatic interpretation. This is based on the consideration that: 1) the clays extracted from the nodules are fairly accurate indicators of syndepositonal climate conditions; and 2) under dry climatic conditions the weathering of felsic and basic rocks will result in illite and montmorillonite, respectively. However, the distinction between authigenic and detrital clay minerals is problematic. Consequently, a further study using a multiproxy approach that combines data derived from clay mineral compositions together with data obtained from the geochemical analysis of stable isotopes of oxygen and carbon would be useful.

# Reference list


**Alonso-Zarza A.M.; Wright V.P. 2010.** Calcretes. In: Alonso-Zarza, A.M.; Tanner, L.H. (Eds). *Carbonates in continental settings: facies, environments and processes. Elsevier Developments in sedimentology* 61, 225-257.

**Andersson P.O.D; Johansson A.; Kumpulainen R.A. 2003.** *Sm-Nd isotope evidence for the provenanace of the Skoorsteenberg Formation, Karoo Supergroup, South Africa.* Journal of African Earth Sciences 36, 173-183.

**Arakel A.V.; McConchie D. 1982.** *Classification and genesis of calcrete and gypsite lithofacies in paleodrainage systems of inland Australia and their relationship to carnotite mineralization*. Journal of Sedimentary Petrology 52, 1149-1170.

**Armenteros I. 2010.** Diagenesis of carbonates in continental settings. In: Alonso-Zarza, A.M. and Tanner, L.H. (Eds). *Carbonates in continental settings: geochemistry, diagenesis and applications. Elsevier Developments in sedimentology* 62, 61-122.

**Astin T.R. 1986.** *Septarian crack formation in carbonate concretions from shales and mudrocks.* Clay Minerals 21, 617-631.

**Beukes N.J. 1970.** Stratigraphy and sedimentology of the Cave Sandstone Stage, Karoo System. In Haughton, S.H. (Ed). *Proceedings of the 2nd IUGS Symposium on Gondwana Stratigraphy and Palaeontology.* CSIR, Pretoria, 321-341.

**Blodgett R.H. 1988.** *Calcareous paleosols in the Triassic Dolores Formation, southwestern Colorado.* Geological Society of America Special Paper 216, 103-121.

**Bordy E.M.; Hancox P.J.; Rubidge B.S. 2004a**. *Fluvial style variations in the Late Triassic – Early Jurassic Elliot formation, main Karoo Basin, South Africa.* Journal of African Earth Sciences 38, 383-400.

**Bordy E.M.; Hancox P.J.; Rubidge B.S. 2004b.** *Basin development during the deposition of the Elliot Formation (Late Triassic – Early Jurassic), Karoo Supergroup, South Africa.* Geological Society of South Africa 107, 397-412.

**Bordy E.M.; Hancox P.J.; Rubidge B.S. 2004c.** *Provenance Study of the Late Triassic – Early Jurassic Elliot Formation, main Karoo Basin, South Africa.* South African Journal of Geology, 107, 587-602.

**Bordy E.M.; Hancox P.J.; Rubidge B.S. 2004d.** *A description of the sedimentology and palaeontology of the Upper Triassic - Lower Jurassic Elliot Formation in Lesotho.* Palaeontologia Africana, 40, 43-58.

**Bordy E.M.; Hancox P.J.; Rubidge B.S. 2005a.** *The contact of the Molteno and Elliot formations through the main Karoo Basin, South Africa: a second-order sequence boundary.* South African Journal of Geology, 108, 349-362.

**Bordy E.M.; Hancox P.J.; Rubidge B.S. 2005b.** *A Reply - Turner, B.R. and Thomson, K., Discussion on 'Basin development during deposition of the Elliot Formation (Late Triassic – Early Jurassic), Karoo Supergroup, South Africa (South African Journal of Geology, 107, 397-412).* South African Journal of Geology, 108, 19-34.

**Bown T.M.; Kraus M.J. (1981).** *Lower Eocene alluvial paleosols (Willwood Formation, Northwest Wyoming, U.S.A.) and their significance for paleoecology, paleoclimatology, and basin analysis.* Palaeogeography, Palaeoclimatology, Palaeoecology 34, 1-30.

**Brewer R. 1964**. *Fabric and mineral analysis of soils*. Wiley, New York, 470p.

**Brewer R.; Sleeman J.R. 1964.** *Glaebules: their definition, classification and interpretation.* European Journal of Soil Science 15, 66-78.

**Brussard L. 1998.** *Soil fauna, guilds, fuctional groups and ecosystem processes.* Applied Soil Ecology 9, 1232-135.

**Buatois L.A.; Mangano M.G.; Genise J.F.; Taylor T.N. 1998.** *The ichologic record of the continental invertebrate invasion: evolutionary trends in environmental expansion, ecospace utilization, and behavioral complexity.* Palaios 13, 217-240.

**Carlise D. 1980.** *Possible variation in the calcrete-gypcrete uranium model*. Open-File Rep. US. Dept. Energy, GJBX-53(80) 38pp.

**Carlise D. 1983.** *Concentration of uranium and vanadium in calcretes and gypcretes.* Geological Society of London, Special Publication 11, 185-195.

**Catuneanu O.; Hancox P.J.; Rubidge B.S. 1998.** *Reciprocal flexural behaviour and contrasting stratigraphies: a new basin development model for the Karoo retroarc foreland system, South Africa.* Basin Research 10, 417-439.

**Cerling T.E. 1984.** *The stable isotopic composition of modern soil carbonate and its relationship to climate.* Earth Planetary Science Letters 71, 229–240.

**Cerling, T.E., Quade, J., 1993.** Stable carbon and oxygen isotopes in soil carbonates. In: Swart P.K.; Lohman K.C.; Mckenzie J.; Savin S. (Eds). *Climate Change in Continental Isotopic Records.* American Geophysical Union, Washington D.C., 217–231.

**Chaudhri A.R.; Singh M. 2012.** *Clay minerals as climate indicators – A case study.* American Journal of Climate Change 1, 231-239.

**Cole D.I. 1992.** Evolution and development of the Karoo Basin. In: de Wit M.J and Ransome I.G.D. (Eds). *Inversion Tectonics and the Cape Fold Belt, Karoo and Cretaceous Basins of Southern Africa.* Balkema, Rotterdam, 87-99.

**Dart R.C.; Barovich K.M.; Chittleborough D.J.; Hill S.M. 2007.** *Calcium in regolith carbonates of central and southern Australia: its source and implications for the global carbon cycle.* Palaeogeography, Palaeoclimatology, Palaeoecology 249, 322-334.

**Deer W.; Howie R.; Zussman, J. 2004.** *Rock-forming Minerals: Silica Minerals, Volume 4B,* Geological Society of London, 965p.

**Dickinson W.R. 1974.** *Plate tectonics and sedimentation.* In Dickinson W.R. (Ed). Society of Economic Paleontologists and Mineralogists, Special Publications 22, 1-27.

**Driese, S.G.; Foreman J.L. 1992.** *Paleopedology and paleoclimatic implications of late Ordovician vertic paleosols, Juniata Formation, Southern Appalachians.* Journal of Sedimentary Petrology 62, 71-83.

**Du Toit A.L. 1954.** *The Geology of South Africa.* 3rd ed. Oliver and Boyd, Edinburgh, 611pp.

**Duncan R.A.; Hooper P.R.; Rehacek J.; Marsh J.S.; Duncan A.R. 1997.** *The timing and duration of the Karoo igneous event, southern Gondwana.* Journal of Geophysical Research 102, 127-138.

**Ehleringer J.R. 1989.** Carbon isotope ratios and physiological processes. In: Rudel P.W.; Ehleringer J.R.; Nagy K.A. (Eds). *Stable Isotopes in Ecological Research.* Springer-Verlag, New York, 525p.

**Ekart D.; Cerling T.; Motanez I.; Tabor N.; 1999.** *A 400 million year carbon isotope record of pedogenic carbonate: implications for palaeoatmosphic carbon dioxide.* American Journal of Science 299, 805-827.

**Eriksson P.G. 1985.** *The Depositional Palaeoenvironment of the Elliot Formation in the Natal Drakensburg and North – Eastern Orange Free State.* Transactions of the Geological Society of South Africa 88, 19-26.

**Eriksson P.G. 1986.** *Aeolian dune sand and alluvial fan deposits in the Clarens Formation of the Natal Drankensburg*. Transactions Geological Society of South Africa 80, 389-393.

**Esteban M.; Klappa C.F. 1983.** *Subaerial exposure environment.* American Association of Petroleum Geologists Memoir 33, 1-54.

**Folk R. L. 1980.** *Petrology of sedimentary rocks.* Hemphill Publishing Company. Austin, Texas, 184pp.

**Frey R.; Pemberton S.G.; Fagerstrom J.A. 1984.** *Morphological ethological, and environmental significance of the ichnogenera Scoyenia and Ancorichnus*. Journal of Paleontology 58, 511-528.

**Gaffney E.S.; Kitching J.W. 1994.** *The most ancient African turtle.* Nature 369, 55-58.

**Galloway W.E.; Hobday, D.K. 1983.** *Terrigenous Clastic Depositional Systems: Applications to Petroleum, Coal, and Uranium Exploration.* Springer-Verlag, New York, p. 51-79.

**Gastaldo R.A.; Knight C.L.; Neveling J.; Tabor N.J. 2014.** *Latest Permian paleosols from Wapadsberg Pass, South Africa: Implications for Changhsingian climate.* Geological Society of America 126, 665-679.

**Gibling M.R. 2006.** *Width and thickness of the fluvial channel bodies and valley fills in the geological record: A literature compilation and classification.* Journal of Sedimentary Research 76, 731-770.

**Goudie A.S. 1983.** Calcrete. In: Goudie A.S.; Pye K. (Eds). *Chemical sediments and geomorphology.* New York, Academic Press, 93-131.

**Groenewald G.H. 1986.** *Geology of the Golden Gate Highlands National Park.* Koedoe 29, 165-181.

**Gustavson T.C. 1991.** *Buried vertisols in lacustrine facies of the Pliocene Fort Hancock Formation, Hueco Bolson, West Texas and Chihuahua, Mexico*. Geological Society of America Buletin 103, 448-460.

**Gustavson T.C.; Holiday V.T. 1999.** *Eolian sedimentation and soil development on a semiarid to subhumid grassland, Tertiary Ogallala and Quaternary Blackwater Draw Formations, Texas and New Mexico high plains.* Journal of Sedimentary Research 69, 622-634.

**Hälbich I.W. 1983.** A tectonogenesis of the Cape Fold Belt (CFB). In: Söhnge, A.P.G., Hälbich, I.W. (Eds). *Geodynamics of the Cape Fold Belt.* Geological Society of South Africa, Special Publication 12, 165–175.

**Haughton S.H. 1924.** *The fauna and stratigraphy of the Stormberg Series.* Annales of the South African Museum 12, 323-495.

**Hawkesworth C.; Kelley S.; Turner S.; le Roex A.; Storey B. 1999.** *Mantle processes during Gondwana break-up and dispersal.* Journal of African Earth Sciences 28, 239-261.

**Herbert C.T.; Compton J.S. 2007.** *Depositional environments of the lower Permian Dwyka diamictite and Prince Albert shale inferred from the geochemistry of early diagenetic concretions, southwest Karoo Basin, South Africa.* Sedimentary Geology 194, 263-277.

**Hounslow M.W. 1997.** *Significance of localized pore pressures to the genesis of septarian concretions.* Sedimentology 44, 1133-1147.

**James N.P. 1972.** *Holocene and Pleistocene calcareous crust (caliche) profiles: Criteria for subaerial exposure.* Journal of Sedimentary Petrology 42, 817-836.

**Johnson D.D.; Beaumont C. 1995.** Preliminary results from a planform kinematic model of orogeny evolution, surface processes and the development of clastic foreland basin

stratigrahy. In: Dorobek S.L.; Ross G.M. (Eds). *Stratigraphic Evolution of Foreland Basins.* Society of Econimic Paleontologists and Mineralogists Special Publications 52, 3-24.

**Johnson M.R. 1991.** *Sandstone petrography, provenance and plate tectonic setting in Gondwana context of the southeastern Cape-Karoo basin.* South African Journal of Geology 94, 137–154.

**Johnson M.R.; van Vuuren C.J.; Hegenberger W.F.; Key R.; Shoko U. 1996.** *Stratigraphy of the Karoo Supergroup in southern Africa: an overview.* Journal of African Earth Sciences 23, 3–15.

**Jones, C.G.; Laawton, J.H.; Shachak, M. 1994.** *Organisms as ecosystem engineers.* Oikos 69, 373-386.

**Khadkikar A.S.; Merh S.S.; Malik J.N.; Chanyal L.S. 1998.** *Calcretes in semi-arid alluvial systems: formative pathways and sinks.* Sedimentary Geology 116, 251-260.

**Kitching J.; Raath M. 1984.** *Fossils From the Elliot and Clarens Formations (Karoo Sequence) of the Northeastern Cape, Orange Free State and Lesotho, and a suggested Biozonation based on Tetrapods.* Palaeotologia Africana 125, 111–125.

**Klappa C.F. 1980.** *Rhizoliths in terrestrial carbonates: classification, recognition, genesis and significance.* Sedimentology 27, 613-629.

**Klappa, C.F., 1983.** A process-response model for the formation of pedogenic calcretes. In: Wilson R.C.L. (Ed). *Residual Deposits.* Geological Society of London Special Publication 11, 211-220.

**Lamplugh G.W. 1902.** *Calcrete.* Geological Magazine 9, 575-575.

**Leeder M.R. 1975.** *Pedogenic carbonates and flood sediment accretion rates: a quantitative model for alluvial arid-zone lithofacies.* Geological Magazine 112, 257-270.

**Leeder M.R. 1982.** *Sedimentology: process and product.* George Allen and Unwin, London, 344p.

**Lindeque A.; Ryberg T.; Stankiewicz J.; Weber M.; de Wit M. 2007.** *Deep Crustal Reflection Experiment across the Southern Karoo Basin, South Africa.* South African Journal of Geology 110, 419-438.

**Lindeque A.; de Wit M.J.; Ryberg T.; Weber M.; Chevallier L. 2011.** *Deep crustal profile across the Southern Karoo basin and Beattie magnetic anomaly, South Africa: An integrated interpretation with tectonic implications.* South African Journal of Geology, 114, 265-292.

**Lock B.E. 1980.** *Flat-plate subduction and the Cape Fold Belt of South Africa.* Geology 8, 35-39.

**Lohmann K.C.; Walker J.C.G. 1989.** *The $\delta^{18}O$ record of Phanerozoic abiotic marine calcite cements.* Geophysical Research Letters 8, 319-322.

**Mack G.H.; James, W.C., 1994.** *Paleoclimate and the global distribution of paleosols*. The Journal of Geology 102, 360-366.

**Miall A.D. 1996.** *The geology of fluvial deposits: Sedimentary facies, basin analysis and petroleum geology.* Berlin: Springer, 582pp.

**Morrow D.W., McIlreath, I.A., 1990.** Diagenesis. General introduction. In: McIlreath, I.A.; Morrow, D.W. (Eds). *Diagenesis.* Geoscience Canada, Reprint series 4, 1-8.

**Mozley P.S.; Matthew Davis J. 1996.** *Relationship between orientated calcite concretions and permeability correlation structure in an alluvial aquifer, Sierra Ladrones Formation, New Mexico.* Journal of sedimentary research 66, 11-16.

**Netterberg F. 1980.** *Geology of Southern Africa Calcretes: 1. Terminology, description, macrofeatures, and classification.* Transactions of the Geological Society of South Africa 83, 255-283.

**Netterberg F.; Caiger, J.H. 1983.** *A geotechnical classification of calcretes and other pedocretes.* Geological Society of London, Special Publications 11, 235-243.

**Parrish J.T. 1990.** Gondwanan paleogeography and paleoclimatology. In: Taylor T.N.; Taylor E.L. (Eds). *Antarctic Paleobiology: Its Role in the Reconstruction of Gondwana.* Spinger Verlag, New York, 12-229.

**Pettijohn F.J. 1957.** *Sedimentary rocks, 2nd Ed.* Harper and Row, 718p.

**Pettijohn F.J. 1975.** *Sedimentary rocks, 3rd Ed.* Harper and Row, 628p.

**Pratt B.R. 2001.** *Septarian concretions: internal cracking caused by synsedimentary earthquakes.* Sedimentology 48, 189-213.

**Pysklywec, R.N.; Mitrovica, J.X. 1999.** *The role of subduction-induced subsidence in the evolution of the Karoo basin.* Journal of Geology 107, 155-164.

**Quade J.; Cater J.M.L.; Ojha T.P.; Adam J.; Harrison T.M. 1995.** *Late Miocene environmental change in Nepal and the northern Indian subcontinent; stable isotopic evidence from paleosols.* Geological Society of America Bulletin 107, 1381–1397.

**Reid I.; Frostick L.E. 1994.** Fluvial sediment transport and deposition. In: Pye, K.; (Ed). *Sediment Transport and Depositional Processes.* Blackwell Scientific Publishers, London, 89-155.

**Reineck H.E.; Singh, I.B.; 1980.** *Depositional Sedimentary Environments,* 2nd ed. Springer-Verlag, New York, 257-314.

**Raiswell R. 1971.** *The growth of Cambrian and Liassic concretions.* Sedimentology 17, 147-171.

**Reeves C.C. 1976.** *Caliche: Origin, Classification, Morphology and Uses.* Estacado Books, Texas, 233p.

**Reeves, C.C. 1970.** *Origin, classification and geologic history of caliche on the southern High Plains, Texas and eastern New Mexico.* The Journal of Geology 78, 352-362.

**Retallack G.J. 1983.** *Late Eocene and Oligocene paleosols from Badlands National Park, South Dakota.* Geological Society of America Special Paper 193, 88p.

**Retallack G.J. 1988.** Field recognition of paleosols. In: Reinhardt J.; Sigleo W.R. (Eds). *Paleosols and Weathering Through Geologic Time: Principles and Applications.* Geological Society of America Special Paper 216, 1-20.

**Retallack G.J. 1991.** *Untangling the effects of burial alteration and ancient soil formation.* Annual Review of Earth and Planetary Sciences 19, 183-206.

**Retallack G.J., 1999.** *Postapocalyptic greenhouse paleoclimate revealed by the earliest Triassic palaeosols in the Sydney Basin, Australia*. The Geological Society of America Bulletin 111, 52-70.

**Retallack G.J.; Alonso-Zarsa 1998.** *Middle Triassic paleosols and paleoclimate of Antarctica*. Journal of Sedimentary Research 68, 169-184.

**Retallack, G. J., 1990.** *Soils of the past - an introduction to paleopedology*. Harper Collins Academic, London, 520p.

**Ruellan, A., 1968.** *Les horizons d'individualization et d'accumulation du calcaire dans les sols du Maroc.* Proc. 9th int. Congr. Soil Sci., 4, 501-510.

**Sciscio, L., 2015.** *The Triassic-Jurassic boundary in southern Africa: a multidisciplinary study using magnetostratigraphical, geochemical and paleo-environmental assessments*. Unpublished PhD thesis. University of Cape Town.

**Scotese C.R.; Boucot A.J.; McKerrow W.S.; 1999.** *Gondwanan paleogeography and paleoclimatology.* Journal of African Earth Sciences 28, 99-114.

**Scotese C.R.; 2015.** *Climate History - Paleomap project***.** [Online] Available at: www.scotese.com

**Sheldon N.D. 2006.** *Using paleosols of the Picture Geoge Basalt to reconstruct the Middle Miocene climatic optimum*. PaleoBios 26, 27-36.

**Sheldon N.D.; Tabor N.J. 2009.** *Quantitative paleoenvironmental and paleoclimatic reconstruction using paleosols.* Earth Science Reviews 95, 1-52.

**Singer A. 1984.** *The paleoclimatic interpretation of clay minerals in sediments – a review.* Earth Science Reviews 21, 251-293.

**Slate J.L.; Smith, G.A.; Wang, Y.; Cerling T.E. 1996.** *Carbonate-paleosol genesis in the Plio-Pleistocene St. David Formation, southeastern Arizona.* Journal of Sedimentary Research 66, 85-94.

**Smith R.; Kitching J. 1997.** *Sedimentology and vertebrate taphonomy of the Tritylodon Acme Zone: a reworked palaeosol in the Lower Jurassic Elliot Formation, Karoo Supergroup, South Africa.* Palaeogeography, Palaeoclimatology, Palaeoecology 131, 29-50.

**Smith R.M.H. 1990.** A review of stratigraphy and sedimenraty environments in the Karoo Basin of South Africa. In: Kogbe C.A.; Lang J. (Eds). *Major African Continental Phanerozoic Complexes and Dynamics of Sedimentation.* Journal of African Earth Sciences 10, 117-137.

**Smith R.M.H.; Erickson P.A.; Botha W.J. 1993.** *A review of the stratigraphy and sedimentary environments of the Karoo-aged basins of Southern Africa.* Journal of African Earth Sciences 16, 143-169.

**Soil Survey Staff, 1975**. Soil taxonomy: Soil Conservation Service, U.S. Department of Agriculture, Agriculture Handbook No. 436, 754 p.

**Spötl C.; Wright V.P. 1992.** *Groundwater dolocretes from the Upper Triassic of the Paris Basin, France: a case study of an arid, continental diagenetic facies.* Sedimentology 39, 1119-1136.

**Stern L.A.; Chamberlain C.P.; Reynolds R.C.; Johnson G.D. 1997.** *Oxygen isotope evidence of climate change from pedogenic clay minerals in the Himalayan molasse.* Geochimca et Cosmochimca Acta 61, 731–744.

**Tandon S.K.; Narayan D. 1981.** *Calcrete conglomerate, case-hardened conglomerate and cornstone – a comparative account of pedogenic and non-pedogenic carbonates from the continental Silwalik Group, Punjab, India.* Sedimentology 28, 353-367.

**Tankard A.J.; Jackson M.P.A.; Eriksson K.A.; Hobday D.K.; Hunter D.R. and Minter W.E.L. 1982.** *Crustal Evolution of Southern Africa: 3.8 Billion Years of Earth History.* Springer-Verlag, Berlin, p.523

**Tankard A.; Welsink H.; Aukes P.; Newton R.; Stettler E. 2009.** *Tectonic evolution of the Cape and Karoo basins of South Africa.* Marine and Petroleum Geology 26, 1379-1412.

**Tankard A.; Welsink H.; Aukes P.; Newton R.; Stettler E. 2012.** *Geodynamic interpretation of the Cape and the Karoo Basins, South Africa.* Phanerozoic Passive Margins, Cratonic Basins and Global Tectonics Maps. USA and UK: Elsevier, 869-942.

**Theron J.N. 1969.** *The Baviaanskloof Range- a South African nappe.* Transactions of the Geological Society of South Africa 72, 29–30.

**Thomas R.J.; Marshall C.G.A.; Du Plesis A.; Miller J.A.; Fitch F.J.; von Brunn V.; Watkeys M.K. 1992.** Geological studies in southern Natal and Transkei: Implications for the Cape Orogen. In: de Wit M.J. and Ransome I.G.D. (Eds), *Inversion Tectonics of the Cape Fold Belt, Karoo and Cretaceous Basin of Southern Africa.* Balkema, Rotterdam, 229-236.

**Turner B.R. 1999.** *Tectonostratigraphical development of the Upper Karoo foreland basin: orogenic unloading versus thermally-induced Gondwana rifting.* Journal of African Earth Sciences 28, 215-238.

**Turner, P., 1980**, *Continental red beds.* Elsevier Scientific Publishing Company, New York, 562p.

**Visser J.N.J. 1992.** Basin tectonics in southwestern Gondwana during the Carboniferous and Permian. In: de Wit, M.J., Ransome, I.G.D. (Eds*.), Inversion Tectonics of the Cape Fold Belt, Karoo and Cretaceous Basins of Southern Africa.* Balkema, Rotterdam, 109–115.

**Visser J.N.J; Botha B.J.V. 1980.** *Meander channel, point bar, crevasse splay, and aeolian deposits from the Elliot Formation in Barkly Pass, North-Eastern Cape.* Transactions of the Geological Society of South Africa 83, 55-62.

**Wagner P.A. 1927.** *The geology of the north-eastern part of the Springbok Flats and surrounding country.* Explanatory sheet 17 (Springbok flats), Geological Survey of South Africa.

**Walker T.R. 1967.** *Formation of red beds in modern and ancient deserts*. Geological Society of America Bulletin 78, 355-368.

**Warren A.; Damiani R. 1999.** *Stereospondyl amphibians from the Elliot Formation of South Africa.* Palaeontologia Africana 35, 45-54.

**Wilson M.J. 1999.** *The origin and formation of clay minerals in soils: past, present and future perspectives.* Clay minerals 34, 7-25.

**Winter H. de la R. 1984.** *Tectonostratigraphy, as applied to the analysis of South African Phanerozoic basins.* South African Journal of Geology 87, 169-179.

**Wright V.P. 1990.** *A micromorphological classification of fossil and recent calcic and petrocalcic microstructures.* Developments in Soil Science 19, 401-407.

**Wright V.P.; Marriot S.B. 1993.** *The sequence stratigraphy of fluvial depositional systems: the role of floodplain sediment storage.* Sedimentary Geology 86, 203-210.

**Wright, V.P.; Tucker M.E. 1991.** Calcretes: An introduction. In Wright V.P.; Tucker M.E. (Eds). *Calcretes.* International Association of Sedimentologists. Reprint Series Vol. 2. Oxford, Blackwell Scientific Publications, 1-22.

**Zhou J.; Chafetz H.S. 2009.** *Biogenic caliches in Texas: The role of organisms and effect of climate*. Sedimentary Geology 222, 207-225.

**Zhou J.; Chafetz H.S. 2010.** *Pedogenic carbonates in Texas: Stable isotope distributions and their implications for reconstructing region-wide palaeoenvironments*. Journal of Sedimentary Research 80. 137-150.

# Appendices

Bulk rock diffractograms of the carbonate nodules from the Elliot Formation.

Bulk Rock Sample P15a (Paradys)

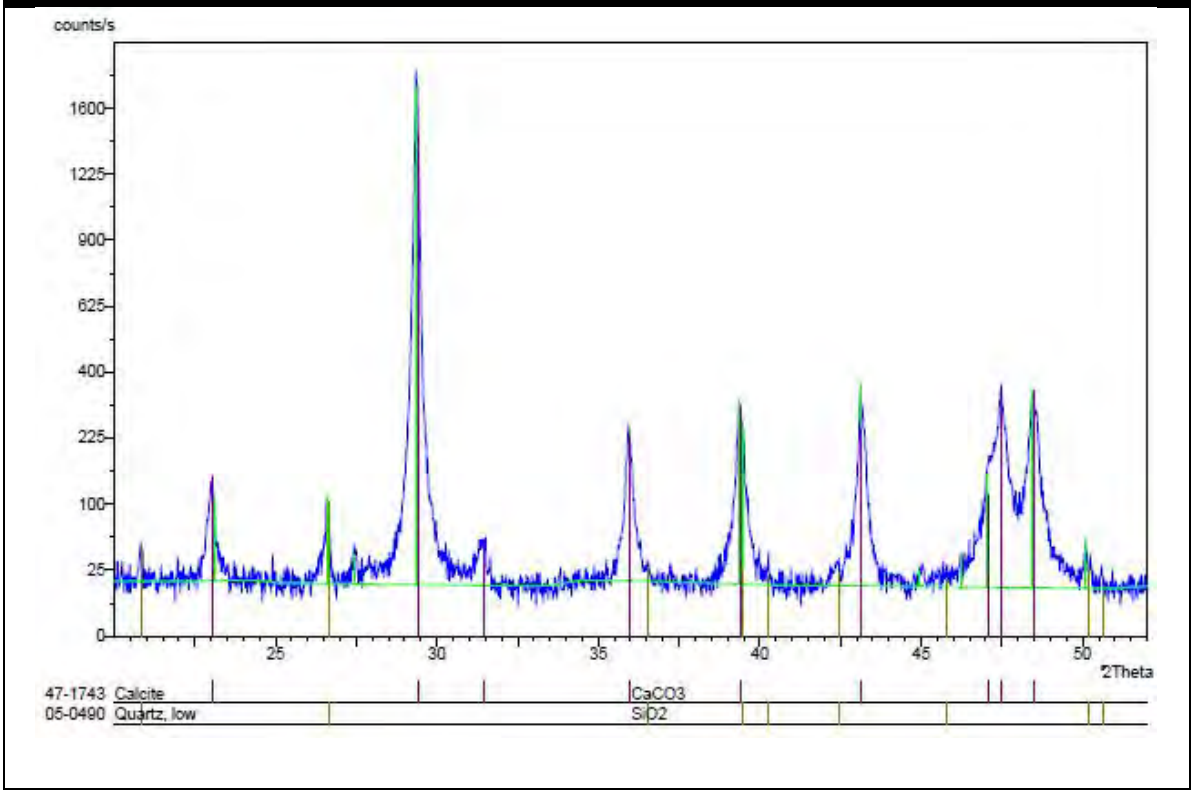

## Bulk Rock Sample P15b (Paradys)

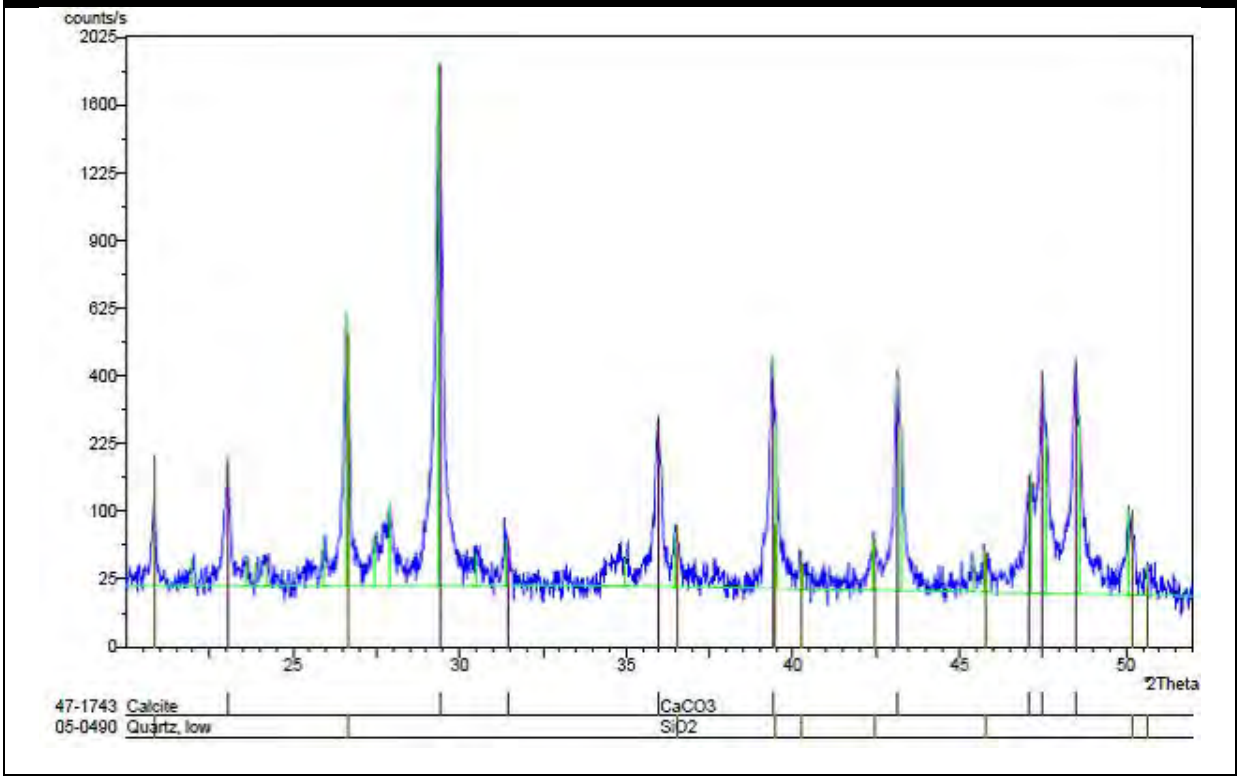


## Bulk Rock Sample GG2a (Golden Gate)

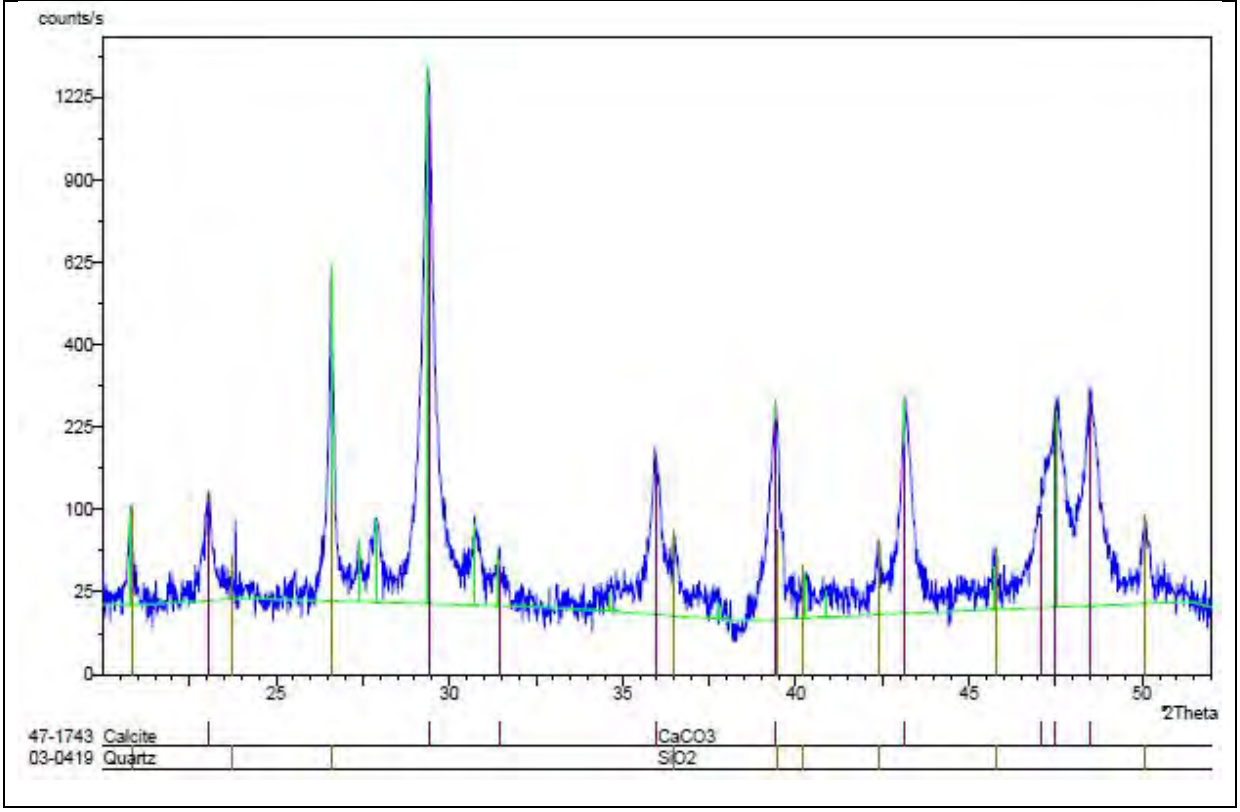

## Bulk Rock Sample GG2b (Golden Gate)

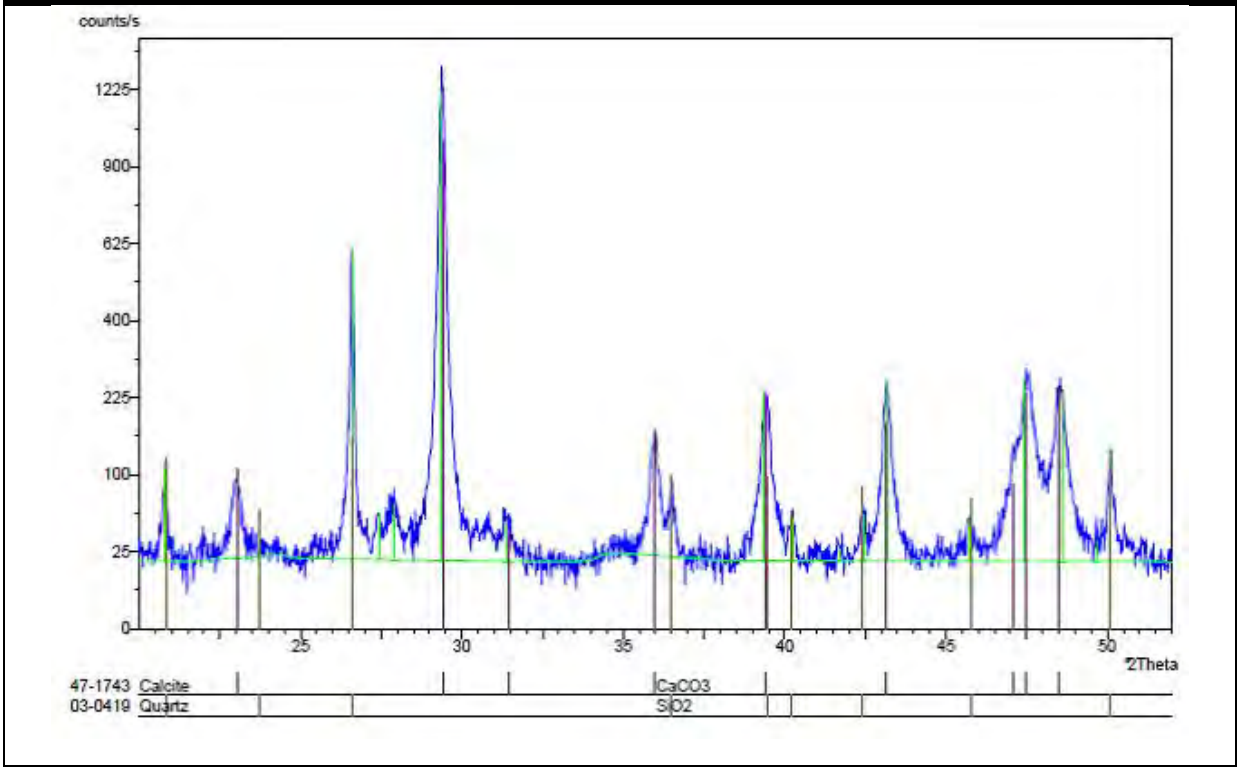


## Bulk Rock Sample SS2a

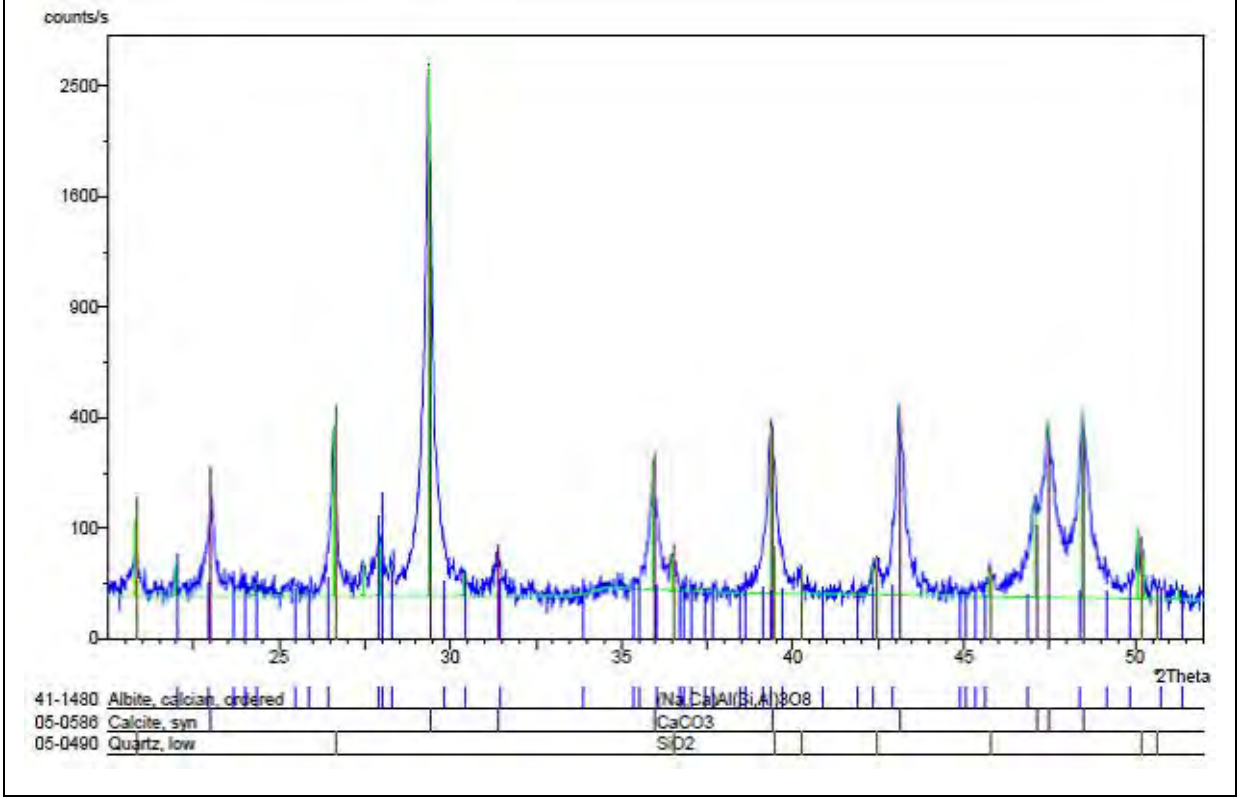

## Bulk Rock Sample SS2b

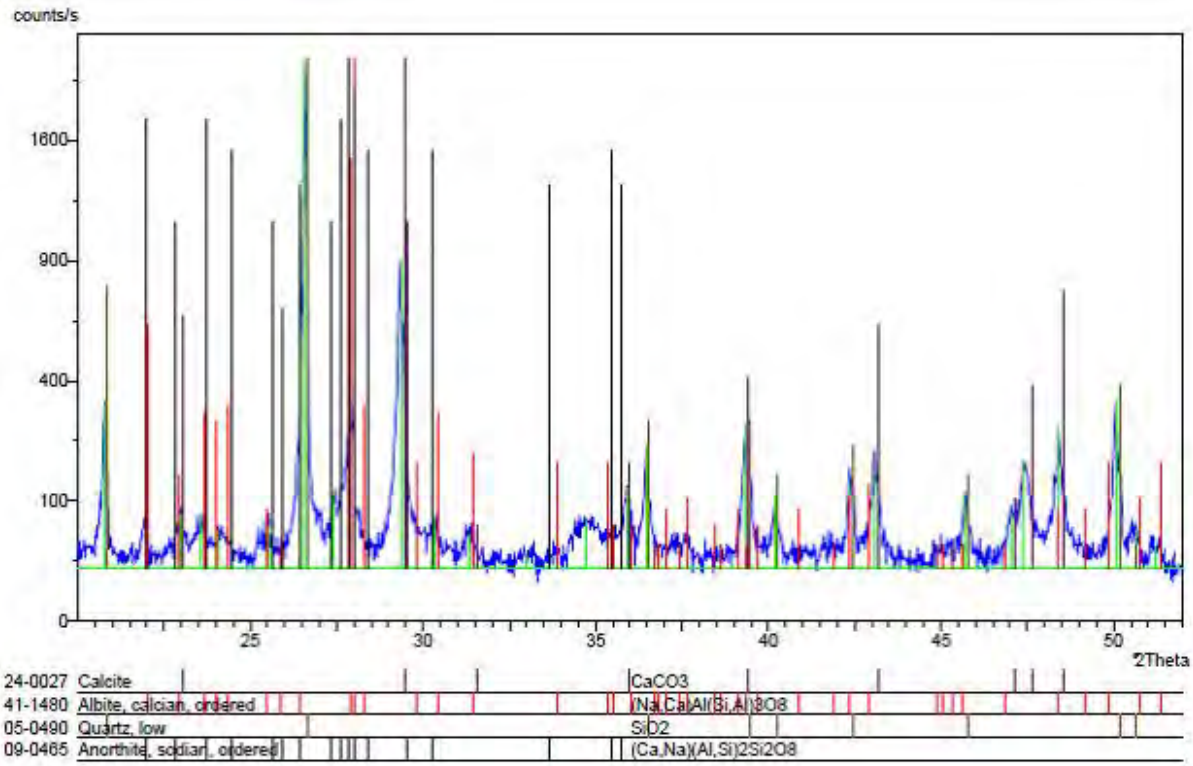


## Bulk Rock Sample SS3

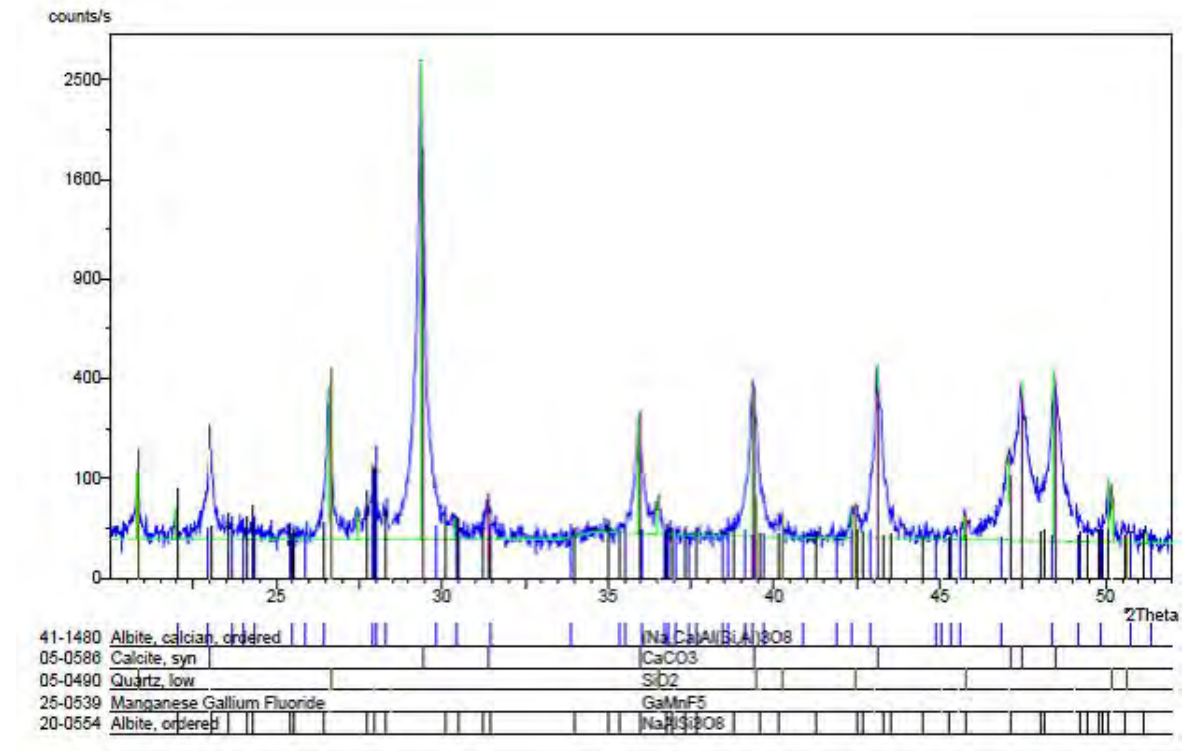

Separated clay fraction diffractograms of the carbonate nodules from the Elliot Formation.

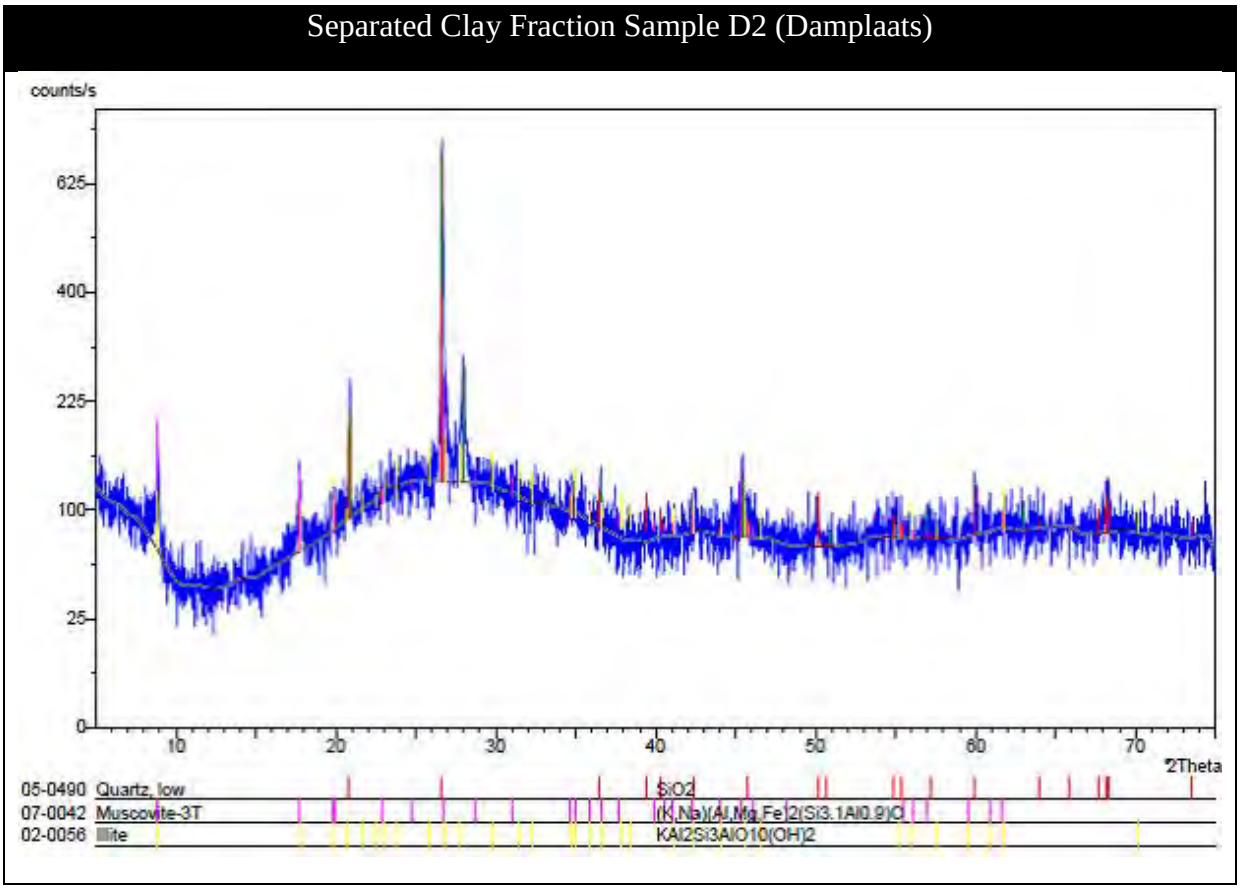

## Separated Clay Fraction Sample ZH8 (Saaihoek)

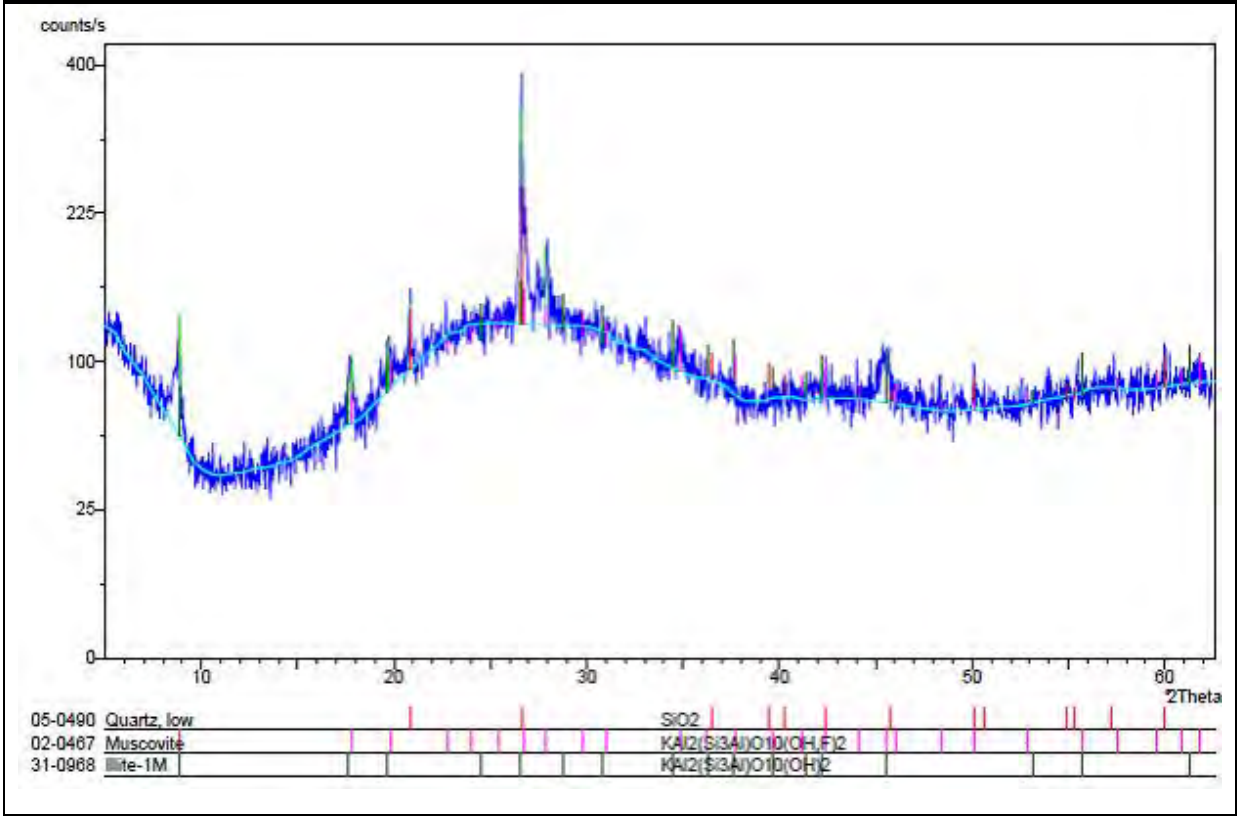


## Separated Clay Fraction Sample BS3 (Boshoek)

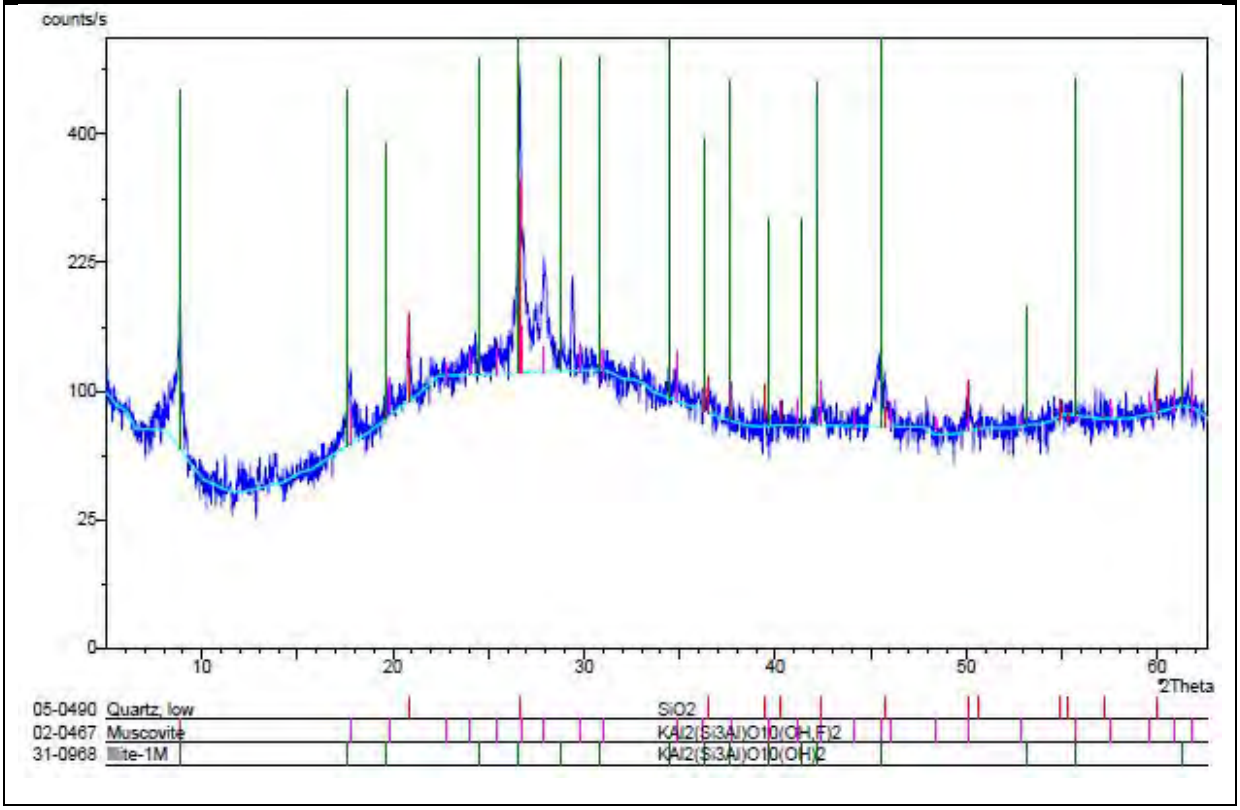

## Separated Clay Fraction Sample T8 (Twee Zusters)

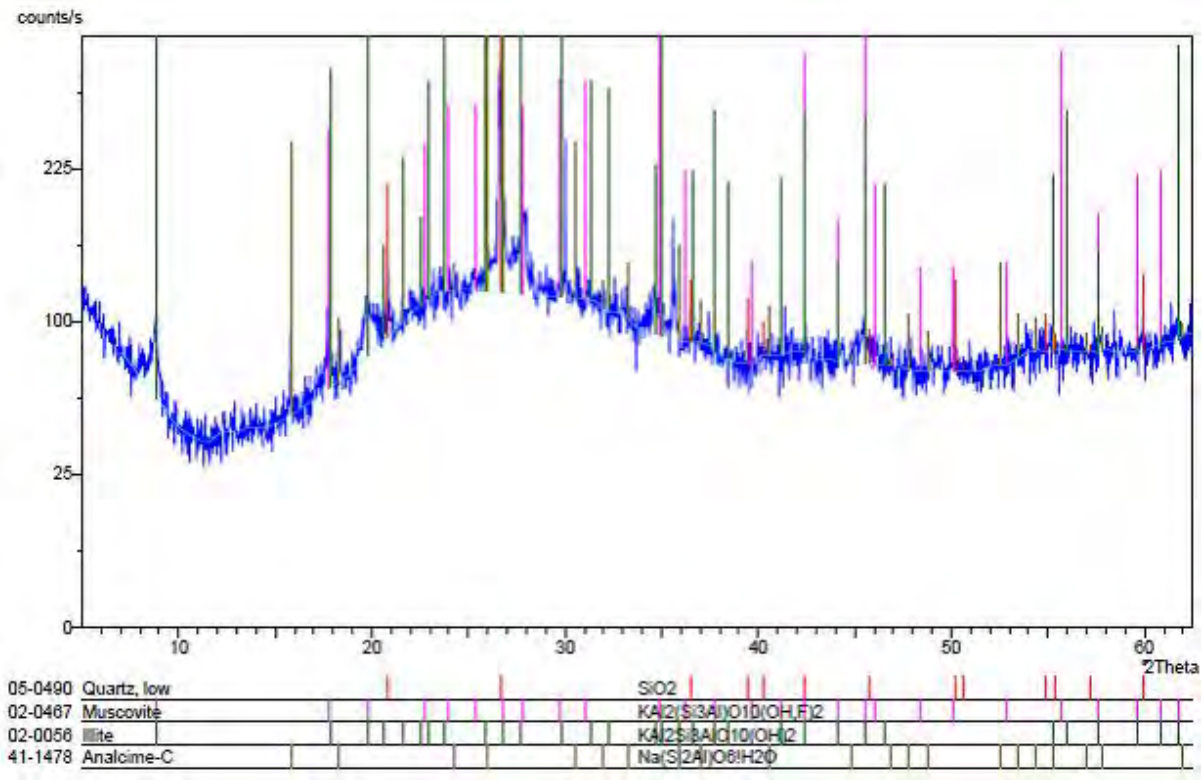


## Separated Clay Fraction Sample GG5 (Golden Gate)

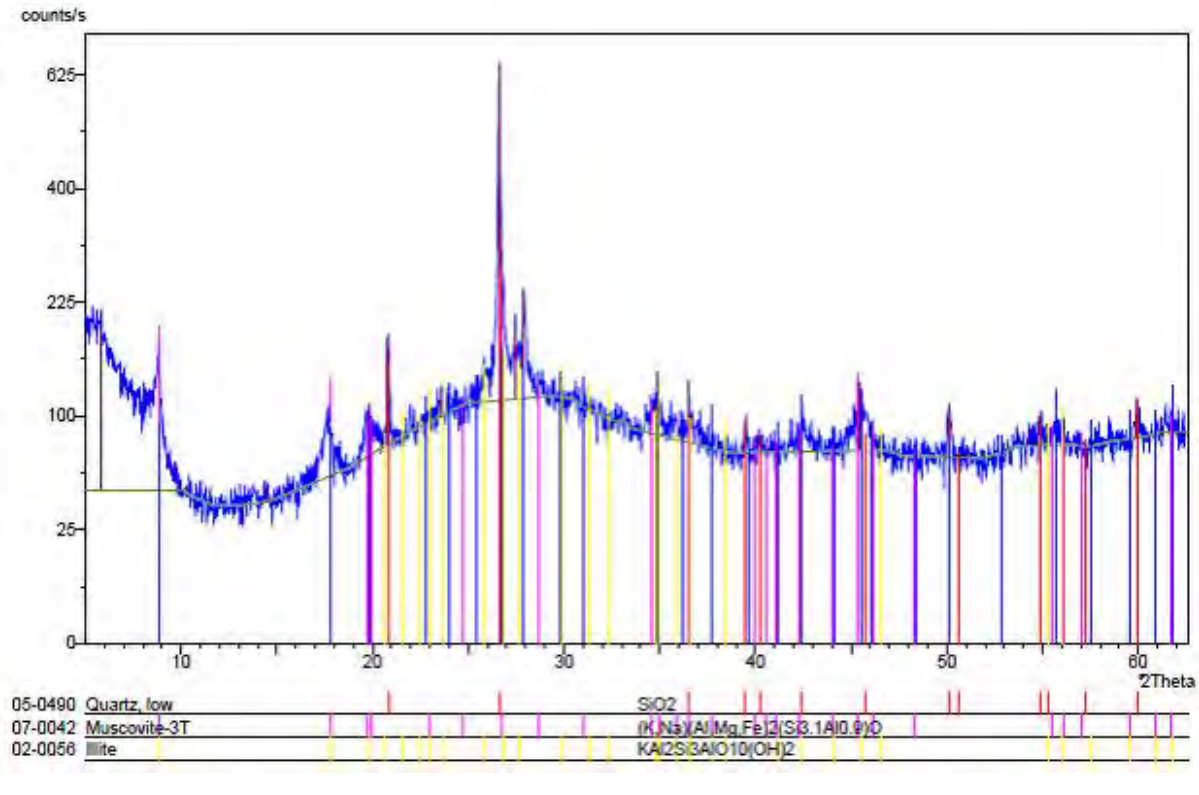

## Separated Clay Fraction Sample OB5A (Oldenburg)

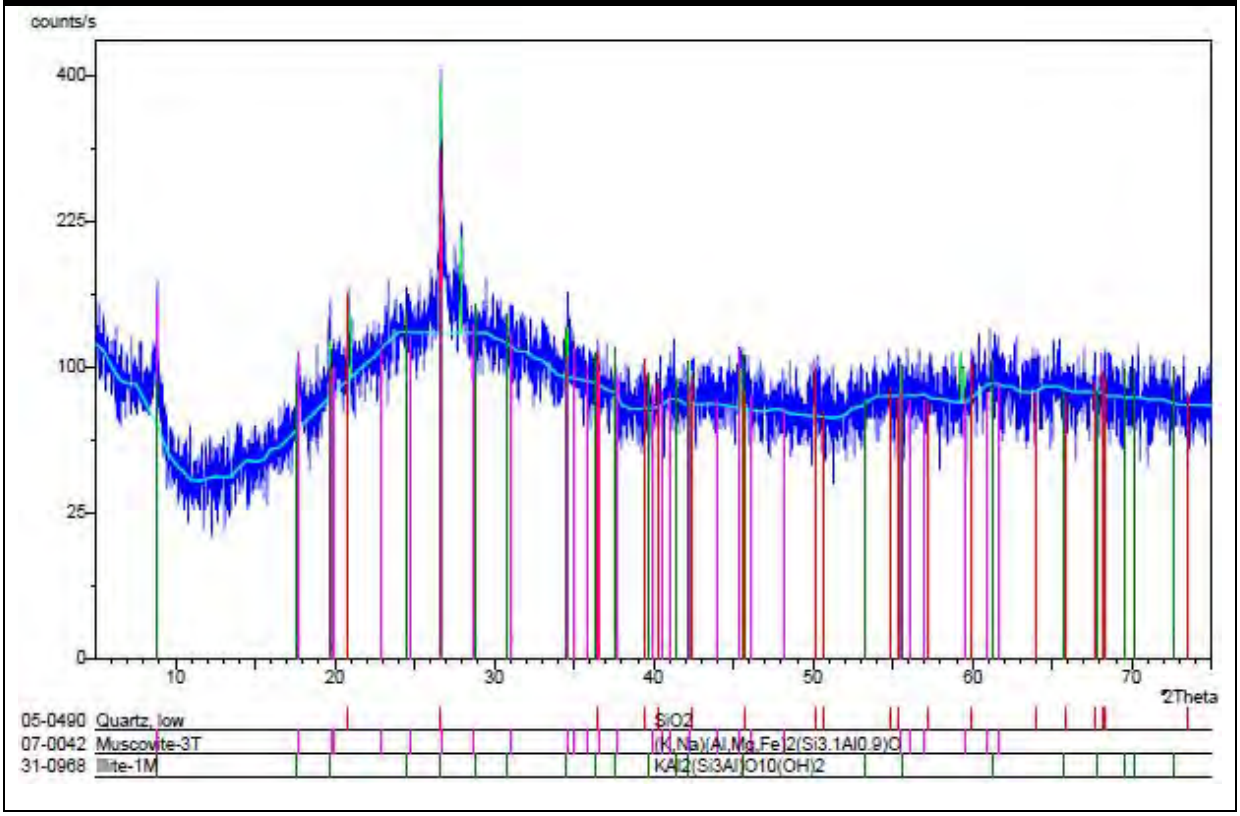


## Separated Clay Fraction Sample SS7 (Sunnyside)